Budapest University of Technology and Economics

Faculty of Architecture

ANALYSIS OF COMPOSITE BEAMS

Anikó Pluzsik

Supervisor:

László P. Kollár

Budapest, January, 2003

Acknowledgments

I would like to thank Professor Laszlo P. Kollar for all of his help and cooperation. He is an extraordinary teacher not only in the classroom, but in life's lessons as well. His approach to people, his endless patience, and his outlook on the world have made a lasting impression. I am privileged to have had the opportunity to work with him.

Thanks to the chairmen of the departments for providing my Ph.D studies:

Professor György Farkas, Chairman of the Department of Structural Engineering,

Professor Tamás Matuscsák and Professor Gábor Domokos, Chairmen of the Department of Mechanics and Structures.

Contents

List of symbols

A	area
$[A]$, $[B]$, $[D]$	stiffness matrices of a plate
$[\widetilde{\alpha}]$, $\left[\widetilde{\beta}\right]$, $\left[\widetilde{\delta}\right]$	compliance matrices of a plate
A_{ij}, B_{ij}, D_{ij}	elements of the stiffness matrices
$\overline{EA}$	tensile stiffness of an orthotropic beam
$\overline{EI}_{yy}$, $\overline{EI}_{yz}$, $\overline{EI}_{zz}$	bending stiffnesses of an orthotropic beam
$\overline{EI}_{\omega}$	warping stiffness of an orthotropic beam
$\overline{GI}_{t}$	torsional stiffness of an orthotropic beam
$\overline{S}_{ij}$	shear stiffnesses of an orthotropic beam
$\overline{s}_{ij}$	shear compliances of an orthotropic beam
h	plate thickness
b_k	width of a wall segment of the beam
K	number of wall segments
L	length of the beam
l	effective length of the beam
$\widehat{N}_x$	axial force acting on a beam
$\widehat{M}_y$, $\widehat{M}_z$	bending moments acting on a beam
$\widehat{M}_{\omega}$	bimoment acting on a beam
$\widehat{T}_x$	torque acting on a beam
$\widehat{T}_{sv}$	Saint Venant torque acting on a beam
$\widehat{T}_{\omega}$	restrained warping induced torque acting on a beam
$\widehat{V}_y$, $\widehat{V}_z$	shear forces acting on a beam
X_1, X_2	force and moment per unit length applied at the cut of a closed section beam
N_x, N_y, N_{zy}	in-plane forces acting on a plate
M_y, M_z, M_{zy}	bending and twist moments acting on a plate
$\widehat{M}_{\omega}$	bimoment acting on a beam
$[P]$	stiffness matrix of a beam refers to the centroid
$\left[\overline{P}\right]$	stiffness matrix of a beam refers to an arbitrarily choosen point
$[W]$	compliance matrix of a beam refers to the centroid
$\left[\overline{W}\right]$	compliance matrix of a beam refers to an arbitrarily choosen point

U	strain energy
u, v, w	displacements in the x, y and z directions
w_B, w_S	displacements due to bending and shear deformations
y_c, z_c	coordinates of the centroid
ϵ_x^o	axial strain of the beam
γ_{xy}	strains of the refernce surface of a plate
$\frac{1}{\rho_y}$, $\frac{1}{\rho_z}$	curvatures of the beam
ϑ	twist per unit length
ϑ^B, ϑ^B	twist per unit length due to bending and shear deformations
Γ	second derivative of the twist of the beam
χ_y, χ_z	rotation of the cross-section of the beam in the $x-z$ and $y-z$ planes
ψ	twist of the beam (rotation of the cross-section about the x axis)
ρ	location of the "tension neutral" surface
ν	location of the "torque neutral" surface
α	parameter for estimating the error of the shear deformation
q	shear flow
C_k	constans in the Ritz method
ϕ_k	basic functions in the Ritz method
$[F]$, $\mathbf{f}$	co-effitient matrix and vector in the Ritz method
$[A_1]$, $[A_1]$, $[B_1]$, $[B_2]$, $[B_3]$	submatrices of $[F]$

List of Figures and Tables

1 Introduction

In structural modeling of beams there are two contradictory requirements: the modeling of a beam must be simple and accurate at the same time. In the literature several beam theories can be found for anisotropic thin-walled beams. Section 1 summarizes these theories, from the simplest, to the more advanced ones.

Beam models that can be found in the literature do not cover all the practical cases. The aim of this thesis is to fulfil the lack on this field.

First we develop beam models for generally anisotropic beams with open and closed cross-sections using the assumptions of classical beam theories (Section 3). (Solution that can be used for practical purposes is available only for closed section beams [16]. However Mansfield [16] neglects the local bending stiffnesses of the wall segments of the beam. Thus, his solution is not applicable for all cases.)

Then we consider orthotropic, closed section beams taking the effect of restrained warping into account (Section 5). (A beam model is available only for pure torsion of symmetric cross-section beams in the literature [20], however, Urban's solution [20] results in an unacceptable error for short beams.) Our aim is to develop a beam model which can be used for all practical cases.

In addition, our aim is to determine the accuracy and applicability of the existing beam models with the aid of numerical comparisons (Section 6).

2 Review of composite beam theories

This section summarizes the different beam theories available in the literature. However, the question remains: how accurate are these models, and under which circumstances they can be used.

The theories differ from each other in

- the allowed deformations of the beam's elements (e.g. the cross-sections remain plane and perpendicular to the axis or they may deform),
- the allowed material types and layups of the walls of the beam (e.g. orthotropic, symmetrical layup, etc.),
- the allowed geometry of the cross-section (open or closed section beams, symmetrical cross-sections, etc.),
- loading conditions (end loads or transverse loads),

- sometimes they apply additional restrictions (such as neglecting the "local" stiffnesses, see Section 2.2.4).

2.1 Constitutive equations

We consider open or closed section thin-walled beams.

The generalized stresses of a wall of the beam are the integrals of the normal and shear stresses $(\sigma_x, \sigma_y, \tau_{xy})$ along the thickness. The generalized stresses of the beam $\{N\}$ are the integral of these stresses of the walls along the circumferences. The generalized strains $\{\varepsilon\}$ are calculated from the displacements of the beam by the geometrical equations. The constitutive equations relate these stresses to the strains. It can be written as follows:

$$\{N\} = \left[\overline{P}\right] \{\varepsilon\} \tag{2.1}$$

where $\left[\overline{P}\right]$ is the stiffness matrix of the beam.

We summarize the beam-theories below according to the following two questions

- How are the generalized stresses ($\{N\}$) and strains ($\{\varepsilon\}$) are defined?
- Which elements of the stiffness matrix ($\left[\overline{P}\right]$) are non-zero?

2.2 Classical beam-theories (no restrained warping, no shear deformation)

In the following we summarize the theories where axial constraints (restrained warping) and shear deformations in bending are not taken into account.

2.2.1 Basic assumptions

1. The effect of change in geometry of the cross-section is not taken into account in the equilibrium equations.
2. The Kirchhoff-Love hypotesis is valid for each plate element.
3. The normal stresses in the contour directions is small compared to the axial stresses.
4. The strains (ϵ_x) vary linearly along the y and z axes:

$$\epsilon_x = \frac{du}{dx} - y\frac{d\chi_y}{dx} - z\frac{d\chi_z}{dx} \tag{2.2}$$

where u is the axial displacement, and the rotation of the cross-section χ_y and χ_z in the $x-y$ and $x-z$ planes can be calculated from the displacements of the axis in the y and z directions (v and w):

$$\begin{aligned} \chi_y &= \frac{dv}{dx} \\ \chi_z &= \frac{dw}{dx} \end{aligned} \tag{2.3}$$

Namely, the shear deformation caused by the transverse shear forces (V_y and V_z) are neglected.

2.2.2 Isotropic beam

A beam is isotropic when it is made of isotropic material. In the Saint Venant theory four generalized stresses are defined: normal force $\left(\widehat{N}_{\overline{x}} = \int N_\xi ds\right)$, bending moments about the y and z axes $\left(\widehat{M}_{\overline{y}} = \int (N_\xi y + M_\xi \cos\alpha)\, ds \text{ and } \widehat{M}_{\overline{z}} = \int (N_\xi z + M_\xi \sin\alpha)\, ds\right)$ and torque $\left(\widehat{T}_{\overline{x}} = -2\int M_{\xi\eta} ds\right)$.

The generalized strains are: the axial strain of the beam's axis $\left(\epsilon_x^o = \frac{\partial u}{\partial x}\right)$, curvatures of the x axis about the y and z axes $\left(\frac{1}{\rho_y} = -\frac{d\chi_y}{dx} \text{ and } \frac{1}{\rho_z} = -\frac{d\chi_z}{dx}\right)$, and the rate of the twist $\left(\vartheta = \frac{d\psi}{dx}\right)$. Because of isotropy torque loads do not cause either axial strain or curvatures. The stiffness matrix ($[\overline{P}]$) can be diagonalized by the proper choice of the coordinate system: When the origin of the coordinate system is attached to the center of gravity of the cross-section, and the axes are in the principal directions, Equation (2.1) becomes

$$\begin{Bmatrix} \widehat{N}_x \\ \widehat{M}_y \\ \widehat{M}_z \\ \widehat{T}_x \end{Bmatrix} = \begin{bmatrix} EA & & & \\ & EI_{yy} & & \\ & & EI_{zz} & \\ & & & GI_t \end{bmatrix} \begin{Bmatrix} \epsilon_x^o \\ \frac{1}{\rho_y} \\ \frac{1}{\rho_z} \\ \vartheta \end{Bmatrix} \tag{2.4}$$

Calculation of the tensile (EA) and bending stiffnesses (EI_{yy} and EI_{zz}) are similar to open and closed section beams, the torsional stiffness (GI_t) is calculated differently, for closed section beams. The torsional stiffness (Bredt-Batho formula) is significantly higher than the torsional stiffness of the equivalent open section beam.

(A simpler beam theory for isotropic beams was derived by Bernoulli and Euler. In this case the last assumption in Section 2.2.1 becomes:

1. In bending the cross-sections of the beam remain plane during the deformation.

2. In bending the cross-sections of the beam remain perpendicular to the axis.

These are the "Bernoulli-Navier" hypoteses.)

2.2.3 Orthotropic beam

A thin-walled beam is orthotropic when each wall segment is made of orthotropic laminates. (A laminate is orthotropic when the 1,6 and 2,6 terms in its stiffness matrices ($[A]$, $[B]$, $[D]$ see Appendix A) are zero [9].) The Saint Venant theory can be easily generalized for orthotropic beams. The stiffness matrix remains diagonal. Analogously to the "center of gravity" the theory defines the centroid such that a normal force acting at the centroid does not cause the curvatures of the beam's axis passing through the centroid. The calculation of the elements of the stiffness matrix and the coordinates of the centroid is straight forward [13], [4]. Formalistically we write

$$\begin{Bmatrix} \widehat{N}_x \\ \widehat{M}_y \\ \widehat{M}_z \\ \widehat{T}_x \end{Bmatrix} = \begin{bmatrix} P_{11} & & & \\ & P_{22} & & \\ & & P_{33} & \\ & & & P_{44} \end{bmatrix} \begin{Bmatrix} \epsilon_x^o \\ \frac{1}{\rho_y} \\ \frac{1}{\rho_z} \\ \vartheta \end{Bmatrix} \tag{2.5}$$

2.2.4 Generally anisotropic beam

A thin-walled beam is called "generally anisotropic" when at least one of its wall is non orthotropic. For generally anisotropic beams tension, bending and twisting modes of displacements interact, which represents a significant difference between the theory of fiber reinforced beams and of classical beams. The constitutive equations becomes

$$\begin{Bmatrix} \widehat{N}_{\overline{x}} \\ \widehat{M}_{\overline{y}} \\ \widehat{M}_{\overline{z}} \\ \widehat{T}_{\overline{x}} \end{Bmatrix} = \begin{bmatrix} \overline{P}_{11} & \overline{P}_{12} & \overline{P}_{13} & \overline{P}_{14} \\ \overline{P}_{12} & \overline{P}_{22} & \overline{P}_{23} & \overline{P}_{24} \\ \overline{P}_{13} & \overline{P}_{23} & \overline{P}_{33} & \overline{P}_{34} \\ \overline{P}_{14} & \overline{P}_{24} & \overline{P}_{34} & \overline{P}_{44} \end{bmatrix} \begin{Bmatrix} \epsilon_{\overline{x}}^o \\ \frac{1}{\rho_{\overline{y}}} \\ \frac{1}{\rho_{\overline{z}}} \\ \overline{\vartheta} \end{Bmatrix} \tag{2.6}$$

The inverse of the stiffness matrix is the compliance matrix:

$$[\overline{W}] = [\overline{P}]^{-1} \tag{2.7}$$

By the proper choice of the centroid of the coordinate system and calculation of the principle directions 3 of these elements of the compliance matrix may be zero:

$$\begin{Bmatrix} \epsilon_x^o \\ \frac{1}{\rho_y} \\ \frac{1}{\rho_z} \\ \vartheta \end{Bmatrix} = \begin{bmatrix} W_{11} & 0 & 0 & W_{14} \\ 0 & W_{22} & 0 & W_{24} \\ 0 & 0 & W_{33} & W_{34} \\ W_{14} & W_{24} & W_{34} & W_{44} \end{bmatrix} \begin{Bmatrix} \widehat{N} \\ \widehat{M}_y \\ \widehat{M}_z \\ \widehat{T}_x \end{Bmatrix} \tag{2.8}$$

Mansfield and Sobey [16] derived the compliance matrix (W) for anisotropic, *closed section* beams. The walls of the beams are made of laminated composite. In each layer there are unidirectional fibers, the direction of the fibers is optional. In additional to the above four assumption (Section 2.2.1), they state

1. The $[B]$ and $[D]$ matrices of the laminates (see Appendix A) are negligible. Accordingly they take into account only the in-plane stiffnesses of the laminate.

The flexibility matrix is completely filled, only W_{12}, W_{13}, W_{23} can be reset to zero with moving the origin to the centroid and rotating the axes to the principal axes of bending. Mansfield and Sobey gave these transformations.

2.3 Vlasov type beam theories (restrained warping, no shear deformations)

In the following we summarize the theories where the axial constraints are taken into account, however the transverse shear deformation is neglected.

2.3.1 Basic assumptions

The first three assumptions in Section 2.2.1 are valid. Instead of Assumption 4 these theories assume that the axial strain varies as follows:

$$\epsilon_x^o = \frac{du}{dx} - y\frac{d\chi_y}{dx} - z\frac{d\chi_z}{dx} - \omega\frac{d\vartheta}{dx} \tag{2.9}$$

where the calculation of χ_y and χ_z is the same as in Section 2.2.1: $\chi_y = \frac{dv}{dx}$, $\chi_z = \frac{dw}{dx}$, $\vartheta = \frac{d\psi}{dx}$ is the rate of twist, and $\omega = \int rds$ is a section property called the sectorial area.

The last term in Equation (2.9) allows to the points of the cross-section an additional axial displacement, called warping, proportional to the rate of twist [17].

2.3.2 Isotropic beam

Vlasov [21] gave a beam theory with the above assumptions for isotropic *open section* beams. If the warping is restrained, normal and shear stresses arise in the beam in addition to those of the classical theory. (If the cross-section is closed, these additional stresses decay in a short distance.) The torque consists of two parts : the Saint Venant torque and the warping induced torque:

$$\widehat{T} = \widehat{T}_{sv} + \widehat{T}_{\omega} \tag{2.10}$$

Vlasov defines an additional generalized stress $\widehat{M}_{\omega}$ (called bimoment)

$$\widehat{M}_{\omega} = \int N_{\xi}\omega ds \tag{2.11}$$

$\widehat{M}_{\omega}$ is related to the generalized strain Γ ($\Gamma = -\frac{d\vartheta}{dx}$) by the warping stiffness (EI_{ω}), and hence the stress-strain relationship becomes:

$$\begin{Bmatrix} \widehat{N}_x \\ \widehat{M}_y \\ \widehat{M}_z \\ \widehat{M}_{\omega} \\ \widehat{T}_{sv} \end{Bmatrix} = \begin{bmatrix} EA & & & & \\ & EI_{yy} & & & \\ & & EI_{zz} & & \\ & & & EI_{\omega} & \\ & & & & GI_t \end{bmatrix} \begin{Bmatrix} \epsilon_x^o \\ \frac{1}{\rho_y} \\ \frac{1}{\rho_z} \\ \Gamma \\ \vartheta \end{Bmatrix} \tag{2.12}$$

The bimoment is related to $\widehat{T}_{\omega}$ as $\widehat{T}_{\omega} = d\widehat{M}_{\omega}/dx$, which yields the well known equation of restrained warping

$$\widehat{T} = \widehat{T}_{sv} + \widehat{T}_{\omega} = GI_t\vartheta + EI_{\omega}\frac{d^2\vartheta}{dx^2} \tag{2.13}$$

2.3.3 Beams with symmetrical laminates

Bauld and Tzeng [6] improved the above theory for laminated composite beams. The cross-section is *open* and the layup is restricted to midplane symmetric fiber reinforced ones ($[B] = 0$). Because of this condition for the layup there is no coupling between tension and torsion, and the 1,5 and 5,1 elements are zero in the $\left[\overline{P}\right]$ stiffness matrix. The whole $\left[\overline{P}\right]$ matrix is filled, except $\overline{P}_{15} = \overline{P}_{51} = 0$. Hence we obtain the relationship between the strains and the stresses of the beam: the stiffness matrix:

$$\left\{ \begin{array}{c} \widehat{N_{\overline{x}}} \\ \widehat{M_{\overline{y}}} \\ \widehat{M_{\overline{z}}} \\ \widehat{M_{\overline{\omega}}} \\ \widehat{T_{\overline{sv}}} \end{array} \right\} = \left[\begin{array}{ccccc} \overline{P}_{11} & \overline{P}_{12} & \overline{P}_{13} & \overline{P}_{14} & 0 \\ \overline{P}_{21} & \overline{P}_{22} & \overline{P}_{23} & \overline{P}_{24} & \overline{P}_{25} \\ \overline{P}_{31} & \overline{P}_{32} & \overline{P}_{33} & \overline{P}_{34} & \overline{P}_{35} \\ \overline{P}_{41} & \overline{P}_{42} & \overline{P}_{43} & \overline{P}_{44} & \overline{P}_{45} \\ 0 & \overline{P}_{52} & \overline{P}_{53} & \overline{P}_{54} & \overline{P}_{55} \end{array} \right] \left\{ \begin{array}{c} \epsilon^o_{\overline{x}} \\ \frac{1}{\rho_{\overline{y}}} \\ \frac{1}{\rho_{\overline{z}}} \\ \overline{\Gamma} \\ \overline{\vartheta} \end{array} \right\} \tag{2.14}$$

2.4 Timoshenko type beam theories (shear deformation, no restrained warping)

In the following we summarize the theories where the axial constraints are neglected, however the transverse shear deformation is taken into account.

2.4.1 Basic assumption

The first three assumptions in Section 2.2.1 is valid. The form of the axial strain is identical to Assumption 4:

$$\epsilon^o_x = \frac{du}{dx} - y\frac{d\chi_y}{dx} - z\frac{d\chi_z}{dx} \tag{2.15}$$

however in this expression χ_y and χ_z are defined as

$$\begin{aligned} \chi_y &= \frac{dv}{dx} - \gamma_y \\ \chi_z &= \frac{dw}{dx} - \gamma_z \end{aligned} \tag{2.16}$$

where γ_y and γ_z are the shear strain in the $x-y$ and $x-z$ planes, respectively. The shear strain is supposed to be constant in the cross-section which is referred to as the first order shear theory.

2.4.2 Isotropic beam

The effect of the shear deformation is included in this theory. Hence the transverse forces and the shear strains are included in the compatibility equations (Equation 2.17). These are related to

each other through the shear stiffnesses [19]. For isotropic case no coupling effects exist.

$$\begin{Bmatrix} \widehat{N}_x \\ \widehat{M}_y \\ \widehat{M}_z \\ \widehat{V}_y \\ \widehat{V}_z \\ \widehat{T}_{sv} \end{Bmatrix} = \begin{bmatrix} EA & & & & & \\ & EI_{yy} & & & & \\ & & EI_{zz} & & & \\ & & & S_y & & \\ & & & & S_z & \\ & & & & & GI_t \end{bmatrix} \begin{Bmatrix} \epsilon_x^o \\ \frac{1}{\rho_y} \\ \frac{1}{\rho_z} \\ \gamma_y \\ \gamma_z \\ \vartheta \end{Bmatrix} \tag{2.17}$$

2.4.3 Generally anisotropic beam

Bank [2], [3] investigated the combined bending and transverse loading of anisotropic, open section beams (torsional and axial loads are not considered). He claims that their model can be used for hand calculation preliminary design studies only. The geometry of the cross-section is restricted to open, singly and doubly symmetrical ones. From $\widehat{M}_z$ and $\widehat{V}_y$ he determines $\epsilon_x^o, 1/\rho_y, 1/\rho_z$ and ϑ for the layers, and gives an average value of these strains for the beam. The stiffness matrix is not presented.

2.5 Theories taking into account restrained warping and shear deformations

2.5.1 Basic assumption

This model uses Assumptions 1 to 3 in Section 2.2.1, and for the axial strain the following assumption:

$$\epsilon_x^o = \frac{du}{dx} - y\frac{d\chi_y}{dx} - z\frac{d\chi_z}{dx} - \omega\frac{d\vartheta}{dx} \tag{2.18}$$

where

$$\begin{aligned} \chi_y &= \frac{dv}{dx} - \gamma_y \\ \chi_z &= \frac{dw}{dx} - \gamma_z \\ \vartheta &= \frac{d\psi}{dx} \end{aligned} \tag{2.19}$$

Hence the effect of warping and shear deformations are included, however warping induced shear is not included. The theory assumes no coupling between normal and shearing effects.

2.5.2 Isotropic and orthotropic beam

Barbero [4], [5] gives the compatibility equations also for *open* and *closed* cross-section. The vectors of the generalized stresses and strains are the sum of these stresses and strains in Section 2.3 and Section 2.4. The non diagonal elements of the stiffness matrix are zero because of orthotropy, and

because of the proper choice of the coordinate system (centroid, shear center, principal axes) and because the coupling between the normal and shearing effects is neglected. Hence the stress-strain relationship is as follows

$$\begin{Bmatrix} \widehat{N}_x \\ \widehat{M}_y \\ \widehat{M}_z \\ \widehat{V}_y \\ \widehat{V}_z \\ \widehat{M}_\omega \\ \widehat{T}_{sv} \end{Bmatrix} = \begin{bmatrix} EA & & & & & & \\ & EI_{yy} & & & & & \\ & & EI_{zz} & & & & \\ & & & S_y & & & \\ & & & & S_z & & \\ & & & & & EI_\omega & \\ & & & & & & GI_t \end{bmatrix} \begin{Bmatrix} \epsilon_x^o \\ \frac{1}{\rho_y} \\ \frac{1}{\rho_z} \\ \gamma_y \\ \gamma_z \\ \Gamma \\ \vartheta \end{Bmatrix} \tag{2.20}$$

2.5.3 Symmetrical beam

Kabir and Sherbourne [10] improved the beam theory of Bauld and Tzeng [6]. The transverse shear deformation of the beam cross-section is included in the expression of the stiffness matrix (see Equation 2.21).

$$\begin{Bmatrix} \widehat{N}_x \\ \widehat{M}_y \\ \widehat{M}_z \\ \widehat{M}_\omega \\ \widehat{T}_{sv} \\ -\widehat{F}_y \\ \widehat{F}_z \\ \widehat{V}_y \\ \widehat{V}_z \end{Bmatrix} = \begin{bmatrix} P_{11} & & & & & & & P_{18} & P_{19} \\ & P_{22} & & & P_{25} & P_{26} & & & \\ & & P_{33} & & P_{35} & & P_{37} & & \\ & & & P_{44} & P_{45} & & & & \\ & P_{52} & P_{53} & P_{54} & P_{55} & P_{56} & P_{57} & & \\ & P_{62} & & & P_{65} & P_{66} & & & \\ & & P_{73} & & P_{75} & & P_{77} & & \\ P_{81} & & & & & & & P_{88} & \\ P_{91} & & & & & & & & P_{99} \end{bmatrix} \begin{Bmatrix} \epsilon_x^o \\ \frac{1}{\rho_y} \\ \frac{1}{\rho_z} \\ \Gamma \\ \vartheta \\ \gamma_z' \\ \gamma_y' \\ \gamma_y \\ \gamma_z \end{Bmatrix} \tag{2.21}$$

The theory is valid for *open section* beams with symmetrical laminates.

2.6 Theories taking into account restrained warping, shear deformations and warping induced shear

2.6.1 Basic assumption

The first three assumptions in Section 2.2.1 is valid. The form of the axial strain is identical to that of in Section 2.5.1:

$$\epsilon_x^o = \frac{du}{dx} - y\frac{d\chi_y}{dx} - z\frac{d\chi_z}{dx} - \omega\frac{d\vartheta_B}{dx} \tag{2.22}$$

where

$$\begin{aligned} \chi_y &= \frac{dv}{dx} - \gamma_y \\ \chi_z &= \frac{dw}{dx} - \gamma_z \end{aligned} \tag{2.23}$$

however in this expression ϑ_B is defined as

$$\vartheta_B = \frac{d\psi}{dx} - \vartheta_S \tag{2.24}$$

The warping is assumed to be proportional to the first derivative of the restrained warping induced twist. Couplings between normal and shearing effects are neglected.

2.6.2 Isotropic and orthotropic beam

Kollár [12] investigated transversely loaded, *open section*, orthotropic beams. The normal stresses induced by the restrained warping result additional shear stresses. These stresses cause an additional twist of the beam, and hence the warping is not proportional to the first derivative of the twist. The twist has two parts: one from bending (which causes warping, like in the previous section) and an other part from the restrained warping induced shear stress:

$$\vartheta = \vartheta_B + \vartheta_S \tag{2.25}$$

Γ is defined as $\Gamma = -\frac{d\vartheta_B}{dx}$. The constitutive equations according Kollár:

$$\begin{Bmatrix} \widehat{M}_{\overline{y}} \\ \widehat{M}_{\overline{z}} \\ \widehat{M}_{\overline{\omega}} \\ \widehat{T}_{\overline{sv}} \\ \widehat{V}_{\overline{y}} \\ \widehat{V}_{\overline{z}} \\ \widehat{T}_{\overline{\omega}} \end{Bmatrix} = \begin{bmatrix} \overline{EI}_{yy} & \overline{EI}_{yz} & & & & & \\ \overline{EI}_{yz} & \overline{EI}_{zz} & & & & & \\ & & \overline{EI}_{\omega} & & & & \\ & & & \overline{GI}_t & & & \\ & & & & \overline{S}_{yy} & \overline{S}_{yz} & \overline{S}_{y\omega} \\ & & & & \overline{S}_{yz} & \overline{S}_{zz} & \overline{S}_{z\omega} \\ & & & & \overline{S}_{y\omega} & \overline{S}_{z\omega} & \overline{S}_{\omega\omega} \end{bmatrix} \begin{Bmatrix} \frac{1}{\rho_{\overline{y}}} \\ \frac{1}{\rho_{\overline{z}}} \\ \overline{\Gamma} \\ \overline{\vartheta} \\ \gamma_{\overline{y}} \\ \gamma_{\overline{z}} \\ \overline{\vartheta}_s \end{Bmatrix} \tag{2.26}$$

Roberts and Ubaidi [18] proposed take into account the shear deformation in torsion by the calculation of the warping stiffness for *open section,* orthotropic beams.

Urban [20] and Kristek [7] investigated the torsion of doubly symmetrical, *closed section,* isotropic beams. Using his basic equations we can derive the same equations as for open section beams (Section 2.6.2). The stiffnesses in the expression of the constitutive equations differ from those of the open sections.

$$\begin{Bmatrix} \widehat{M}_{\omega} \\ \widehat{T}_{sv} \\ \widehat{T}_{\omega} \end{Bmatrix} = \begin{bmatrix} EI_{\omega} & & \\ & GI_t & \\ & & S_{\omega\omega} \end{bmatrix} \begin{Bmatrix} \Gamma \\ \vartheta \\ \vartheta_s \end{Bmatrix} \tag{2.27}$$

In additional to the assumptions of [12], they state

1. The shear flow distribution is constant along the cross-section.

   Their results together with other more general approaches will be discussed in Section 5.1.

2.6.3 Generally anisotropic beam

Wu and Sun [23] use the same generalized strains as Kollár [12]. A differential equation system is stated for the problem. There is no restriction for the layers of the plates consisting the beam. The cross-section can be either *open* or *closed*. The stiffness matrix is not expressed, and the solution becomes very complicated.

2.7 Generalized beam theories

2.7.1 Isotropic and orthotropic beam

In the Timoshenko type beam theories (first order shear theories, Section 2.4) the distribution of the shear strain across the cross-section is uniform. There are higher order shear theories with more general assumptions for the distribution of the shear strain.

The Vlasov type beam theories (Section 2.3) allows the cross-section to warp according to a determined function. In Bachau theory no assumption is made on axial displacement distribution. In this beam theory a set of orthonormal eigenwarpings ($\omega_i(s)$) is derived. With these the axial strain (ϵ_x^o) of the classical theories (including shear deformations or not) can be improved:

$$\epsilon_x^o = \epsilon_{xb}^o + \sum W_i(s) \times F_i'(x) \tag{2.28}$$

where $F_i(x)$ and $W_i(s)$ are unknown functions of x and s, which can be determined by minimizing the potential energy.

2.8 Transversely loaded beams

2.8.1 Classical beam-theories (no restrained warping, no shear deformation)

From the transverse loads we can calculate the resultant normal force and the bending moments, and with these force and moments we can examine the beam similarly to the analysis discussed in the previous section. To calculate the resultant torque resulting from the transverse loads we have to introduce the notion of the shear center, about which the torque due to a shear force have to be measured.

For isotropic beams the definition of the shear center is as follows: transverse forces acting at the shear center do not cause twist. The shear flow and hence the location of the shear center are different for open and for closed cross-section beams.

For orthotropic beams the definition of the shear center and the procedure of calculating its location are the same as for isotropic beams. Barbero [5] gives the expressions of coordinates of the shear center's for *open* and *closed section* beams.

For generally anisotropic beams the twist is induced not only by the torque but also by the bending moments. Consequently, the transverse forces acting at any point of the cross-section the beam may twist. Mansfield and Sobey [16] gave the definition of the shear center for anisotropic, *closed section* beams: the shear center is at the point where the twist is solely due to the resultant bending moments. Mansfield and Sobey gave the expression of the location of the shear center for closed cross-sections. Because of the complexity of this expression a simpler approximation is also given.

2.8.2 Theories taking into account restrained warping induced shear (restrained warping, shear deformation)

When warping induced shear is taken into account, even for orthotropic beams, as a rule, the cross-section of the beam will rotate. In this case there is no location for the external transverse loads, for which, the rotation of the beam is zero. For orthotropic, *open section* beams Kollár [12] defined two specified points on the cross-section: the shear deformation shear center (when the shear forces are applied at that point, there is no shear induced twist) and the bending deformation shear center (when the shear forces are applied at that point, there is no bending induced twist).

3 Theory of open and closed section, generally anisotropic thin-walled beams - no restrained warping

In this section we will derive the stiffness matrix of thin walled open or closed section composite beams [24] (see $\boxed{P}$ in Section 2.2.4 (Equation 2.6)). There is no restriction on the layup of the wall segments and the local bending stiffnesses are taken into account. We will neglect the effects of restrained warping and shear deformation. (The effect of this approximation will be investigated in Section 6.)

3.1 Problem statement

We consider thin-walled open and closed section prismatic beams. The walls of the beams may consist of a single layer or of several layers, each layer may be made of composite materials. The beam's wall consists of flat segments (Figure 1) designated by the subscript k ($k = 1, 2, \ldots, K$, where K is the total number of wall segments). The cross-section may be symmetrical or unsymmetrical and the layup of the beam is arbitrary (i.e. the layers are not necessarily orthotropic or symmetrical).

The beam is subjected to an axial force $\widehat{N}$, bending moments $\widehat{M}_y$, $\widehat{M}_z$, and torque $\widehat{T}$ acting at the centroid (the centroid is defined such that the force $\widehat{N}$ does not result in the curvatures of the axis of the beam).

We employ the following coordinate systems (Figure 2).

For the beam we use the x-y-z coordinate system with the origin at the centroid and the $\overline{x}$-$\overline{y}$-$\overline{z}$ coordinate system with the origin at an arbitrarily chosen point. For the k-th segment we employ the ξ_k-η_k-ζ_k coordinate system with the origin at the center of the reference plane of the k-th segment. ξ is parallel to the x coordinate, η is along the circumference of the wall, and ζ is perpendicular to the circumference.

The displacements of the longitudinal axis, passing through the centroid, are u, v, w, ψ (Figure 3), where u is the axial displacement, v and w are the transverse displacements in the y and z directions, and ψ is the rotation of the cross-section (twist).

The relationships between these displacements, and the axial strain ϵ_x^o and the curvatures $1/\rho_y$, $1/\rho_z$ of the x axis, and the rate of twist ϑ are

$$\frac{\partial u}{\partial x} = \epsilon_x^o \qquad \frac{\partial^2 v}{\partial x^2} = -\frac{1}{\rho_z} \qquad \frac{\partial^2 w}{\partial x^2} = -\frac{1}{\rho_y} \qquad \frac{\partial \psi}{\partial x} = \vartheta \tag{3.1}$$

In the $\overline{x}$-$\overline{y}$-$\overline{z}$ coordinate system these relationships become

$$\frac{\partial \overline{u}}{\partial \overline{x}} = \epsilon_{\overline{x}}^o \qquad \frac{\partial^2 \overline{v}}{\partial \overline{x}^2} = -\frac{1}{\rho_{\overline{z}}} \qquad \frac{\partial^2 \overline{w}}{\partial \overline{x}^2} = -\frac{1}{\rho_{\overline{y}}} \qquad \frac{\partial \overline{\psi}}{\partial \overline{x}} = \overline{\vartheta} \tag{3.2}$$

where $\epsilon_{\overline{x}}^o$, $1/\rho_{\overline{y}}$, $1/\rho_{\overline{z}}$, are the axial strain and the curvatures of the longitudinal axis passing through the origin of the $\overline{x}$-$\overline{y}$-$\overline{z}$ coordinate system. $\overline{u}$, $\overline{v}$, $\overline{w}$, and $\overline{\psi}$ are the displacements of the $\overline{x}$ axis.

The cross-sections of beams with arbitrary layup do not remain plane and the Bernoulli-Navier hypothesis is inapplicable. Nonetheless, in a long body subjected to the loads given in Figure 1, such as a beam, the strains may be considered to be constant in the axial direction, and the plane-strain condition (the stresses and strains vary only in planes perpendicular to the x axis) may be applied in the analysis [15].

3.2 Open section beams

The analysis of thin-walled open section beams is performed in four steps.

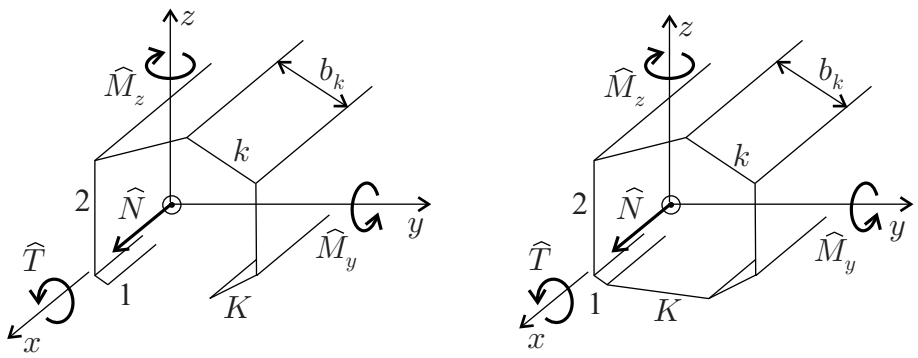

Figure 1: Forces in open and closed section thin-walled beams with flat wall segments

1. The strains in each wall segment are related to the axial strain, curvatures and twist of the beam's axis.

2. The forces in each wall segment are determined from the strains in the wall segment.

3. The resultant axial force, moments, and torque acting at the axis of the beam are determined from the wall segment forces.

4. The stiffness matrix is established by relating the resultant axial force, moments, and torque to the axial strain, curvatures and twist of the beam's axis.

3.2.1 Step 1. Strains in the wall segments

At a point on the reference plane of each *wall segment* the axial strain is calculated by the plane strain condition

$$\epsilon^o_{\xi k} = \epsilon^o_{\overline{x}} + \overline{z}\frac{1}{\rho_{\overline{y}}} + \overline{y}\frac{1}{\rho_{\overline{z}}} \tag{3.3}$$

where $\overline{z}$ and $\overline{y}$ are the coordinates of an arbitrary point on the k-th segment's reference surface and $\epsilon^o_{\xi k}$ is the axial strain at this point.

The strains of the axis of the k-th wall segment can be expressed as

$$\begin{Bmatrix} \epsilon^w_k \\ \kappa^w_{\xi k} \\ \kappa^w_{mk} \\ \vartheta^w_k \end{Bmatrix} = \underbrace{\begin{bmatrix} 1 & \overline{z}_k & \overline{y}_k & 0 \\ 0 & \cos\alpha_k & -\sin\alpha_k & 0 \\ 0 & \sin\alpha_k & \cos\alpha_k & 0 \\ 0 & 0 & 0 & 1 \end{bmatrix}}_{[R_k]} \begin{Bmatrix} \epsilon^o_{\overline{x}} \\ \frac{1}{\rho_{\overline{y}}} \\ \frac{1}{\rho_{\overline{z}}} \\ \overline{\vartheta} \end{Bmatrix} \tag{3.4}$$

where $\overline{y}_k$ and $\overline{z}_k$ are the coordinates of the ξ_k-η_k-ζ_k coordinate system's origin, which is at the midpoint of the reference plane (Figure 2), and α_k is the angle between the η_k and $\overline{y}$ coordinate axes. The superscript w refers to the segment's longitudinal axis which passes through the midpoint of the reference plane ($\eta = 0, \zeta = 0$). The first of these equations is written by virtue of Equation

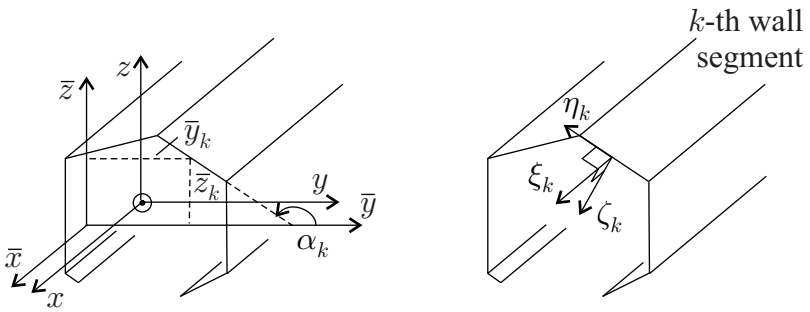

Figure 2: Coordinate systems employed in the analysis of thin-walled beams with arbitrary layup

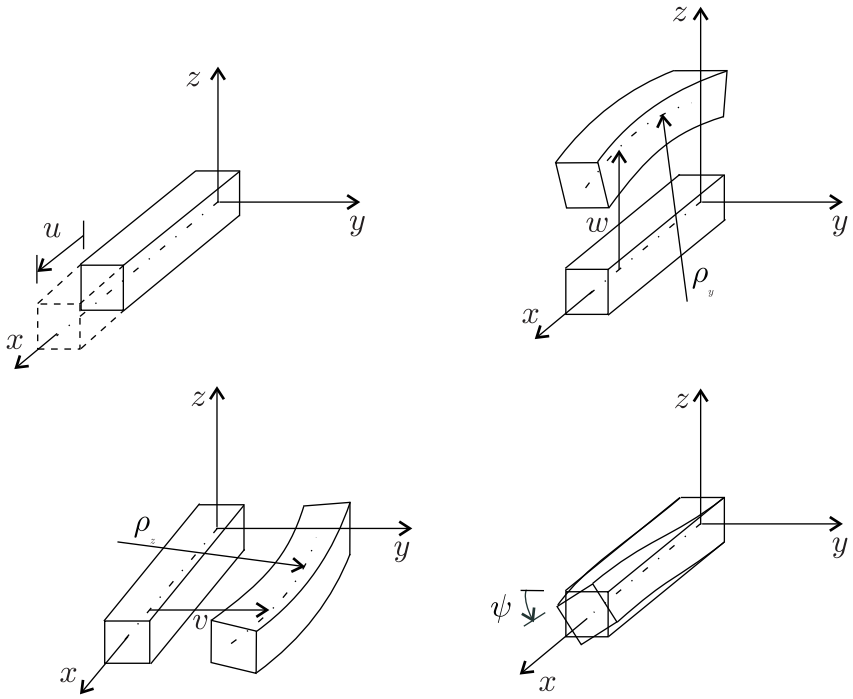

Figure 3: Displacements of a beam

(3.3). $\kappa^w_{\xi k}$ and κ^w_{mk} are the curvatures of the k-th wall segment's axis in the ξ-ζ and η-ξ planes, respectively (Figure 4). The last equation ($\vartheta^w_k = \overline{\vartheta}$) is written by observing that the twist of every point in the wall segment is equal to the twist of the beam.

The axial strain in the k-th segment varies linearly with η (see Equation 3.3) and we can write

$$\epsilon^o_{\xi k} = \epsilon^w_k + \eta \kappa^w_{mk} \tag{3.5}$$

The curvature $\kappa_{\xi k}$ is uniform in each flat segment

$$\kappa_{\xi k} = \frac{1}{\rho_{\overline{y}}} \cos\alpha_k - \frac{1}{\rho_{\overline{z}}} \sin\alpha_k \tag{3.6}$$

The ratio of twist can be written as

$$\vartheta = \frac{\partial \psi}{\partial x} = \frac{\partial \frac{\partial w^0}{\partial y}}{\partial x} = \frac{\partial^2 w^0}{\partial x \partial y} \tag{3.7}$$

which, by using the definition of $\kappa_{\xi\eta}$ ($\kappa_{\xi\eta} = -2\frac{\partial^2 w}{\partial x \partial y}$) can be written as

$$\vartheta = -\frac{1}{2}\kappa_{\xi\eta} \tag{3.8}$$

hence we have $\kappa_{\xi k} = \kappa^w_{\xi k}$ and $\kappa_{\xi\eta k} = -2\vartheta^w_k = -2\overline{\vartheta}$. These relationships together with Equation (3.5) may be written in matrix form as

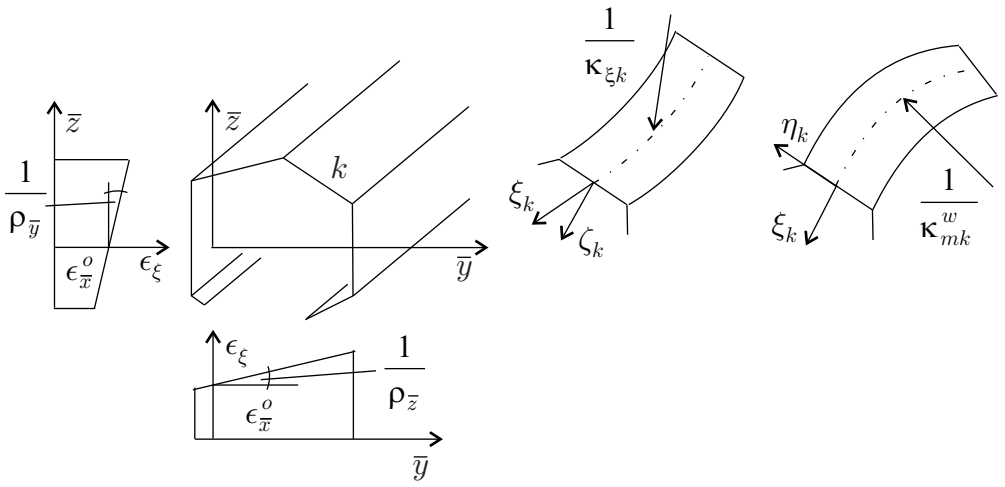

Figure 4: Deformations of an open section thin-walled beam

$$\left\{\begin{array}{c}\epsilon^o_{\xi k}\\ \kappa_{\xi k}\\ \kappa_{\xi\eta k}\end{array}\right\} = \left\{\begin{array}{c}\epsilon^o_{\xi}\\ \kappa_{\xi}\\ \kappa_{\xi\eta}\end{array}\right\}_k = \underbrace{\left[\begin{array}{cccc}1&0&\eta&0\\0&1&0&0\\0&0&0&-2\end{array}\right]}_{[R_\eta]} \left\{\begin{array}{c}\epsilon^w_k\\ \kappa^w_{\xi k}\\ \kappa^w_{mk}\\ \vartheta^w_k\end{array}\right\} \tag{3.9}$$

3.2.2 Step 2. Forces and moments in the wall segments

The strain-force relationship in each wall segment is given by:

$$\left\{\begin{array}{c}\epsilon^o_{\xi}\\ \epsilon^o_{\eta}\\ \gamma^0_{\xi\eta}\\ \kappa_{\xi}\\ \kappa_{\eta}\\ \kappa_{\xi\eta}\end{array}\right\}_k = \left[\begin{array}{cccccc}\alpha_{11}&\alpha_{12}&\alpha_{16}&\beta_{11}&\beta_{12}&\beta_{16}\\ \alpha_{12}&\alpha_{22}&\alpha_{26}&\beta_{21}&\beta_{22}&\beta_{26}\\ \alpha_{16}&\alpha_{26}&\alpha_{66}&\beta_{61}&\beta_{62}&\beta_{66}\\ \beta_{11}&\beta_{21}&\beta_{61}&\delta_{11}&\delta_{12}&\delta_{16}\\ \beta_{12}&\beta_{22}&\beta_{62}&\delta_{12}&\delta_{22}&\delta_{26}\\ \beta_{16}&\beta_{26}&\beta_{66}&\delta_{16}&\delta_{26}&\delta_{66}\end{array}\right]_k \left\{\begin{array}{c}N_\xi\\ N_\eta\\ N_{\xi\eta}\\ M_\xi\\ M_\eta\\ M_{\xi\eta}\end{array}\right\}_k \tag{3.10}$$

where the $[\alpha]$, $[\beta]$, $[\delta]$ matrices are the inverse of the $[A]$, $[B]$, $[D]$ matrices of the wall segment [9]

$$\left[\begin{array}{cc}[\alpha]&[\beta]\\ [\beta]^T&[\delta]\end{array}\right] = \left[\begin{array}{cc}[A]&[B]\\ [B]^T&[D]\end{array}\right]^{-1} \tag{3.11}$$

$N_\eta, N_{\xi\eta}, M_\eta$ are zero along the free longitudinal edges (see Figure 5) and, consequently, are approximately zero everywhere ($N_\eta = N_{\xi\eta} = M_\eta = 0$).

With these approximations the strain-force relationships for the k-th wall segment become (see Equation 3.10)

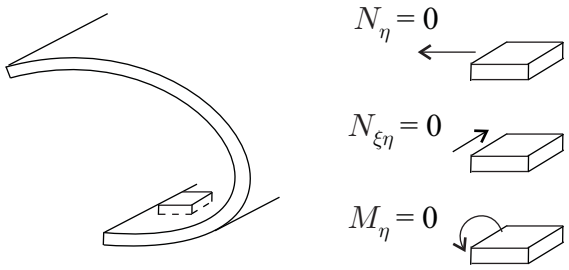

Figure 5: The forces and moments along the longitudinal edge of an open section thin-walled beam

$$\left\{ \begin{array}{c} \epsilon_\xi^o \\ \kappa_\xi \\ \kappa_{\xi\eta} \end{array} \right\}_k = \underbrace{\left[\begin{array}{ccc} \alpha_{11} & \beta_{11} & \beta_{16} \\ \beta_{11} & \delta_{11} & \delta_{16} \\ \beta_{16} & \delta_{16} & \delta_{66} \end{array} \right]_k}_{[\widetilde{\mu}_k]} \left\{ \begin{array}{c} N_\xi \\ M_\xi \\ M_{\xi\eta} \end{array} \right\}_k = [\widetilde{\mu}_k] \left\{ \begin{array}{c} N_\xi \\ M_\xi \\ M_{\xi\eta} \end{array} \right\}_k \tag{3.12}$$

We introduce the following stress resultants in the segment's ξ_k-η_k-ζ_k coordinate system (Figure 6, left)

$$\widehat{N}_{\xi k}^w = \int\limits_{(b_k)} N_{\xi k} d\eta = b_k N_{\xi k, \text{ at } \eta=0} \tag{3.13}$$

$$\widehat{M}_{\xi k}^w = \int\limits_{(b_k)} M_{\xi k} d\eta = b_k M_{\xi k, \text{ at } \eta=0} \tag{3.14}$$

$$\widehat{M}_{mk}^w = \int\limits_{(b_k)} N_{\xi k} \eta d\eta \tag{3.15}$$

b_k is the width of the wall segment (Figure 1). The torque is [5]

$$\widehat{T}_{\xi k}^w = -2 \int\limits_{(b_k)} M_{\xi\eta k} d\eta = -2 b_k M_{\xi\eta k, \text{ at } \eta=0} \tag{3.16}$$

Note that $\widehat{N}^w$, $\widehat{M}^w$, and $\widehat{T}^w$ represent forces and moments, and the superscript w refers to the wall segment. The same symbols without hat represent forces and moments per unit length.

The second equalities in Equations (3.13), (3.14) and (3.16) are written by observing that in each segment $\left\{\epsilon_\xi^o, \kappa_\xi, \kappa_{\xi\eta}\right\}$ varies linearly along the width (η direction, see Equation 3.9), and, consequently, N_ξ, M_ξ, $M_{\xi\eta}$ also vary linearly along the width (see Equation 3.12). Equations (3.13), (3.14), (3.16), (3.12), and (3.9) result in

$$\left\{ \begin{array}{c} \epsilon_k^w \\ \kappa_{\xi k}^w \\ \vartheta_k^w \end{array} \right\} = \frac{1}{b_k} \left[\begin{array}{ccc} \alpha_{11} & \beta_{11} & -\frac{1}{2}\beta_{16} \\ \beta_{11} & \delta_{11} & -\frac{1}{2}\delta_{16} \\ -\frac{1}{2}\beta_{16} & -\frac{1}{2}\delta_{16} & \frac{1}{4}\delta_{66} \end{array} \right] \left\{ \begin{array}{c} \widehat{N}_{\xi k}^w \\ \widehat{M}_{\xi k}^w \\ \widehat{T}_{\xi k}^w \end{array} \right\} \tag{3.17}$$

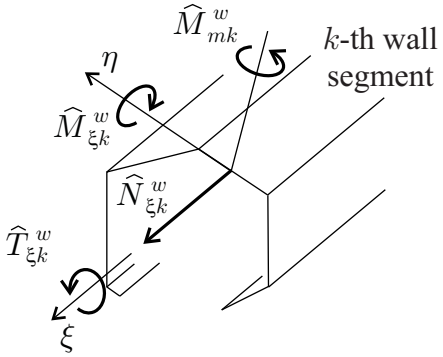

Figure 6: The force resultants in the k-th wall segment

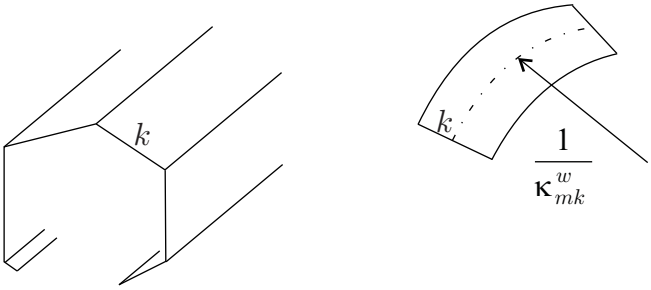

Figure 7: Curvature κ^{w}_{mk} of the wall segment

To evaluate the integral in Equation (3.15) we consider only the curvature κ^{w}_{mk} of the segment, and assume that the flat segment remains flat ($\kappa_{\xi} = 0$, $\kappa_{\xi\eta} = 0$, Figure 7).

With this approximation the inverse of Equation (3.12) yields

$$\left\{ \begin{array}{c} N_{\xi} \\ M_{\xi} \\ M_{\xi\eta} \end{array} \right\}_k = \left[\begin{array}{ccc} \widetilde{A}_{11} & \widetilde{A}_{12} & \widetilde{A}_{13} \\ \widetilde{A}_{12} & \widetilde{A}_{22} & \widetilde{A}_{23} \\ \widetilde{A}_{13} & \widetilde{A}_{23} & \widetilde{A}_{33} \end{array} \right]_k \left\{ \begin{array}{c} \epsilon^{o}_{\xi k} \\ 0 \\ 0 \end{array} \right\} \tag{3.18}$$

The matrix $\left[\widetilde{A}\right]$ is defined as

$$\left[\begin{array}{ccc} \widetilde{A}_{11} & \widetilde{A}_{12} & \widetilde{A}_{13} \\ \widetilde{A}_{12} & \widetilde{A}_{22} & \widetilde{A}_{23} \\ \widetilde{A}_{13} & \widetilde{A}_{23} & \widetilde{A}_{33} \end{array} \right]_k = \left[\begin{array}{ccc} \alpha_{11} & \alpha_{12} & \alpha_{16} \\ \alpha_{12} & \alpha_{22} & \alpha_{26} \\ \alpha_{16} & \alpha_{26} & \alpha_{66} \end{array} \right]^{-1}_k \tag{3.19}$$

With this definition $N_{\xi k}$ is $N_{\xi k} = \left(\widetilde{A}_{11}\right)_k \epsilon^{o}_{\xi k}$. By substituting this expression and Equation (3.5) into Equation (3.15) and by performing the integration, we obtain

$$\widehat{M}^{w}_{mk} = \frac{\left(\widetilde{A}_{11}\right)_k b_k^3}{12} \kappa^{w}_{mk} \tag{3.20}$$

Equations (3.17) and (3.20) give the following strain-force relationship in the ξ_k-η_k-ζ_k coordinate system

$$\left\{\begin{array}{c}\epsilon_k^w\\ \kappa_{\xi k}^w\\ \kappa_{mk}^w\\ \vartheta_k^w\end{array}\right\} = \underbrace{\frac{1}{b_k}\left[\begin{array}{cccc}\alpha_{11} & \beta_{11} & 0 & -\frac{1}{2}\beta_{16}\\ \beta_{11} & \delta_{11} & 0 & -\frac{1}{2}\delta_{16}\\ 0 & 0 & \frac{12}{\left(A_{11}\right)_k b_k^2} & 0\\ -\frac{1}{2}\beta_{16} & -\frac{1}{2}\delta_{16} & 0 & \frac{1}{4}\delta_{66}\end{array}\right]}_{[\omega_k]} \left\{\begin{array}{c}\widehat{N}_{\xi k}^w\\ \widehat{M}_{\xi k}^w\\ \widehat{M}_{mk}^w\\ \widehat{T}_{\xi k}^w\end{array}\right\} \tag{3.21}$$

3.2.3 Step 3. Forces in the beam

In the bar coordinate system ($\overline{x}$-$\overline{y}$-$\overline{z}$) the forces in the beam are the sum of the forces in the wall segments (Figures 6 and 2)

$$\left\{\begin{array}{c}\widehat{N}_{\overline{x}}\\ \widehat{M}_{\overline{y}}\\ \widehat{M}_{\overline{z}}\\ \widehat{T}_{\overline{x}}\end{array}\right\} = \sum_{k=1}^{K} \underbrace{\left[\begin{array}{cccc}1 & 0 & 0 & 0\\ \overline{z}_k & \cos\alpha_k & \sin\alpha_k & 0\\ \overline{y}_k & -\sin\alpha_k & \cos\alpha_k & 0\\ 0 & 0 & 0 & 1\end{array}\right]}_{[R_k]^T} \left\{\begin{array}{c}\widehat{N}_{\xi k}^w\\ \widehat{M}_{\xi k}^w\\ \widehat{M}_{mk}^w\\ \widehat{T}_{\xi k}^w\end{array}\right\} \tag{3.22}$$

We note that $[R_k]^T$ is the transpose of the matrix $[R_k]$ (see Equation 3.4).

3.2.4 Step 4. Stiffness matrix

Equations (3.22), (3.21), and (3.4) yield

$$\left\{\begin{array}{c}\widehat{N}_{\overline{x}}\\ \widehat{M}_{\overline{y}}\\ \widehat{M}_{\overline{z}}\\ \widehat{T}_{\overline{x}}\end{array}\right\} = \sum_{k=1}^{K} [R_k]^T \left\{\begin{array}{c}\widehat{N}_{\xi k}^w\\ \widehat{M}_{\xi k}^w\\ \widehat{M}_{mk}^w\\ \widehat{T}_{\xi k}^w\end{array}\right\} = \sum_{k=1}^{K} [R_k]^T [\omega_k]^{-1} \left\{\begin{array}{c}\epsilon_k^w\\ \kappa_{\xi k}^w\\ \kappa_{mk}^w\\ \vartheta_k^w\end{array}\right\} = \tag{3.23}$$

$$= \underbrace{\sum_{k=1}^{K} \left([R_k]^T [\omega_k]^{-1} [R_k]\right)}_{[\overline{P}]} \left\{\begin{array}{c}\epsilon_{\overline{x}}^o\\ \frac{1}{\rho_{\overline{y}}}\\ \frac{1}{\rho_{\overline{z}}}\\ \overline{\vartheta}\end{array}\right\} \tag{3.24}$$

$[\overline{P}]$ is the stiffness matrix in the bar coordinate system (Table 1).

The displacements must be determined by solving the governing equations (i.e. the equilibrium equations, the strain displacement relationships (Equation 3.1), and the constitutive equations (Equation 2.6)) for the beam under consideration. These equations are given in the x, y, z coordinate system. Hence the stiffness (and compliance) matrices must also be expressed in this

Open section beam:

$$\left[\overline{P}\right] = \sum_{k=1}^{K} \left[R_k\right]^T \left[\omega_k\right]^{-1} \left[R_k\right]$$

Closed section beam:

$$\left[\overline{P}\right] = \sum_{k=1}^{K} \left(\left[R_k\right]^T \left[\omega_k\right]^{-1} \left[R_k\right]\right) + \left[L\right]^T \left[F\right]^{-1} \left[L\right]$$

$$\left[\overline{W}\right] = \left[\overline{P}\right]^{-1}$$

$$\left[R_k\right] = \begin{bmatrix} 1 & \overline{z}_k & \overline{y}_k & 0 \\ 0 & \cos\alpha_k & -\sin\alpha_k & 0 \\ 0 & \sin\alpha_k & \cos\alpha_k & 0 \\ 0 & 0 & 0 & 1 \end{bmatrix} \qquad \begin{bmatrix} \widetilde{A}_{11} & \widetilde{A}_{12} & \widetilde{A}_{13} \\ \widetilde{A}_{12} & \widetilde{A}_{22} & \widetilde{A}_{23} \\ \widetilde{A}_{13} & \widetilde{A}_{23} & \widetilde{A}_{33} \end{bmatrix}_k = \begin{bmatrix} \alpha_{11} & \beta_{11} & \beta_{16} \\ \beta_{11} & \delta_{11} & \delta_{16} \\ \beta_{16} & \delta_{16} & \delta_{66} \end{bmatrix}_k^{-1}$$

$$\left[\omega_k\right] = \frac{1}{b_k} \begin{bmatrix} \alpha_{11} & \beta_{11} & 0 & -\frac{1}{2}\beta_{16} \\ \beta_{11} & \delta_{11} & 0 & -\frac{1}{2}\delta_{16} \\ 0 & 0 & \frac{12}{\left(\widetilde{A}_{11}\right)_k b_k^2} & 0 \\ -\frac{1}{2}\beta_{16} & -\frac{1}{2}\delta_{16} & 0 & \frac{1}{4}\delta_{66} \end{bmatrix}$$

$$\left[L\right] = \begin{bmatrix} 0 & 0 & 0 & 2A \\ 0 & 0 & 0 & 0 \end{bmatrix} - \left[I\right] \qquad \left[I\right] = \sum_{k=1}^{K} \begin{bmatrix} \alpha_{16} & \beta_{61} & 0 & -\frac{1}{2}\beta_{66} \\ \beta_{12} & \delta_{12} & 0 & -\frac{1}{2}\delta_{26} \end{bmatrix}_k \left[\omega_k\right]^{-1} \left[R_k\right]$$

$$\left[F\right] = \sum_{k=1}^{K} \left(b_k \begin{bmatrix} \alpha_{66} & \beta_{62} \\ \beta_{62} & \delta_{22} \end{bmatrix}_k - \begin{bmatrix} \alpha_{16} & \beta_{61} & 0 & -\frac{1}{2}\beta_{66} \\ \beta_{12} & \delta_{12} & 0 & -\frac{1}{2}\delta_{26} \end{bmatrix}_k \left[\omega_k\right]^{-1} \begin{bmatrix} \alpha_{16} & \beta_{12} \\ \beta_{61} & \delta_{12} \\ 0 & 0 \\ -\frac{1}{2}\beta_{66} & -\frac{1}{2}\delta_{26} \end{bmatrix}_k \right)$$

Table 1: Stiffness $\left[\overline{P}\right]$ and compliance $\left[\overline{W}\right]$ matrices in the bar coordinate system of open and closed section beams with arbitrary layup. The elements α_{ij}, β_{ij}, δ_{ij} are evaluated at the ξ_k-η_k-ζ_k coordinate system of each wall segment. The superscript T denotes transpose

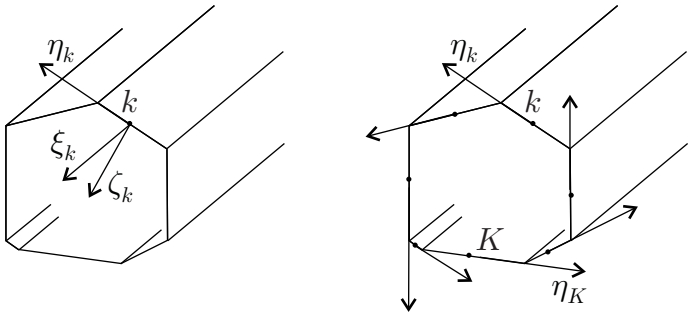

Figure 8: The local coordinate system attached to the k-th wall segment (left) and the directions of the η coordinates (right) in a closed section beam

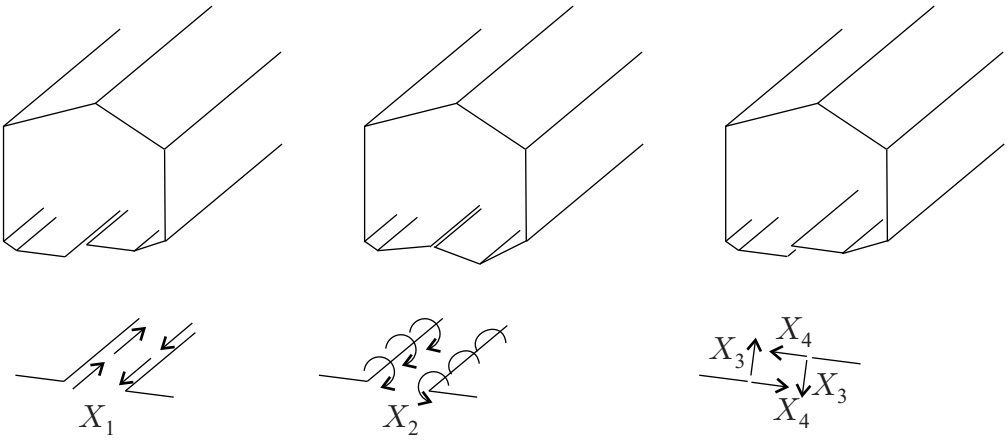

Figure 9: Deformations at the "cut" of a closed section beam and the forces acting along the cut

coordinate system. Therefore, the above stiffness matrices must be transformed to the x, y, z coordinate system. This transformation is given by Equation (3.55).

3.3 Closed section beams

We consider a single cell closed section beam with flat wall segments. In each segment we use a ξ_k-η_k-ζ_k coordinate system with the origin at the midpoint of the reference plane of the k-th segment, and with η_k pointing in the counter clockwise direction (Figure 8).

If a closed section beam were cut lengthwise the two cut edges would move relative to each other as shown in Figure 9. In the uncut beam this deformation is prevented by force X_1, bending moment X_2, and two transverse forces X_3, X_4 acting along the cut (Figure 9).

X_1, X_2, X_3, and X_4 give rise to V_η, N_η, $N_{\xi\eta}$, and M_η in each wall segment, as illustrated in Figure 10 for the k-th wall segment.

The transverse forces X_3, X_4 are generally small, and may be neglected. Hence N_η (and V_η) are zero in each wall segment, and $N_{\xi\eta}$ and M_η do not change along the circumference and are identical to X_1 and X_2, respectively

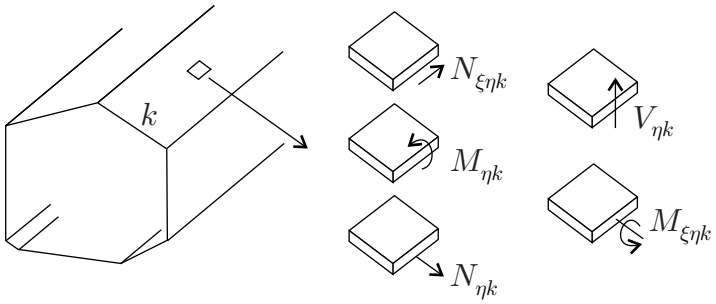

Figure 10: The forces and moments (per unit length) acting in the k-th wall of a closed section beam

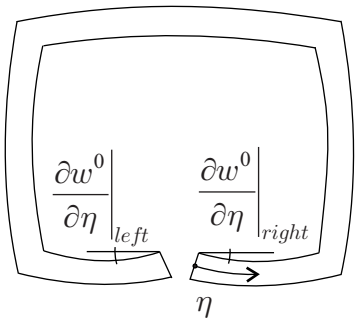

Figure 11: Relative rotation of the cut edges

$$\left\{ \begin{array}{c} N_{\xi\eta} \\ M_\eta \end{array} \right\}_k = \left\{ \begin{array}{c} X_1 \\ X_2 \end{array} \right\} \tag{3.25}$$

$N_{\xi\eta}$ is the shear flow

$$N_{\xi\eta} = X_1 \equiv q \tag{3.26}$$

The axial displacements and the rotation along the two edges of the "cut" must be identical (see Figure 11).

These conditions give the compatibility equations

$$u|_{left} = u|_{right} \qquad \left.\frac{\partial w^o}{\partial \eta}\right|_{right} = \left.\frac{\partial w^o}{\partial \eta}\right|_{left} \tag{3.27}$$

where u is the displacement of the wall in the axial direction and w^o is the displacement of the wall perpendicular to the wall segment's reference surface.

The first compatibility equation can be expressed as [17]

$$-2A\overline{\vartheta} + \oint \gamma^o_{\xi\eta} d\eta = 0 \tag{3.28}$$

while the second compatibility equation can be written by using the definition $\kappa_\eta = -\partial^2 w^0/\partial\eta^2$. with this definition the second equation in Equation 3.27 becomes

$$\oint \kappa_\eta d\eta = 0 \tag{3.29}$$

η is the coordinate along the circumference and A is the enclosed area. The integrals must be performed along the entire circumference.

The analysis of thin-walled closed section beams is performed in five steps. The first three steps are identical with those of open section beams with the modification that $N_{\xi\eta}\,(= X_1)$ and $M_\eta\,(= X_2)$ are non-zero and are as yet unknown. They are determined in the fourth step. The five steps are

1. The strains in each wall segment are related to the axial strain, curvatures and twist of the beam's axis.
2. The forces in each wall segment are expressed in terms of the strains in the wall segment and X_1, X_2.
3. The resultant axial force, moments, and torque acting at the axis of the beam are determined from the wall segment forces.
4. X_1 and X_2 are determined from the compatibility equations.
5. The stiffness matrix is established by relating the resultant axial force, moments, and torque to the axial strain, curvatures and twist of the beam's axis.

3.3.1 Step 1. Strains in the wall segments

The strains in the wall segments are calculated in the same way as in open section beams. The axial strain, curvatures, and twist of the k-th segments axis (where $\eta = 0, \zeta = 0$) are given by Equation (3.4).

The axial strain in the k-th segment varies linearly with η, while the curvatures $\kappa_{\xi k}$, $\kappa_{\xi\eta k}$ do not vary with η (see Equation 3.9).

3.3.2 Step 2. Forces and moments in the wall segments

As is discussed in Section 3.3, when X_3 and X_4 are neglected N_η is zero, and $N_{\xi\eta} = X_1, M_\eta = X_2$ do not vary along the circumference. With these approximations the strain-force relationships of the k-th segment become (see Equation 3.10 and 3.12)

$$\left\{\begin{array}{c}\epsilon^o_\xi\\ \kappa_\xi\\ \kappa_{\xi\eta}\end{array}\right\}_k = \underbrace{\left[\begin{array}{ccc}\alpha_{11} & \beta_{11} & \beta_{61}\\ \beta_{11} & \delta_{11} & \delta_{16}\\ \beta_{16} & \delta_{16} & \delta_{66}\end{array}\right]_k}_{[\widetilde{\mu}_k]} \left\{\begin{array}{c}N_\xi\\ M_\xi\\ M_{\xi\eta}\end{array}\right\}_k + \underbrace{\left[\begin{array}{cc}\alpha_{16} & \beta_{12}\\ \beta_{61} & \delta_{12}\\ \beta_{66} & \delta_{26}\end{array}\right]_k}_{[\widetilde{\nu}_k]} \left\{\begin{array}{c}X_1\\ X_2\end{array}\right\} \tag{3.30}$$

$$\left\{\begin{array}{c}\gamma^o_{\xi\eta}\\ \kappa_\eta\end{array}\right\}_k = \left[\begin{array}{ccc}\alpha_{16} & \beta_{61} & \beta_{66}\\ \beta_{12} & \delta_{12} & \delta_{26}\end{array}\right]_k \left\{\begin{array}{c}N_\xi\\ M_\xi\\ M_{\xi\eta}\end{array}\right\}_k + \left[\begin{array}{cc}\alpha_{66} & \beta_{26}\\ \beta_{26} & \delta_{22}\end{array}\right]_k \left\{\begin{array}{c}X_1\\ X_2\end{array}\right\} \tag{3.31}$$

Equations (3.13)-(3.16), and (3.20), derived for open section beams, are also applicable for closed section beams. These equations, together with Equation (3.30), give

$$\left\{\begin{array}{c}\epsilon^w_k\\ \kappa^w_{\xi k}\\ \kappa^w_{mk}\\ \vartheta^w_k\end{array}\right\} = [\omega_k] \left\{\begin{array}{c}\widehat{N}^w_{\xi k}\\ \widehat{M}^w_{\xi k}\\ \widehat{M}^w_{mk}\\ \widehat{T}^w_{\xi k}\end{array}\right\} + \left[\begin{array}{cc}\alpha_{16} & \beta_{12}\\ \beta_{61} & \delta_{12}\\ 0 & 0\\ -\frac{1}{2}\beta_{66} & -\frac{1}{2}\delta_{26}\end{array}\right]_k \left\{\begin{array}{c}X_1\\ X_2\end{array}\right\} \tag{3.32}$$

where $[\omega_k]$ is defined in Equation (3.21) and is also given in Table 1. By inverting this equation, we obtain

$$\left\{\begin{array}{c}\widehat{N}^w_{\xi k}\\ \widehat{M}^w_{\xi k}\\ \widehat{M}^w_{mk}\\ \widehat{T}^w_{\xi k}\end{array}\right\} = [\omega_k]^{-1} \left\{\begin{array}{c}\epsilon^w_k\\ \kappa^w_{\xi k}\\ \kappa^w_{mk}\\ \vartheta^w_k\end{array}\right\} - [\omega_k]^{-1} \left[\begin{array}{cc}\alpha_{16} & \beta_{12}\\ \beta_{61} & \delta_{12}\\ 0 & 0\\ -\frac{1}{2}\beta_{66} & -\frac{1}{2}\delta_{26}\end{array}\right]_k \left\{\begin{array}{c}X_1\\ X_2\end{array}\right\} \tag{3.33}$$

3.3.3 Step 3. Forces in the beam

The forces inside the beam in the bar coordinate system are given by Equation (3.22) with the following modification. For an open section beam the torque is due to the twist moment $M_{\xi\eta}$ only, while for a closed section beam it is due to the twist moment $M_{\xi\eta}$ and to the shear flow X_1. The torque due to X_1 is given by the Bredt-Batho formula [17]

$$\left(\widehat{T}_{\overline{x}}\right)_{\text{due to } X_1} = 2AX_1 \tag{3.34}$$

where A is the enclosed area. With this additional torque Equation (3.22) becomes

$$\left\{\begin{array}{c}\widehat{N}_{\overline{x}}\\ \widehat{M}_{\overline{y}}\\ \widehat{M}_{\overline{z}}\\ \widehat{T}_{\overline{x}}\end{array}\right\} = \sum_{k=1}^{K} [R_k]^T \left\{\begin{array}{c}\widehat{N}^w_{\xi k}\\ \widehat{M}^w_{\xi k}\\ \widehat{M}^w_{mk}\\ \widehat{T}^w_{\xi k}\end{array}\right\} + \left[\begin{array}{cc}0 & 0\\ 0 & 0\\ 0 & 0\\ 2A & 0\end{array}\right] \left\{\begin{array}{c}X_1\\ X_2\end{array}\right\} \tag{3.35}$$

where $[R_k]^T$ is given in Equation (3.22).

3.3.4 Step 4. Forces X_1 and X_2

By introducing Equation (3.31) into Equation (3.28) and (3.29), we obtain

$$0 = -\left\{ \begin{array}{c} 2A\overline{\vartheta} \\ 0 \end{array} \right\} + \oint \left[\begin{array}{ccc} \alpha_{16} & \beta_{61} & \beta_{66} \\ \beta_{12} & \delta_{12} & \delta_{26} \end{array} \right] \left\{ \begin{array}{c} N_\xi \\ M_\xi \\ M_{\xi\eta} \end{array} \right\} d\eta + \oint \left[\begin{array}{cc} \alpha_{66} & \beta_{62} \\ \beta_{62} & \delta_{22} \end{array} \right] d\eta \left\{ \begin{array}{c} X_1 \\ X_2 \end{array} \right\} \quad (3.36)$$

The integral around the circumference may be obtained by performing the integration along each segment and then summing these integrals

$$\oint ()d\eta = \sum_{k=1}^{K} \int_{(b_k)} ()d\eta \quad (3.37)$$

Applying Equation (3.37) for N_ξ, M_ξ and $M_{\xi\eta}$ we obtain

$$\int_{(b_k)} N_\xi d\eta = \widehat{N}^w_{\xi k} \qquad \int_{(b_k)} M_\xi d\eta = \widehat{M}^w_{\xi k} \qquad \int_{(b_k)} M_{\xi\eta} d\eta = -\frac{1}{2}\widehat{T}^w_{\xi k} \quad (3.38)$$

Hence Equation (3.36) becomes

$$0 = -\left\{ \begin{array}{c} 2A\overline{\vartheta} \\ 0 \end{array} \right\} + \sum_{k=1}^{K} \left(\left[\begin{array}{ccc} \alpha_{16} & \beta_{61} & -\frac{1}{2}\beta_{66} \\ \beta_{12} & \delta_{12} & -\frac{1}{2}\delta_{26} \end{array} \right]_k \left\{ \begin{array}{c} \widehat{N}^w_{\xi k} \\ \widehat{M}^w_{\xi k} \\ \widehat{T}^w_{\xi k} \end{array} \right\} + b_k \left[\begin{array}{cc} \alpha_{66} & \beta_{62} \\ \beta_{62} & \delta_{22} \end{array} \right]_k \left\{ \begin{array}{c} X_1 \\ X_2 \end{array} \right\} \right) \quad (3.39)$$

By taking Equation (3.33) and (3.4) into account, we can write

$$0 = -\left\{ \begin{array}{c} 2A\overline{\vartheta} \\ 0 \end{array} \right\} + [I] \left\{ \begin{array}{c} \epsilon^o_{\overline{x}} \\ \frac{1}{\rho_{\overline{y}}} \\ \frac{1}{\rho_{\overline{z}}} \\ \overline{\vartheta} \end{array} \right\} + [F] \left\{ \begin{array}{c} X_1 \\ X_2 \end{array} \right\} \quad (3.40)$$

where the matrices $[I]$ and $[F]$ are defined in Table 1. By inverting this equation we obtain

$$\left\{ \begin{array}{c} X_1 \\ X_2 \end{array} \right\} = [F]^{-1} [L] \left\{ \begin{array}{c} \epsilon^o_{\overline{x}} \\ \frac{1}{\rho_{\overline{y}}} \\ \frac{1}{\rho_{\overline{z}}} \\ \overline{\vartheta} \end{array} \right\} \quad (3.41)$$

where the matrix $[L]$ is given in Table 1.

3.3.5 Step 5. Stiffness matrix

Equations (3.35), (3.33), and (3.4) give

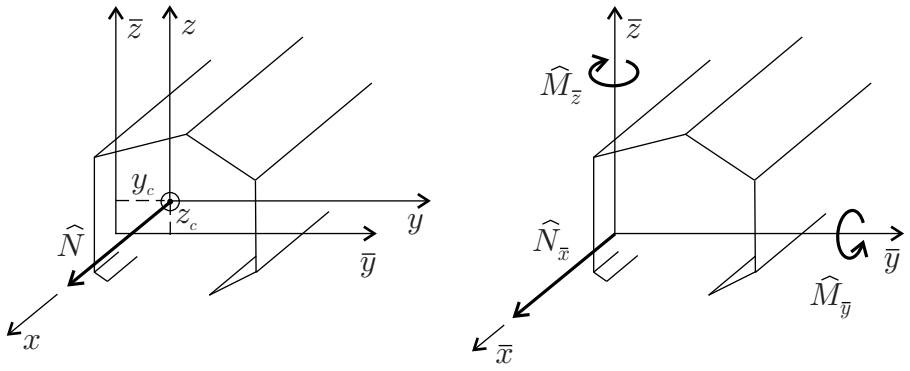

Figure 12: Beam subjected to an axial force at the centroid and the resultant axial force and moments in the $\overline{x}$-$\overline{y}$-$\overline{z}$ coordinate system

$$\begin{Bmatrix} \widehat{N}_{\overline{x}} \\ \widehat{M}_{\overline{y}} \\ \widehat{M}_{\overline{z}} \\ \widehat{T}_{\overline{x}} \end{Bmatrix} = \sum_{k=1}^{K} [R_k]^T [\omega_k]^{-1} [R_k] \begin{Bmatrix} \epsilon^o_{\overline{x}} \\ \frac{1}{\rho_{\overline{y}}} \\ \frac{1}{\rho_{\overline{z}}} \\ \overline{\vartheta} \end{Bmatrix} + \left(\begin{bmatrix} 0 & 0 \\ 0 & 0 \\ 0 & 0 \\ 2A & 0 \end{bmatrix} - [I]^T \right) \begin{Bmatrix} X_1 \\ X_2 \end{Bmatrix} \tag{3.42}$$

where $[I]^T$ is the transpose of $[I]$ (Table 1). By introducing Equation (3.41) into Equation (3.42) we obtain

$$\begin{Bmatrix} \widehat{N}_{\overline{x}} \\ \widehat{M}_{\overline{y}} \\ \widehat{M}_{\overline{z}} \\ \widehat{T}_{\overline{x}} \end{Bmatrix} = \underbrace{\left(\sum_{k=1}^{K} \left([R_k]^T [\omega_k]^{-1} [R_k] \right) + [L]^T [F]^{-1} [L] \right)}_{[\overline{P}]} \begin{Bmatrix} \epsilon^o_{\overline{x}} \\ \frac{1}{\rho_{\overline{y}}} \\ \frac{1}{\rho_{\overline{z}}} \\ \overline{\vartheta} \end{Bmatrix} \tag{3.43}$$

where $[\overline{P}]$ is the stiffness matrix of the closed section beam in the bar coordinate system (see Table 1).

3.4 Centroid

The aforementioned expressions give the stiffness matrices of open and closed section beams in an arbitrarily chosen coordinate system. To determine these matrices in the x-y-z coordinate system attached to the centroid, the location of the centroid must be known. The centroid is located such that the beam's axis remains straight when a pure axial force $\widehat{N}$ is applied at the centroid. While this axis remains straight, the beam may twist about the axis of twist, which does not necessarily coincide with the axis passing through the centroid.

The coordinates of the centroid in the bar coordinate system (chosen arbitrarily) are denoted by z_c and y_c (Figure 12).

The force and moment resultants at the origin of the bar coordinate system $\widehat{N}_{\overline{x}}$, $\widehat{M}_{\overline{y}}$, $\widehat{M}_{\overline{z}}$ are related to the force applied at the centroid by the expressions

$$\widehat{N}_{\overline{x}} = \widehat{N} \qquad \widehat{M}_{\overline{y}} = z_c \widehat{N} \qquad \widehat{M}_{\overline{z}} = y_c \widehat{N} \tag{3.44}$$

For both open and closed section beams the strain-force relationships may be written as

$$\left\{ \begin{array}{c} \epsilon^o_{\overline{x}} \\ \frac{1}{\rho_{\overline{y}}} \\ \frac{1}{\rho_{\overline{z}}} \\ \overline{\vartheta} \end{array} \right\} = \left[\begin{array}{cccc} \overline{W}_{11} & \overline{W}_{12} & \overline{W}_{13} & \overline{W}_{14} \\ \overline{W}_{12} & \overline{W}_{22} & \overline{W}_{23} & \overline{W}_{24} \\ \overline{W}_{13} & \overline{W}_{23} & \overline{W}_{33} & \overline{W}_{34} \\ \overline{W}_{14} & \overline{W}_{24} & \overline{W}_{34} & \overline{W}_{44} \end{array} \right] \left\{ \begin{array}{c} \widehat{N}_{\overline{x}} \\ \widehat{M}_{\overline{y}} \\ \widehat{M}_{\overline{z}} \\ \widehat{T}_{\overline{x}} \end{array} \right\} \tag{3.45}$$

where $\left[\overline{W}\right]$ is the compliance matrix in the bar coordinate system

$$\left[\overline{W}\right] = \left[P\right]^{-1} \tag{3.46}$$

where $\left[P\right]$ is the stiffness matrix given by Equation (3.23) and (3.43) for open and closed section beams, respectively.

Equations (3.45) and (3.44) yield the curvatures

$$\left\{ \begin{array}{c} \frac{1}{\rho_{\overline{y}}} \\ \frac{1}{\rho_{\overline{z}}} \end{array} \right\} = \left[\begin{array}{ccc} \overline{W}_{12} & \overline{W}_{22} & \overline{W}_{23} \\ \overline{W}_{13} & \overline{W}_{23} & \overline{W}_{33} \end{array} \right] \left\{ \begin{array}{c} 1 \\ z_c \\ y_c \end{array} \right\} \widehat{N} \tag{3.47}$$

Since $\widehat{N}$ is applied at the centroid, by definition the curvatures of the beam are zero

$$\frac{1}{\rho_{\overline{y}}} = \frac{1}{\rho_{\overline{z}}} = 0 \tag{3.48}$$

Equations (3.47) and (3.48) yield the location of the centroid with respect to the origin of the bar coordinate system

$$\left\{ \begin{array}{c} z_c \\ y_c \end{array} \right\} = - \left[\begin{array}{cc} \overline{W}_{22} & \overline{W}_{23} \\ \overline{W}_{23} & \overline{W}_{33} \end{array} \right]^{-1} \left[\begin{array}{c} \overline{W}_{12} \\ \overline{W}_{13} \end{array} \right] \tag{3.49}$$

3.4.1 Stiffness and compliance matrices in the centroid coordinate system

We now apply the expressions of the compliance matrix (Equation 3.45) at the centroid to which the x-y-z coordinate system is attached. The forces $\widehat{N}_{\overline{x}}$, $\widehat{M}_{\overline{y}}$, $\widehat{M}_{\overline{z}}$ in the bar coordinate system are related to the axial force $\widehat{N}$ in the x-y-z coordinate system by (Equation 3.44), while the torques in the two coordinate systems are identical

$$\widehat{T}_{\overline{x}} = \widehat{T} \tag{3.50}$$

Equations (3.44) and (3.50) in matrix form are

$$\begin{Bmatrix} \widehat{N}_{\overline{x}} \\ \widehat{M}_{\overline{y}} \\ \widehat{M}_{\overline{z}} \\ \widehat{T}_{\overline{x}} \end{Bmatrix} = [R_b] \begin{Bmatrix} \widehat{N} \\ \widehat{M}_y \\ \widehat{M}_z \\ \widehat{T} \end{Bmatrix} \tag{3.51}$$

where $[R_b]$ is defined as

$$[R_b] = \begin{bmatrix} 1 & 0 & 0 & 0 \\ z_c & 1 & 0 & 0 \\ y_c & 0 & 1 & 0 \\ 0 & 0 & 0 & 1 \end{bmatrix} \tag{3.52}$$

The axial strain of the axis x (passing through the centroid) is related to the strain and curvatures of the axis $\overline{x}$ (passing through the origin at the bar coordinate system) by (Equation 3.3)

$$\epsilon_x^o = \epsilon_{\overline{x}}^o + \frac{1}{\rho_{\overline{y}}} z_c + \frac{1}{\rho_{\overline{z}}} y_c \tag{3.53}$$

The curvatures and the twists per unit length of the x and $\overline{x}$ axis are identical. These conditions, together with Equation (3.53), can be expressed as

$$\begin{Bmatrix} \epsilon_x^o \\ \frac{1}{\rho_y} \\ \frac{1}{\rho_z} \\ \vartheta \end{Bmatrix} = [R_b]^T \begin{Bmatrix} \epsilon_{\overline{x}}^o \\ \frac{1}{\rho_{\overline{y}}} \\ \frac{1}{\rho_{\overline{z}}} \\ \overline{\vartheta} \end{Bmatrix} \tag{3.54}$$

where $[R_b]^T$ is the transpose of $[R_b]$. By substituting Equation (3.51) and (3.54) into Equation (3.45), we obtain the strain-force relationship with respect to the x-y-z coordinate system

$$\begin{Bmatrix} \epsilon_x^o \\ \frac{1}{\rho_y} \\ \frac{1}{\rho_z} \\ \vartheta \end{Bmatrix} = [R_b]^T \underbrace{\begin{bmatrix} \overline{W}_{11} & \overline{W}_{12} & \overline{W}_{13} & \overline{W}_{14} \\ \overline{W}_{12} & \overline{W}_{22} & \overline{W}_{23} & \overline{W}_{24} \\ \overline{W}_{13} & \overline{W}_{23} & \overline{W}_{33} & \overline{W}_{34} \\ \overline{W}_{14} & \overline{W}_{24} & \overline{W}_{34} & \overline{W}_{44} \end{bmatrix}}_{[W]} [R_b] \begin{Bmatrix} \widehat{N} \\ \widehat{M}_y \\ \widehat{M}_z \\ \widehat{T} \end{Bmatrix} \tag{3.55}$$

By performing the matrix multiplications in Equation (3.55), we obtain the compliance matrix in the x-y-z coordinate system which has four zero elements (see Equation 3.49)

$$[W] = \begin{bmatrix} W_{11} & 0 & 0 & W_{14} \\ 0 & W_{22} & W_{23} & W_{24} \\ 0 & W_{23} & W_{33} & W_{34} \\ W_{14} & W_{24} & W_{34} & W_{44} \end{bmatrix} \tag{3.56}$$

The zero elements of the compliance matrix are zero by virtue of the fact that a normal force applied at the centroid does not result in bending. The inverse of Equation (3.56) is

$$\begin{bmatrix} P_{11} & P_{12} & P_{13} & P_{14} \\ P_{12} & P_{22} & P_{23} & P_{24} \\ P_{13} & P_{23} & P_{33} & P_{34} \\ P_{14} & P_{24} & P_{34} & P_{44} \end{bmatrix} = \begin{bmatrix} W_{11} & 0 & 0 & W_{14} \\ 0 & W_{22} & W_{23} & W_{24} \\ 0 & W_{23} & W_{33} & W_{34} \\ W_{14} & W_{24} & W_{34} & W_{44} \end{bmatrix}^{-1} \tag{3.57}$$

where P_{ij} are the elements of the stiffness matrix in the x-y-z coordinate system.

3.4.2 Stiffness matrix of orthotropic beams

When the 16 and 26 elements of the $[A]$, $[B]$, $[D]$ matrices of a laminate are zero ($A_{16} = A_{26} = B_{16} = B_{26} = D_{16} = D_{26} = 0$) the laminate is called orthotropic. A thin-walled beam is orthotropic when each of its walls is orthotropic. For an orthotropic beam the calculation results in $W_{14} = W_{24} = W_{34} = 0$ and $P_{14} = P_{24} = P_{34} = 0$. Thus, for an orthotropic beam we have

$$[P] = \begin{bmatrix} P_{11} & 0 & 0 & 0 \\ 0 & P_{22} & P_{23} & 0 \\ 0 & P_{23} & P_{33} & 0 \\ 0 & 0 & 0 & P_{44} \end{bmatrix} \tag{3.58}$$

By comparing Equation (3.58) and the stiffness matrix of an isotropic beam [17] we see that the replacement stiffnesses of thin-walled orthotropic open and closed section beams are

$$P_{11} = \widehat{EA} \tag{3.59}$$

$$P_{22} = \widehat{EI}_{yy} \qquad P_{33} = \widehat{EI}_{zz} \qquad P_{23} = \widehat{EI}_{yz} \tag{3.60}$$

$$P_{44} = \widehat{GI}_t \tag{3.61}$$

where $\widehat{EA}$ is the tensile stiffness, $\widehat{EI}_{yy}$, $\widehat{EI}_{zz}$ and $\widehat{EI}_{yz}$ are bending stiffnesses, $\widehat{GI}_t$ is the torsional stiffness. For this case our results simplify to those of Barbero ([4]).

3.5 Stresses and strains

We consider a thin-walled open section beam subjected to axial force $\widehat{N}_{\overline{x}}$, bending moments $\widehat{M}_{\overline{y}}$, $\widehat{M}_{\overline{z}}$, and torque $\widehat{T}_{\overline{x}}$, (acting at the origin of the arbitrarily chosen $\overline{x}$-$\overline{y}$-$\overline{z}$ bar coordinate system). The axial strain ($\epsilon^o_{\overline{x}}$), curvatures ($\frac{1}{\rho_{\overline{y}}}$, $\frac{1}{\rho_{\overline{z}}}$), and twist of the longitudinal axis is given by Equation (3.45).

3.5.1 Open section beams

For the k-th segment Equation (3.4) and (3.9) give

$$\left\{ \begin{array}{c} \epsilon_\xi^o \\ \kappa_\xi \\ \kappa_{\xi\eta} \end{array} \right\}_k = [R_\eta]\,[R_k] \left\{ \begin{array}{c} \epsilon_{\overline{x}}^o \\ \frac{1}{\rho_{\overline{y}}} \\ \frac{1}{\rho_{\overline{z}}} \\ \overline{\vartheta} \end{array} \right\} \tag{3.62}$$

where ϵ_ξ^o is the axial strain, and κ_ξ and $\kappa_{\xi\eta}$ are the curvatures of the axis through the midpoint of the wall segment's reference plane.

The forces in the k-th segment are given by Equation (3.12).

Equations (3.45), (3.62) and (3.12) give

$$\left\{ \begin{array}{c} N_\xi \\ M_\xi \\ M_{\xi\eta} \end{array} \right\}_k = [\widetilde{\mu}_k]^{-1}\,[R_\eta]\,[R_k]\,[\overline{W}] \left\{ \begin{array}{c} \widehat{N}_{\overline{x}} \\ \widehat{M}_{\overline{y}} \\ \widehat{M}_{\overline{z}} \\ \widehat{T}_{\overline{x}} \end{array} \right\} \tag{3.63}$$

We recall that in an open section beam $N_{\eta k}, N_{\xi\eta k}$, and $M_{\eta k}$ are zero

$$N_{\eta k} = N_{\xi\eta k} = M_{\eta k} = 0 \tag{3.64}$$

From the three forces ($N_{\xi k}$, $N_{\eta k}$, $N_{\xi\eta k}$) and the three moments ($M_{\xi k}$, $M_{\eta k}$, $M_{\xi\eta k}$) for unit length we can calculate the stresses and strains using the laminate plate theory ([9]).

3.5.2 Closed section beams

The strains ($\epsilon_{\xi k}^o$, $\kappa_{\xi k}$, $\kappa_{\xi\eta k}$) at the axis through the midpoint of the k-th segment reference plane are given by Equation (3.62).

In a closed section beam $N_{\eta k}$ is zero and $N_{\xi\eta k}, M_{\eta k}$ are equal to X_1 and X_2 (Equation 3.25)

$$N_{\eta k} = 0 \qquad N_{\xi\eta k} = X_1 = q \qquad M_{\eta k} = X_2 \tag{3.65}$$

where X_1 and X_2 are calculated by Equation (3.41) and (3.45)

$$\left\{ \begin{array}{c} X_1 \\ X_2 \end{array} \right\} = [F]^{-1}\,[L] \left\{ \begin{array}{c} \epsilon_{\overline{x}}^o \\ \frac{1}{\rho_{\overline{y}}} \\ \frac{1}{\rho_{\overline{z}}} \\ \overline{\vartheta} \end{array} \right\} = [F]^{-1}\,[L]\,[\overline{W}] \left\{ \begin{array}{c} \widehat{N}_{\overline{x}} \\ \widehat{M}_{\overline{y}} \\ \widehat{M}_{\overline{z}} \\ \widehat{T}_{\overline{x}} \end{array} \right\} \tag{3.66}$$

The forces in the k-th segment are (see Equation 3.30)

$$\left\{ \begin{array}{c} N_\xi \\ M_\xi \\ M_{\xi\eta} \end{array} \right\}_k = [\widetilde{\mu}_k]^{-1} \left(\left\{ \begin{array}{c} \epsilon_\xi^o \\ \kappa_\xi \\ \kappa_{\xi\eta} \end{array} \right\}_k - [\widetilde{\nu}_k] \left\{ \begin{array}{c} X_1 \\ X_2 \end{array} \right\} \right) \tag{3.67}$$

where $[\widetilde{\mu}_k]$ and $[\widetilde{\nu}_k]$ are defined in Equation (3.30).

	E_1 [MPa]	E_2 [MPa]	G_{12} [MPa]	ν_{12}
T300/CFRP	148000	9650	4550	0.3

Table 2: Material properties of a carbon epoxy ply

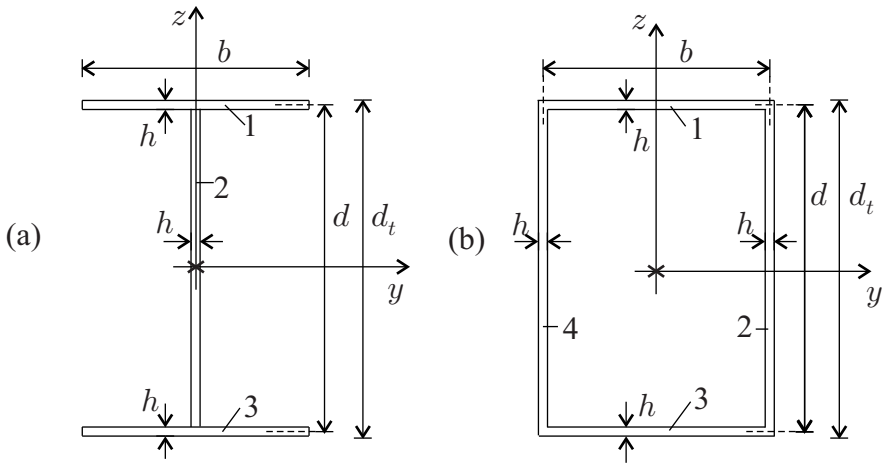

Figure 13: Open and closed sections considered in the numerical examples

Equations (3.62), (3.66), and (3.67) yield

$$\left\{ \begin{array}{c} N_\xi \\ M_\xi \\ M_{\xi\eta} \end{array} \right\}_k = [\widetilde{\mu}_k]^{-1} \left([R_\eta]\,[R_k] - [\widetilde{\nu}_k]\,[F]^{-1}\,[L] \right) [\overline{W}] \left\{ \begin{array}{c} \widehat{N}_{\overline{x}} \\ \widehat{M}_{\overline{y}} \\ \widehat{M}_{\overline{z}} \\ \widehat{T}_{\overline{x}} \end{array} \right\} \tag{3.68}$$

Once the forces and moments (per unit length) are calculated for each wall segment by Equation (3.65) and (3.68), the strains and curvatures for each segment are calculated by using the laminate plate theory [9].

3.6 Verification

To verify the derived expressions for open and closed section beams we analyzed carbon fiber reinforced composite beams. The material properties of a ply made of unidirectional fibers are given in Table 12.

E_1 is the Young modulus in the fiber (x_1) direction, E_2 is the Young modulus perpendicular to the fiber (x_2), G_{12} is the shear modulus in the $x_1 - x_2$ plane and ν_{12} is the major Poisson's ratio.

We consider two cross-sections as shown in Figure 13. The thickness of the wall is 2 mm. (The effect of the thickness will be investigated in Section 3.7.2.)

We analyzed different layups which are listed in the first column of Table 3. The thickness of each ply was 1/6 mm, hence the total thickness of the laminates are 2 mm.

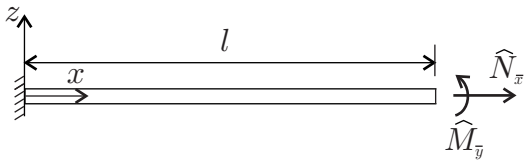

Figure 14: Loads on a cantilever beam

Here we present analysis of a cantilever beam subjected to a moment ($\widehat{M}_y$) and to a normal force ($\widehat{N}_x$) at the free end (Figure 14). We assume that warping of each cross-section may freely develop. (Simply supported beams subjected to a distributed load will be presented in Section 6.)

	E_1 [MPa]	E_2 [MPa]	G_{12} [MPa]	ν_{12}
T300/CFRP	148000	9650	4550	0.3

Table 3: Material properties of a carbon epoxy ply

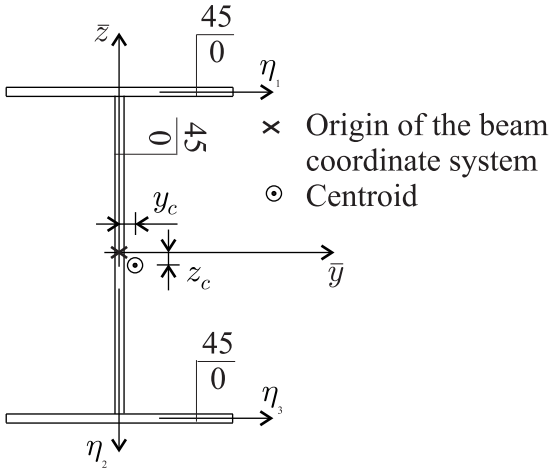

Figure 15: Cross-section of the beam considered in section 3.6.1

3.6.1 I-beam with unsymmetrical layup $[0_6/45_6]$

First we present the analysis of an I-beam with the layup $[0_6/45_6]$ (See Appendix A) given in the fifth row of Table 3, subjected to an axial load $\widehat{N}_x = 170$ N at the middle of the web (Figure 15). The length of the cantilever beam (L) is 1000 mm, while the dimensions of the cross-section are $b = 50$ mm, $d = 70$ mm, $h = 2$ mm.

We wish to determine the end displacements of the beam.

The solution is given in steps (which are not identical to those given in Section 3.2).

Step 1. Calculation of the stiffness matrices of the laminate.

The $[A]$, $[B]$, and $[D]$ stiffness matrices are calculated according to classical laminate plate theory [9]. The results (for the midplane of the laminate) are

$$[\mathbf{A}] = \begin{bmatrix} 1.9452 & 0.3946 & 0.3479 \\ 0.3946 & 0.5536 & 0.3479 \\ 0.3479 & 0.3479 & 0.4274 \end{bmatrix} \times 10^5 \text{ N/mm} \tag{3.69}$$

$$[\mathbf{B}] = \begin{bmatrix} \text{-}5.1611 & 1.6820 & 1.7396 \\ 1.6820 & 1.7972 & 1.7396 \\ 1.7396 & 1.7396 & 1.6820 \end{bmatrix} \times 10^4 \text{ N}$$

$$[\mathbf{D}] = \begin{bmatrix} 6.4842 & 1.3154 & 1.1597 \\ 1.3154 & 1.8453 & 1.1597 \\ 1.1597 & 1.1597 & 1.4246 \end{bmatrix} \times 10^4 \text{ Nmm}$$

Here and below the forces are given in N and the distances in mm. For simplicity the dimensions are omitted below.

Step 2. Calculation of the compliance matrices of the laminate.

The $[\alpha]$, $[\beta]$ and $[\delta]$ compliance matrices are

$$\begin{bmatrix} \alpha & \beta \\ \beta^T & \delta \end{bmatrix} = \begin{bmatrix} A & B \\ B^T & D \end{bmatrix}^{-1} = 10^{-3} \times \tag{3.70}$$

$$\begin{bmatrix} 0.01344 & -0.004854 & -0.00707 & 0.01707 & -0.006012 & -0.01106 \\ -0.004854 & 0.04180 & -0.02123 & -0.006012 & -0.005045 & -0.01106 \\ -0.00707 & -0.02123 & 0.064953 & -0.01106 & -0.01106 & -0.02405 \\ 0.01707 & -0.006012 & -0.01106 & 0.04031 & -0.01456 & -0.02141 \\ -0.006012 & -0.005045 & -0.01106 & -0.01456 & 0.1254 & -0.06368 \\ -0.01106 & -0.01106 & -0.02405 & -0.02141 & -0.06368 & 0.1948 \end{bmatrix}$$

The results are also presented in Table 3.

Step 3. Calculation of the $[R_k]$ and $[\omega_k]$ *matrices.*

Figure 15 shows the η axes of the local coordinate system of the walls. Equation (3.4) gives

$$[R_1] = \begin{bmatrix} 1 & 35 & 0 & 0 \\ 0 & 1 & 0 & 0 \\ 0 & 0 & 1 & 0 \\ 0 & 0 & 0 & 1 \end{bmatrix} \quad [R_2] = \begin{bmatrix} 1 & 0 & 0 & 0 \\ 0 & 0 & -1 & 0 \\ 0 & 1 & 0 & 0 \\ 0 & 0 & 0 & 1 \end{bmatrix} \quad [R_3] = \begin{bmatrix} 1 & -35 & 0 & 0 \\ 0 & 1 & 0 & 0 \\ 0 & 0 & 1 & 0 \\ 0 & 0 & 0 & 1 \end{bmatrix} \tag{3.71}$$

while Equation (3.21) with $b_1 = b_3 = 50,\ b_2 = 68$ and $\left(\widetilde{A}_{11}\right)_1 = \left(\widetilde{A}_{11}\right)_2 = \left(\widetilde{A}_{11}\right)_3 = 1.6150 \times 10^5$ (see Equation 3.19) yields

$$[\omega_1] = [\omega_3] = \begin{bmatrix} 0.2688 & 0.3414 & 0 & 0.1106 \\ 0.3414 & 0.8064 & 0 & 0.2141 \\ 0 & 0 & 0.0005944 & 0 \\ 0.1106 & 0.2141 & 0 & 0.9743 \end{bmatrix} \times 10^{-6} \tag{3.72}$$

$$[\omega_2] = \begin{bmatrix} 0.1976 & 0.2510 & 0 & 0.0813 \\ 0.2510 & 0.5929 & 0 & 0.1574 \\ 0 & 0 & 0.0002363 & 0 \\ 0.0813 & 0.1574 & 0 & 0.7164 \end{bmatrix} \times 10^{-6} \tag{3.73}$$

Step 4. Calculation of the stiffness and compliance matrices of the beam.

The stiffness matrix of the beam $[\overline{P}]$ is given by Equation (3.24)

$$[\overline{P}] = [R_1]^T [\omega_1]^{-1} [R_1] + [R_2]^T [\omega_2]^{-1} [R_2] + [R_3]^T [\omega_3]^{-1} [R_3] \tag{3.74}$$

$$= \begin{bmatrix} 0.002713 & -0.0006744 & 0.0004586 & -0.00005890 \\ -0.0006744 & 2.4021 & 0 & -0.00004325 \\ 0.0004586 & 0 & 0.3368 & 0.00002941 \\ -0.00005890 & -0.00004325 & 0.00002941 & 0.0003675 \end{bmatrix} \times 10^{10}$$

The compliance matrix of the beam $[\overline{W}]$ is given by Equation (3.46)

$$[\overline{W}] = [\overline{P}]^{-1} = \begin{bmatrix} 0.03700 & 0.00001049 & -0.00005089 & 0.005934 \\ 0.000010 & 0.00004163 & 0 & 0.000006582 \\ -0.00005089 & 0 & 0.0002970 & -0.00003192 \\ 0.005934 & 0.000006582 & -0.00003192 & 0.2730 \end{bmatrix} \times 10^{-6} \quad (3.75)$$

Step 5. Calculation of the location of the centroid.

The coordinates of the centroid are (Equation 3.49)

$$\begin{Bmatrix} z_c \\ y_c \end{Bmatrix} = - \begin{bmatrix} \overline{W}_{22} & \overline{W}_{23} \\ \overline{W}_{23} & \overline{W}_{33} \end{bmatrix}^{-1} \begin{bmatrix} \overline{W}_{12} \\ \overline{W}_{13} \end{bmatrix} = \begin{Bmatrix} -0.2520 \\ 0.1714 \end{Bmatrix} \quad (3.76)$$

Step 6. Stiffness and compliance matrices of the beam in the centroid coordinate system.

The $[R_b]$ matrix is (see Equation 3.52):

$$[R_b] = \begin{bmatrix} 1 & 0 & 0 & 0 \\ -0.2520 & 1 & 0 & 0 \\ 0.1714 & 0 & 1 & 0 \\ 0 & 0 & 0 & 1 \end{bmatrix} \quad (3.77)$$

The compliance matrix W is (Equation 3.55)

$$[W] = [R_b]^T [\overline{W}] [R_b] = \begin{bmatrix} 0.03698 & 0 & 0 & 0.005927 \\ 0 & 0.00004163 & 0 & 0.000006582 \\ 0 & 0 & 0.0002970 & -0.00003192 \\ 0.005927 & 0.000006582 & -0.00003192 & 0.2730 \end{bmatrix} \times 10^{-6} \quad (3.78)$$

The stiffness matrix is the inverse of the compliance matrix:

$$[P] = [W]^{-1} = \begin{bmatrix} 0.002713 & 0.000009335 & -0.000006457 & -0.00005890 \\ 0.000009335 & 2.4020 & 0.0001140 & -0.00005809 \\ -0.000006457 & 0.0001140 & 0.3368 & 0.00003950 \\ -0.00005890 & -0.00005809 & 0.00003950 & 0.0003675 \end{bmatrix} \times 10^{10} \quad (3.79)$$

Step 7. Strains in the beam.

When an axial force is applied at the free end of the cantilever, the strains and curvatures are uniform along the beam.

The vector of the forces acting at the origin of the bar coordinate system is:

$$\left\{\begin{array}{c}\widehat{N}_{\overline{x}}\\ \widehat{M}_{\overline{y}}\\ \widehat{M}_{\overline{z}}\\ \widehat{T}_{\overline{x}}\end{array}\right\}=\left\{\begin{array}{c}170\\ 0\\ 0\\ 0\end{array}\right\} \tag{3.80}$$

The force $\widehat{N}_{\overline{x}}$ acting at the middle of the web is equivalent to applying the following force and moments at the centroid:

$$\left\{\begin{array}{c}\widehat{N}\\ \widehat{M}_y\\ \widehat{M}_z\\ \widehat{T}\end{array}\right\}=\left\{\begin{array}{c}\widehat{N}_{\overline{x}}\\ -z_c\widehat{N}_{\overline{x}}\\ -y_c\widehat{N}_{\overline{x}}\\ \widehat{T}_{\overline{x}}\end{array}\right\}=\left\{\begin{array}{c}170\\ 42.84\\ -29.14\\ 0\end{array}\right\} \tag{3.81}$$

which result in the following strains:

$$\left\{\begin{array}{c}\epsilon_x^o\\ \frac{1}{\rho_y}\\ \frac{1}{\rho_z}\\ \vartheta\end{array}\right\}=10^{-6}\times\left[\begin{array}{cccc}0.03698 & 0 & 0 & 0.005927\\ 0 & 0.00004163 & 0 & 0.000006582\\ 0 & 0 & 0.0002970 & -0.00003192\\ 0.005927 & 0.000006582 & -0.00003192 & 0.2730\end{array}\right]\left\{\begin{array}{c}170\\ 42.84\\ -29.14\\ 0\end{array}\right\}=$$

$$=\left\{\begin{array}{c}0.6289\times10^{-5}\\ 0.1784\times10^{-7}\\ -0.8651\times10^{-8}\\ 0.1009\times10^{-5}\end{array}\right\} \tag{3.82}$$

From these uniform strains the end displacements and the rotation of the cross-section at the end are

$$\begin{aligned}u &= \epsilon_x^o\times L=0.6289\times10^{-5}\times1000=0.6289\times10^{-2}\text{mm}\\ v &= \frac{1}{\rho_y}\times\frac{L^2}{2}=0.1784\times10^{-7}\times\frac{10^6}{2}=0.8920\times10^{-2}\text{mm}\\ w &= \frac{1}{\rho_z}\times\frac{L^2}{2}=-0.8651\times10^{-8}\times\frac{10^6}{2}=-0.4325\times10^{-2}\text{mm}\\ \psi &= \vartheta\times L=0.1009\times10^{-5}\times1000=0.1009\times10^{-2}\end{aligned} \tag{3.83}$$

The displacements were also calculated by the ANSYS finite element program. The results are

$$\begin{aligned}u &= 0.6216\times10^{-2}\text{mm}\\ v &= 0.8662\times10^{-2}\text{mm}\\ w &= -0.4395\times10^{-2}\text{mm}\\ \psi &= 0.1046\times10^{-2}\end{aligned} \tag{3.84}$$

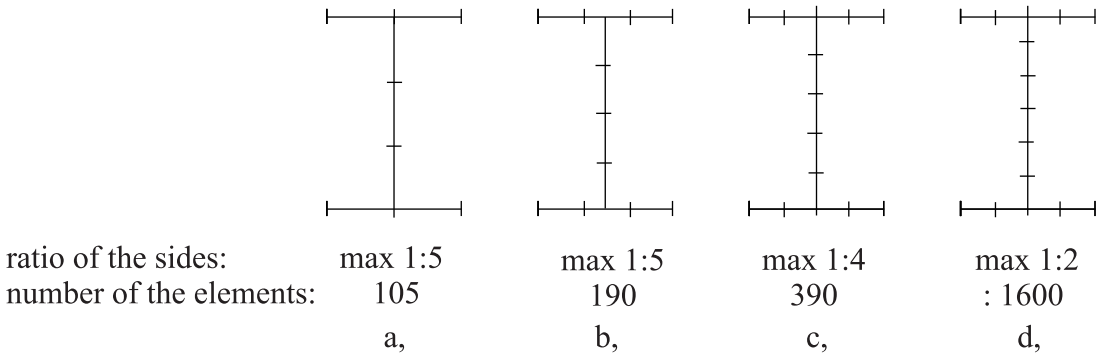

Figure 16: FE models for an I-beam

which agree closely with the results given by Equation (3.83).

In the numerical calculations we used the SHELL91 element type of the Ansys program. This is a shell element with 8 nodes, which can be used for anisotropic, layered composite plates. The nodes have 6 degrees of freedom (u, v, w, ψ_x, ψ_y and ψ_z).

The fixed end cross-section was supported in such a way that the cross-section was free to warp. (The effect of restrained warping will be considered in Section 6.)

For examine the accuracy of the numerical calculations we have divided the cross-section by four ways (Figure 16a, 16b, 16c and 16d). We made the above calculation all the four cases. For simplicity the layup was $[0_{12}]$. The displacement u along the x axis of the end of the beam

$$u_a = 0.2735 \times 10^{-2}\text{mm} \qquad \text{105 elements} \tag{3.85}$$

$$u_b = 0.3032 \times 10^{-2}\text{mm} \qquad \text{190 elements} \tag{3.86}$$

$$u_c = 0.3225 \times 10^{-2}\text{mm} \qquad \text{390 elements} \tag{3.87}$$

$$u_d = 0.3378 \times 10^{-2}\text{mm} \qquad \text{1600 elements} \tag{3.88}$$

The result of our calculation is

$$u = 0.3418 \times 10^{-2}\text{mm} \tag{3.89}$$

In all the numerical calculations we use the fourth model (Figure 16d).

3.6.2 I-beam with different layups

Calculations similar to those given in Section 3.6.1 were carried out for all the layups listed in Table 3. The results of the analytical and FE calculations are summarized in Table 4. It can be seen that the analytical and FE calculations are in agreement.

3.6.3 Box-beam with unsymmetrical layup ($[0_6/45_6]$)

We present the analysis of a box-beam with the layup $[0_6/45_6]$, given in the fifth row of Table 3 subjected to an axial load $\widehat{N}_x = 240N$ at the middle of the cross-section (Figure 17). The length

layup	$\widehat{N}$ (N)	$\widehat{M_y}$ (10^3Nmm)		$\epsilon^o_{\overline{x}}$ $\left(10^{-5}\right)$	$\frac{1}{\rho_{\overline{y}}}$ $\left(10^{-5}\right)$	$\frac{1}{\rho_{\overline{z}}}$ $\left(10^{-5}\right)$	$\overline{\vartheta}$ $\left(10^{-5}\right)$
$[0_{12}]$	0	100.022	An	0	0.2272	0	0
			FE	0	0.2236	0	0
			Error	0	-1.61	0	0
$[0_{12}]$	170	0	An	0.3418	0	0	0
			FE	0.3378	0	0	0
			Error	-1.18	0	0	0
$[45_{12}]$	0	100.022	An	0	2.741	0.0006	0.4848
			FE	0	2.697	0.0006	0.4658
			Error	0	-1.64	-	-4.08
$[45_6/-45_6]$	170	0	An	3.5099	0	0	0.9975
			FE	3.4686	0	0	0.9857
			Error	-1.19	0	0	1.20
$[0_6/45_6]$	170	0	An	0.6289	0.0018	-0.0009	0.1009
			FE	0.6216	0.0017	-0.0009	0.1046
			Error	-1.17	-	-	3.58
$[0_6/45_6]$	0	100.022	An	0.1050	0.4164	0.0001	0.0658
			FE	0.1022	0.4099	0.0001	0.0667
			Error	-2.74	-1.58	-	-1.35
$[10_4/20_4/30_4]$	0	100.022	An	0.1211	0.6988	0.0005	0.3239
			FE	0.1207	0.6903	0.0005	0.2979
			Error	-0.33	-1.23	-	-8.73

Table 4: Results of the present analysis (An), the Finite Element analysis (FE) and the error in percentage (Error) for different layups.

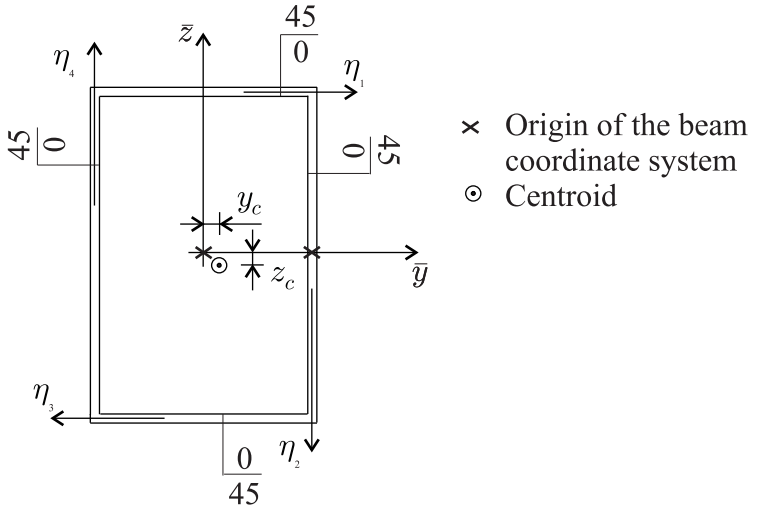

Figure 17: Cross-section of the beam considered in section 3.6.3

of the cantilever beam (L) is 1000 mm. The dimensions of the cross-section (Figure 17) are $b = 50$ mm, $d = 70$ mm, $h = 2$ mm. We wish to determine the end displacements.

Solution of the problem is given below in steps (which are different from the steps given in Section 3.3).

Step 1 and Step 2. The first two steps are identical to those for an I-beam given in Section 3.6.1

Step 3. Calculation of the $[R_k]$, $[\omega_k]$, $[F]$, $[I]$, *and* $[L]$ *matrices.*

Figure 17 shows the η-axes of the local coordinate systems of the walls. Equation (3.4) gives

$$[R_1] = \begin{bmatrix} 1 & -35 & 0 & 0 \\ 0 & 1 & 0 & 0 \\ 0 & 0 & 1 & 0 \\ 0 & 0 & 0 & 1 \end{bmatrix} \quad [R_2] = \begin{bmatrix} 1 & 0 & 25 & 0 \\ 0 & 0 & -1 & 0 \\ 0 & 1 & 0 & 0 \\ 0 & 0 & 0 & 1 \end{bmatrix}$$

$$[R_3] = \begin{bmatrix} 1 & 35 & 0 & 0 \\ 0 & -1 & 0 & 0 \\ 0 & 0 & -1 & 0 \\ 0 & 0 & 0 & 1 \end{bmatrix} \quad [R_4] = \begin{bmatrix} 1 & 0 & -25 & 0 \\ 0 & 0 & 1 & 0 \\ 0 & -1 & 0 & 0 \\ 0 & 0 & 0 & 1 \end{bmatrix} \tag{3.90}$$

Equation (3.21) with $b_1 = b_3 = 50$, $b_2 = b_4 = 70$ and with $\left(\widetilde{A}_{11}\right)_1 = \left(\widetilde{A}_{11}\right)_2 = \left(\widetilde{A}_{11}\right)_3 =$

1.6150×10^5 see (Equation 3.19) give

$$[\omega_1] = [\omega_3] = \begin{bmatrix} 0.2688 & 0.3414 & 0 & 0.1106 \\ 0.3414 & 0.8064 & 0 & 0.2141 \\ 0 & 0 & 0.0005944 & 0 \\ 0.1106 & 0.2141 & 0 & 0.9743 \end{bmatrix} \times 10^{-6}$$

$$[\omega_2] = [\omega_4] = \begin{bmatrix} 0.1920 & 0.2438 & 0 & 0.0790 \\ 0.2438 & 0.5760 & 0 & 0.1529 \\ 0 & 0 & 0.0002166 & 0 \\ 0.0790 & 0.1529 & 0 & 0.6959 \end{bmatrix} \times 10^{-6} \qquad (3.91)$$

The $[F]$, $[I]$, and $[L]$ matrices are given in Table 1. They yield ($K = 4$)

$$\begin{aligned} [F] &= \begin{bmatrix} 0.01339 & \text{-}0.006474 \\ \text{-}0.006474 & 0.02215 \end{bmatrix} \\ [I] &= \begin{bmatrix} \text{-}107.8176 & 0 & 0 & 80.6088 \\ \text{-}24.1002 & 0 & 0 & 187.3554 \end{bmatrix} \\ [L] &= \begin{bmatrix} 0.1078 & 0 & 0 & 6.9194 \\ 0.02410 & 0 & 0 & \text{-}0.1874 \end{bmatrix} \times 10^3 \end{aligned} \qquad (3.92)$$

Step 4. Calculation of the stiffness and compliance matrices of the beam.

The stiffness matrix of the beam $[\overline{P}]$ is given by Equation (3.43).

$$\begin{aligned} [\overline{P}] &= \left([R_1]^T [\omega_1]^{-1} [R_1] + [R_2]^T [\omega_2]^{-1} [R_2] + [R_3]^T [\omega_3]^{-1} [R_3] + [L]^T [F]^{-1} [L] \right) = \\ &= \begin{bmatrix} 0.003993 & 0 & 0 & 0.006753 \\ 0 & 2.9494 & 0 & 0 \\ 0 & 0 & 1.7976 & 0 \\ 0.006753 & 0 & 0 & 0.4105 \end{bmatrix} \times 10^{10} \end{aligned} \qquad (3.93)$$

The compliance matrix of the beam $[\overline{W}]$ yields (Equation 3.46)

$$[\overline{W}] = [\overline{P}]^{-1} = \begin{bmatrix} 0.2576 & 0 & 0 & \text{-}0.004237 \\ 0 & 0.0003390 & 0 & 0 \\ 0 & 0 & 0.0005363 & 0 \\ \text{-}0.004237 & 0 & 0 & 0.002506 \end{bmatrix} \times 10^{-7} \qquad (3.94)$$

Step 5. Calculation of the location of the centroid.

The centroid is at the middle of the cross-section (Equation 3.49):

$$\left\{ \begin{array}{c} z_c \\ y_c \end{array} \right\} = - \left[\begin{array}{cc} \overline{W}_{22} & \overline{W}_{23} \\ \overline{W}_{23} & \overline{W}_{33} \end{array} \right]^{-1} \left[\begin{array}{c} \overline{W}_{12} \\ \overline{W}_{13} \end{array} \right] = \left\{ \begin{array}{c} 0 \\ 0 \end{array} \right\} \tag{3.95}$$

Step 6. Strains in the beam.

When the cantilever is loaded by an axial force at the end, the strains and curvatures are uniform along the beam.

The forces acting at the origin of the bar coordinate system is:

$$\left\{ \begin{array}{c} \widehat{N}_{\overline{x}} \\ \widehat{M}_{\overline{y}} \\ \widehat{M}_{\overline{z}} \\ \widehat{T}_{\overline{x}} \end{array} \right\} = \left\{ \begin{array}{c} 240 \\ 0 \\ 0 \\ 0 \end{array} \right\} \tag{3.96}$$

The strains are calculated by Equation (3.45)

$$\left\{ \begin{array}{c} \epsilon^o_{\overline{x}} \\ \frac{1}{\rho_{\overline{y}}} \\ \frac{1}{\rho_{\overline{z}}} \\ \overline{\vartheta} \end{array} \right\} = 10^{-7} \times \left[\begin{array}{cccc} 0.2576 & 0 & 0 & \text{-}0.004237 \\ 0 & 0.0003390 & 0 & 0 \\ 0 & 0 & 0.0005363 & 0 \\ \text{-}0.004237 & 0 & 0 & 0.002506 \end{array} \right] \left\{ \begin{array}{c} 240 \\ 0 \\ 0 \\ 0 \end{array} \right\} =$$

$$= \left\{ \begin{array}{c} 0.6182 \\ 0 \\ 0 \\ -0.0102 \end{array} \right\} \times 10^{-5} \tag{3.97}$$

From these uniform strains displacements and the rotation of the cross-section at the end are

$$\begin{aligned} u &= \epsilon^o_x \times L = 0.6182 \times 10^{-5} \times 1000 = 0.6182 \times 10^{-2}\text{mm} \\ \psi &= \vartheta \times L = -0.0102 \times 10^{-5} \times 1000 = -0.102 \times 10^{-3} \end{aligned} \tag{3.98}$$

The displacements were also calculated by the ANSYS finite element program. The results are

$$\begin{aligned} u &= 0.6157 \times 10^{-2}\text{mm} \\ \psi &= -0.09899 \times 10^{-3} \end{aligned} \tag{3.99}$$

3.6.4 Box-beam with different layups

Calculations similar to those given in 30 were carried out for all the layups listed in Table 3. The results of the analytical and FE calculations are summarized in Table 5. It can be seen that the analytical results compare well with the FE calculations.

layup	$\widehat{N}$ (N)		$\epsilon_{\overline{x}}^{o}\left(10^{-5}\right)$	$\overline{\vartheta}\left(10^{-6}\right)$
$[0_{12}]$	240	An	0.3378	0.0000
		FE	0.3378	0.0000
		Error	0	0
$[45_{12}]$	240	An	4.0694	-0.8247
		FE	4.0705	-0.7999
		Error	0.02	-3.10
$[45_6/-45_6]$	240	An	3.0516	-0.0065
		FE	3.0690	-0.0063
		Error	0.55	-3.17
$[0_6/45_6]$	240	An	0.6182	-0.10169
		FE	0.6157	-0.09899
		Error	-0.406	-2.72
$[10_4/20_4/30_4]$	0	An	1.0489	-0.6470
		FE	1.0340	-0.6260
		Error	-1.45	-3.35

Table 5: Results of the present analysis (An), the Finite Element analysis (FE) and the error in percentage (Error) for different layups

3.7 Discussion

In the numerical examples (Section 3.6) we considered cantilever beams. The internal forces ($\widehat{N}$, $\widehat{M_y}$, $\widehat{M_z}$, $\widehat{T}$) can be calculated from the equilibrium equations and hence the calculation of the strains, stresses, and displacements are straightforward.

For other end supports, when the beam is statically indeterminate, all the governing equations (equilibrium, strain-displacement (Equation 3.1), material law (Equation 3.10)) must be considered simultaneously to determine the internal forces and the displacements. When the beam is orthotropic the 1,4; 2,4; and 3,4 elements of the stiffness matrix ($[P]$) are zero and the solution of the governing equations are readily available (see e.g. [9]).

The following questions arise: (i) how big is the error when for an anisotropic beam, which is not orthotropic, these elements of the stiffness matrix are neglected? If the error is small, the classical solutions can be applied for non-orthotropic beams.

Authors (see [16]) sometimes neglect the local stiffnesses of the laminates of thin walled beams, i.e. they take into account only the $[A]$ (or $[\alpha]$) matrix, while neglecting the $[B]$ and $[D]$ (or $[\beta]$ and $[\delta]$) matrices. This approximation simplifies the analysis considerably. In the following we will investigate the error caused by this approximation, and the following question is also addressed: (ii) how big is the error resulting from neglecting the local bending stiffnesses?

The first question will be investigated in Section 3.7.1 while the second one in Section 3.7.2.

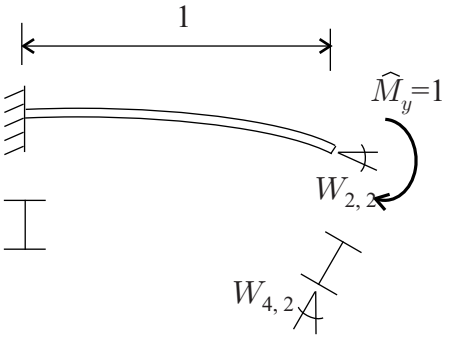

Figure 18: Displacements of a cantilever beam subjected to an end moment

layup		
top flange and web	bootom flange	$W_{4,2}/W_{2,2}$
$[0_{12}]$	$[0_{12}]$	0
$[45_{12}]$	$[45_{12}]$	0.1748
$[45_6/-45_6]$	$[-45_6/45_6]$	-5.9728
$[0_6/45_6]$	$[45_6/0_6]$	3.4572
$[10_4/20_4/30_4]$	$[30_4/20_4/10_4]$	-8.7580

Table 6: The ratio of $W_{4,2}/W_{2,2}$ for different layups

3.7.1 Effect of anisotropy

Tension-twist coupling. An axial force causes the twist of an anisotropic beam while for an orthotropic beam axial force does not cause twist. The amount of twist can be calculated from the 4,1 element of the stiffness matrix. This term must not be neglected.

Bending-twist coupling An applied bending moment may also cause the beam to twist. When bending moment $\widehat{M}_y = 1$ is applied the amount of twist per unit length (i.e. the rotation of the cross-section with respect to the x axis) is equal to the 4,2 element of the compliance matrix (Figure 18).

The rotation of the cross-section with respect to the y axis per unit length is equal to the 2,2 element of the compliance matrix. The ratio W_{42}/W_{22} is given in Table 6 for the cross-section shown in Figure 13a. We can see that for unsymmetrical layups (row 3 to 5) W_{42} cannot be neglected.

3.7.2 Effect of local stiffness

Symmetrical layup For *open-section beams*: As a rule, the $[D]$ matrix can be neglected in the calculation of the $\overline{P}_{ij}$ $(i,j = 1,2,3)$ elements of the stiffness matrix and the simplified analysis

layup	I beam	error in the elements of the stiffness matrix [%]		
	h/d_t	P_{11}	P_{22}	P_{33}
$[0_{12}]$	0.08	0	0.18	0.92
	0.16	0	0.73	3.58
	0.32	0	2.84	12.94
$[45_{12}]$	0.08	0	0.24	1.22
	0.16	0	0.97	4.73
	0.32	0	3.7	16.57
$[0_6/90_6]$	0.08	0	0.08	0.39
	0.16	0	0.31	1.55
	0.32	0	1.22	5.91
$[0_6/\pm 45_6]$	0.08	0	0.09	0.48
	0.16	0	0.38	1.90
	0.32	0	1.50	7.17

Table 7: Effect of neglecting the local stiffnesses on the elements of the stiffness matrix of open section beams as a function of the wall thickness, h

suggested by [16] is applicable, if the layup is symmetrical (thus $[B] = 0$). The error in the $\overline{P}_{11}$, $\overline{P}_{22}$, and $\overline{P}_{33}$ terms of the stiffness matrix is illustrated in Table 7 for I-beams, which results if local bending stiffnesses are neglected, are presented in Table 7 as a function of wall thickness, h. (Note the $\overline{P}_{i4}$ elements for open section beams depend directly on the thickness of the wall.)

For *closed-section beams*: When the layup is symmetrical, as a rule, the $[D]$ matrix can be neglected in the calculation of the elements of the stiffness matrix ($\overline{P}_{ij}$, $i, j = 1, 2, 3, 4$). This is illustrated in Table 8 where the elements $\overline{P}_{11}$, $\overline{P}_{22}$, $\overline{P}_{33}$, $\overline{P}_{44}$ are shown as a function of h.

Unsymmetrical layup When the layup is unsymmetrical, the omission of the $[\beta]$ matrix may cause considerable errors. The reason being the β_{16} term in the compliance matrix of the laminate may cause tension-twist coupling. (We may neglect the $[\delta]$ matrix, though this approximation does not simplify the analysis.)

Unsymmetrical-orthotropic layup When the layup is orthotropic the 1,6 and 2,6 elements of the $[A]$, $[B]$, $[D]$ (and consequently of the $[\alpha]$, $[\beta]$, $[\delta]$) matrices are zero.

For *open-section beams*, the most important term in the laminate's compliance matrix (which plays a role in the bending and tensile stiffnesses of the beam) is α_{11} which relates the axial force per unit length (N_ξ) to the axial strain ϵ_ξ. The value of α_{11} depends on the choice of the reference plane. We found that the $[\beta]$ and $[\delta]$ matrices can be neglected in the calculation of the bending and tensile stiffnesses only if the reference surface is chosen such, that β_{11} is equal to zero ($\beta_{11} = 0$)

layup	Box beam	error in the elements of the stiffness matrix (%)			
	h/d_t	P_{11}	P_{22}	P_{33}	P_{44}
$[0_{12}]$	0.08	0.00	0.15	0.36	1.28
	0.16	0.00	0.61	1.41	4.94
	0.32	0.00	2.40	5.41	17.22
$[45_{12}]$	0.08	0.00	0.20	0.48	4.08
	0.16	0.00	0.82	1.87	14.54
	0.32	0.00	3.18	7.10	40.49
$[0_6/90_6]$	0.08	0.18	0.07	0.14	1.28
	0.16	0.18	0.29	0.51	4.94
	0.32	0.18	1.26	1.74	17.22
$[0_6/\pm 45_6]$	0.08	0.76	0.08	0.17	0.81
	0.16	0.76	0.35	0.64	3.71
	0.32	0.76	1.52	2.19	17.98

Table 8: Effect of neglecting the local stiffnesses on the elements of the stiffness matrix of closed section beams as a function of the wall thickness, h

(as it was suggested by [5]). This condition gives the following expression for the location of the ("tension neutral") reference surface (see Appendix D).

$$\rho = -\frac{\beta_{11}}{\delta_{11}} \tag{3.100}$$

By this choice of the reference surface the $[\alpha]$, $[\beta]$ and $[\delta]$ matrices of the $[0_6/90_6]$ and $[0_6/\pm 45_6]$ layups (see Table 3) simplify as shown in Table 9.

We note that the results of the analysis given in Section 3.6 are practically unaffected by the choice of the reference surface. However, in this case the $[\beta]$ and $[\delta]$ matrices may be neglected, which is illustrated in Table 7.

(Note that the torsional stiffness depends on the δ_{66} term which is unaffected by the choice of the reference surface.)

For *closed-section beams* α_{11} plays an important role in the bending and tensile stiffnesses of the beam and the reference surface given by Equation (3.100) must be used in the evaluation of α_{11}. We found the α_{66} term dominates the torsional stiffness. In the calculation of the torsional stiffness the $[\beta]$ and $[\delta]$ matrices may be neglected only if the reference surface is chosen such that β_{66} is zero. To determine the location of the reference surface, where β_{66} is zero (referred to as the ("torque neutral") reference surface, see Appendix D)

$$\nu = -\frac{\beta_{66}}{\delta_{66}} \tag{3.101}$$

Layups	$[0_6/90_6]$	$[0_6/\pm 45_6]$
ρ	-0.4388	-0.4000
ν	0	0.3935
$[\alpha]$ $(10^{-3}$mm/N)	$\begin{bmatrix} 0.0063 & -0.0009 & 0 \\ -0.0009 & 0.0409 & 0 \\ 0 & 0 & 0.1734 \end{bmatrix}$	$\begin{bmatrix} 0.0061 & -0.0029 & 0 \\ -0.0029 & 0.0612 & 0 \\ 0 & 0 & 0.1060 \end{bmatrix}$
$[\beta]$ $(10^{-3}1$/N)	$\begin{bmatrix} 0 & 0.0007 & 0 \\ 0.0007 & -0.0394 & 0 \\ 0 & 0 & -0.1447 \end{bmatrix}$	$\begin{bmatrix} 0 & -0.0019 & 0 \\ -0.0019 & -0.0551 & 0 \\ 0 & 0 & -0.1040 \end{bmatrix}$
$[\delta]$ $(10^{-3}1$/Nmm)	$\begin{bmatrix} 0.0449 & -0.0017 & 0 \\ -0.0017 & 0.0449 & 0 \\ 0 & 0 & 0.3297 \end{bmatrix}$	$\begin{bmatrix} 0.0349 & -0.0257 & 0 \\ -0.0257 & 0.0988 & 0 \\ 0 & 0 & 0.1311 \end{bmatrix}$

Table 9: The compliance matrices of two laminates with respect to the "tension neutral" (ρ) reference plane, and the location of the "tension neutral" and "torque neutral" (ν) surfaces

Therefore the torsional stiffness must be evaluated for a reference surface which is different from the reference surface used in calculating the bending and tensile stiffnesses.

To use two reference surfaces is unpractical.. Instead, we suggest to attach the reference surface to the location given by Equation (3.100), and use the compliances α_{11}, α_{22}, $\alpha_{12}, \alpha^{\nu}_{66}$, where

$$\alpha^{\nu}_{66} = \alpha_{66} + 2\nu\beta_{66} + \nu^2\delta_{66} \tag{3.102}$$

α_{66}, β_{66} and δ_{66} are evaluated at the reference surface given by Equation (3.100). (α^{ν}_{66} is identical to the α_{66} stiffness evaluated at the reference surface defined by Equation (3.101)).

4 Theory of open section, orthotropic, thin-walled beams - with restrained warping

In Section 2.6.2 the stress-strain relationship for open section, orthotropic, thin-walled beams are given according to [12]. The basic assumptions of this beam theory are given in Section 2.6.1. We summarize below the governing equations of open section, orthotropic thin-walled beams ([12]), and present the expressions for calculating the shear stiffnesses.

The equilibrium equations in matrix form are as follows:

$$\begin{bmatrix} & & & -\frac{d}{dx} & & \\ & & & & -\frac{d}{dx} & \\ & & -\frac{d}{dx} & & & -\frac{d}{dx} \\ \frac{d}{dx} & & & -1 & & \\ & \frac{d}{dx} & & & -1 & \\ & & \frac{d}{dx} & & & -1 \end{bmatrix} \begin{Bmatrix} \widehat{M}_{\overline{y}} \\ \widehat{M}_{\overline{z}} \\ \widehat{M}_{\overline{\omega}} \\ \widehat{T}_{\overline{sv}} \\ \widehat{V}_{\overline{y}} \\ \widehat{V}_{\overline{z}} \\ \widehat{T}_{\overline{\omega}} \end{Bmatrix} = \begin{Bmatrix} p_y \\ p_z \\ t \\ 0 \\ 0 \\ 0 \end{Bmatrix} \tag{4.1}$$

where p_y and p_z are the external loads in the $y-x$ and $z-x$ planes and t is the distributed torque (see Figure 19), and the internal forces $\left(\widehat{M}_{\overline{y}},\ \widehat{M}_{\overline{z}},\ \widehat{M}_{\overline{\omega}},\ \widehat{T}_{\overline{sv}},\ \widehat{V}_{\overline{y}},\ \widehat{V}_{\overline{z}} \text{ and } \widehat{T}_{\overline{\omega}}\right)$ were defined on pages 11 and 13.

The stress-strain relationship (Equation 2.26) *is the following*:

$$\begin{Bmatrix} \widehat{M}_{\overline{y}} \\ \widehat{M}_{\overline{z}} \\ \widehat{M}_{\overline{\omega}} \\ \widehat{T}_{\overline{sv}} \\ \widehat{V}_{\overline{y}} \\ \widehat{V}_{\overline{z}} \\ \widehat{T}_{\overline{\omega}} \end{Bmatrix} = \begin{bmatrix} \overline{EI}_{yy} & \overline{EI}_{yz} & & & & & & \\ \overline{EI}_{yz} & \overline{EI}_{zz} & & & & & & \\ & & \overline{EI}_{\omega} & & & & & \\ & & & \overline{GI}_t & & & & \\ & & & & \overline{S}_{yy} & \overline{S}_{yz} & \overline{S}_{y\omega} \\ & & & & \overline{S}_{yz} & \overline{S}_{zz} & \overline{S}_{z\omega} \\ & & & & \overline{S}_{y\omega} & \overline{S}_{z\omega} & \overline{S}_{\omega\omega} \end{bmatrix} \begin{Bmatrix} \frac{1}{\rho_{\overline{y}}} \\ \frac{1}{\rho_{\overline{z}}} \\ \overline{\Gamma} \\ \overline{\vartheta} \\ \gamma_{\overline{y}} \\ \gamma_{\overline{z}} \\ \overline{\vartheta}_s \end{Bmatrix} \tag{4.2}$$

where the generalized strains $\left(\frac{1}{\rho_{\overline{y}}},\ \frac{1}{\rho_{\overline{z}}},\ \overline{\Gamma},\ \overline{\vartheta},\ \gamma_{\overline{y}},\ \gamma_{\overline{z}} \text{ and } \overline{\vartheta}_s\right)$ were defined on pages 11, 13, 14 and 17. In the stiffness matrix $\overline{EI}_{yy}$, $\overline{EI}_{zz}$, $\overline{EI}_{yz}$ are the bending stiffnesses, $\overline{EI}_{\omega}$ is the warping stiffness, $\overline{GI}_t$ is the torsional stiffness and $\overline{S}_{ij}$ are the shear stiffnesses.

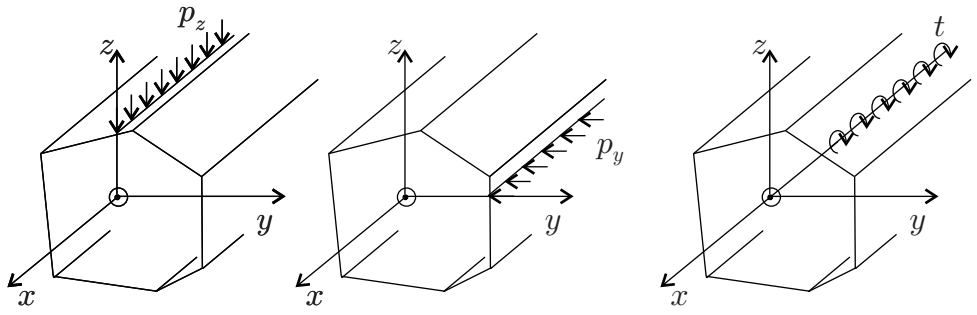

Figure 19: Loads on a closed section thin-walled beam

The strain-displacement relationship is given by:

$$\begin{Bmatrix} \frac{1}{\rho_{\overline{y}}} \\ \frac{1}{\rho_{\overline{z}}} \\ \overline{\Gamma} \\ \overline{\vartheta} \\ \gamma_{\overline{y}} \\ \gamma_{\overline{z}} \\ \overline{\vartheta}_s \end{Bmatrix} = \begin{bmatrix} & & & -\frac{d}{dx} & & \\ & & & & -\frac{d}{dx} & \\ & & & & & -\frac{d}{dx} \\ & & \frac{d}{dx} & & & \\ \frac{d}{dx} & & & -1 & & \\ & \frac{d}{dx} & & & -1 & \\ & & \frac{d}{dx} & & & -1 \end{bmatrix} \begin{Bmatrix} v \\ w \\ \psi \\ \chi_y \\ \chi_z \\ \overline{\vartheta}_B \end{Bmatrix} \tag{4.3}$$

It can be seen that the shear deformation in torsion is defined analogously to the shear deformation in bending. We can calculate the bending, torsional and warping stiffnesses in the same way as for beams made of isotropic material [5]. Below we will give the calculation of the shear compliances which are defined as

$$\begin{bmatrix} \overline{s}_{yy} & \overline{s}_{yz} & \overline{s}_{y\omega} \\ \overline{s}_{yz} & \overline{s}_{zz} & \overline{s}_{z\omega} \\ \overline{s}_{y\omega} & \overline{s}_{z\omega} & \overline{s}_{\omega\omega} \end{bmatrix} = \begin{bmatrix} \overline{S}_{yy} & \overline{S}_{yz} & \overline{S}_{y\omega} \\ \overline{S}_{yz} & \overline{S}_{zz} & \overline{S}_{z\omega} \\ \overline{S}_{y\omega} & \overline{S}_{z\omega} & \overline{S}_{\omega\omega} \end{bmatrix}^{-1} \tag{4.4}$$

According to [12] the shear flow consist of three parts:

$$q = \widehat{V}_{\overline{y}} q_y + \widehat{V}_{\overline{z}} q_z + \widehat{T}_{\overline{\omega}} q_\omega \tag{4.5}$$

where q_y, q_z and q_ω are the shear flows caused by unit shear loads ($\widehat{V}_{\overline{y}} = 1$, $\widehat{V}_{\overline{z}} = 1$) and by a unit torque ($\widehat{T} = \widehat{T}_{\overline{\omega}} = 1$), respectively. The shear flows q_y, q_z and q_ω can be calculated according to the classical analysis of thin walled beams [17]. The expressions of $\overline{s}_{yy}$, $\overline{s}_{zz}$, $\overline{s}_{\omega\omega}$, $\overline{s}_{yz}$, $\overline{s}_{y\omega}$ and $\overline{s}_{z\omega}$ are as follows [12]

$$\begin{aligned} \overline{s}_{yy} &= \oint \widetilde{\alpha}_{66} q_y^2 ds \qquad \overline{s}_{zz} = \oint \widetilde{\alpha}_{66} q_z^2 ds \qquad \overline{s}_{\omega\omega} = \oint \widetilde{\alpha}_{66} q_\omega^2 ds \\ \overline{s}_{yz} &= \oint \widetilde{\alpha}_{66} q_y q_z ds \qquad \overline{s}_{y\omega} = \oint \widetilde{\alpha}_{66} q_y q_\omega ds \qquad \overline{s}_{z\omega} = \oint \widetilde{\alpha}_{66} q_y q_\omega ds \end{aligned} \tag{4.6}$$

5 Theory of closed section, orthotropic, thin-walled beams - with restrained warping

First we summarize those theories which —at least in principle— may provide the stresses and displacements with reasonable accuracy (Section 5.1). Then a new theory for closed section, orthotropic, thin-walled beams will be presented. We will compare the accuracy of this new and that of the available theories in Section 5.7.5.

5.1 Literature

Urban-Kristek theory

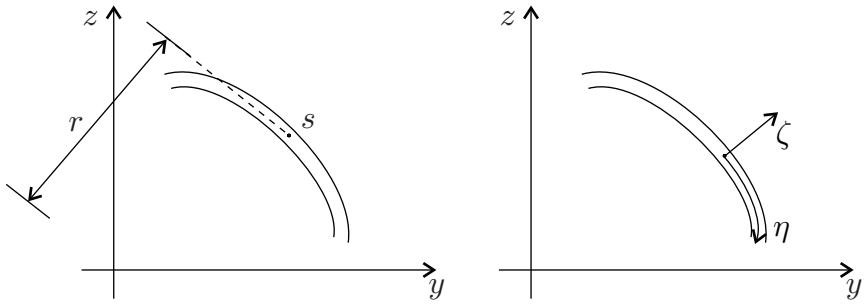

Figure 20: Definition of r

Urban [20] investigated the torsion of doubly symmetrical, closed section, isotropic, prismatic beams by using the basic assumptions given in Section 2.6.1. These results were generalized by Kristek [7] for beams with variable cross-section (see Section 2.6.2). We present below the governing equations for uniform cross-section (prismatic beams).

Kristek [7] took into account the torque due to the shear flow (and neglect the small effect of the distributed torque moment), hence the torque is

$$\widehat{T} = \oint qrd\eta \tag{5.1}$$

where r is the distance between the tangent of the wall and the axis of rotation (see Figure 20), and q is the shear flow, defined as

$$q = \int_{(h)} \oint \tau_{x\eta} d\zeta \tag{5.2}$$

The torque consist of two parts:

$$\widehat{T} = \widehat{T}_{sv} + \widehat{T}_{\omega} \tag{5.3}$$

which can be expressed as:

$$\widehat{T}_{sv} = GI_t\vartheta \qquad \widehat{T}_{\omega} = -EI_{\omega}\frac{d^2\vartheta_B}{dx^2} \tag{5.4}$$

Kristek assumed that the shear flow is uniform, and can be calculated as:

$$q = \frac{1}{\widetilde{\alpha}_{66}}\gamma_{xs} \tag{5.5}$$

where the shear strain γ_{xs} of the middle surface is

$$\gamma_{xs} = \frac{\partial u}{\partial \eta} + \frac{\partial v_s}{\partial x} \tag{5.6}$$

Here, u is the axial, while v_s is the tangential displacements, calculated as:

$$u = \omega\overline{\vartheta}_B \qquad v_s = r\overline{\psi} \tag{5.7}$$

The warping function ω for closed section beams is calculated by

$$\omega = \frac{2A\int \frac{1}{h}d\eta}{\oint \frac{1}{h}d\eta} - \int rd\eta \tag{5.8}$$

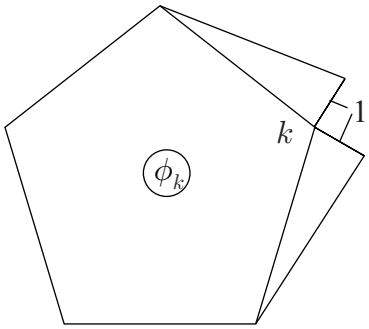

Figure 21: Circumferential distribution of the k-th axial displacement function (ϕ_k)

From Equations (5.1) – (5.8) Kristek derived the following differential equation for pure torsion:

$$\frac{d^2\vartheta_B}{dx^2} - \vartheta_B \frac{GI_t}{EI_\omega} H = -\widehat{T}\frac{H}{EI_\omega} \tag{5.9}$$

where the stiffnesses are defined as:

$$GI_k = G\frac{4A^2}{\oint \frac{1}{h} d\eta} \tag{5.10}$$

$$EI_\omega = E \oint \omega^2 d\eta \tag{5.11}$$

$$GI_c = G \oint r^2 d\eta \tag{5.12}$$

$$H = 1 - \frac{GI_t}{GI_c} \tag{5.13}$$

Vlasov theory

Vlasov applied the principle of virtual displacements for calculating the displacements, stresses and strains of multicell non-symmetrical beams made of isotropic material.

He approximated the axial displacement as

$$u(x,s) = \sum_{k=1}^{K} U_k(x)\phi_k(s) \tag{5.14}$$

where K is the number of the wall segments, ϕ_k represents the "generalized coordinates of the warped elementary transverse strip of a thin walled beam with respect to the plane of the initial cross-section", and U_k are the unknown generalized longitudinal displacements of the thin-walled beam. The suggested ϕ_k function is presented in Figure 21. (Vlasov assumed the tangential displacements (v_s) in the same form as given by Equation (5.14). Consequently, the cross-section may deform in its own plane. The modifications because of the deformable cross-section are not presented in this section.) By applying the principle of virtual displacements he arrived at the following equations:

$$\int \frac{\partial \sigma_x}{\partial x}\phi_k dF - \int \tau \frac{\partial \phi_k}{\partial \eta} dF - \int r\phi_k d\eta = 0 \qquad k = 1, \ldots, K \tag{5.15}$$

The normal and the shear stress are:

$$\sigma_x = E\frac{\partial u}{\partial x} \qquad \tau = G\left(\frac{\partial u}{\partial \eta} + \frac{\partial v_s}{\partial x}\right) \tag{5.16}$$

Substituting Equation (5.14) and Equation (5.16) into Equation (5.15) we obtain a system of K linear differential equations for the required K longitudinal displacements U_k :

$$\sum_{i=1}^{K} \int E\frac{\partial \phi_k}{\partial \eta}\frac{\partial \phi_i}{\partial \eta} dF \frac{\partial^2 U_k}{\partial x^2} - \sum_{i=1}^{K} \int G\phi_i\phi_k dF U_k - \int r_k\phi_k d\eta = 0 \qquad k = 1, \ldots, K \tag{5.17}$$

We have to emphasize that Vlasov's theory is not a beam theory in the sense that the order of the governing differential equation system depends on the number of the wall segments of the cross-section.

In addition, because of the assumptions for the displacement field neither of the above theories provides the results with acceptable accuracy when the stiffnesses of the wall segments differ from each other significantly (see Section 5.7.5).

Numerical comparisons with Kristek's theory will be given in Section 5.7.5.

In the following we present a new theory for the calculation of the displacements of closed section, orthotropic, thin-walled beams.

5.2 Problem statement

In the following sections we consider thin-walled closed section prismatic beams. The walls of the beams may consist of a single layer or of several layers, each layer may be made of composite materials. The beam consists of flat segments (Figure 22) designated by the subscript k ($k = 1, 2, \ldots, K$, where K is the total number of the wall segments). The cross-section may be symmetrical or unsymmetrical and the layup of the wall is orthotropic.

5.3 Assumptions

In the present theory we use the first three assumptions given in Section 2.2.1, which are reiterated here:

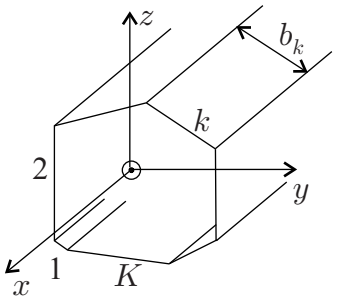

Figure 22: Cross-section of the thin-walled beam

1. The effect of change in geometry of the cross-section is not taken into account in the equilibrium equations.

2. The Kirchhoff-Love hypotesis is valid for each plate element.

3. The normal stresses in the contour directions is small compared to the axial stresses.

5.4 Governing equations

We employ the same coordinate systems as in Section 3 (Figure 23).

For the beam we use the x-y-z coordinate system with the origin at the centroid and the $\overline{x}$-$\overline{y}$-$\overline{z}$ coordinate system with the origin at an arbitrarily chosen point. For the k-th segment we employ the ξ_k-η_k-ζ_k coordinate system with the origin at the center of the reference plane of the k-th segment. ξ is parallel to the x coordinate, η is along the circumference of the wall, and ζ is perpendicular to the circumference.

The axial displacements of an arbitrary point's of the cross-section (Figure 24) is given by [13]:

$$u\left(s\right) = -\int_0^s r d\eta \vartheta + \int_0^s \gamma^0_{\xi\eta} d\eta \tag{5.18}$$

where η is the circumferential coordinate, r is given in Figure 20, ϑ is the rate of twist and $\gamma^0_{\xi\eta}$ is the shear strain. For an orthotropic wall the stress-strain relationship is given as [9]

$$\left\{\begin{array}{c} \epsilon^o_\xi \\ \epsilon^o_\eta \\ \gamma^0_{\xi\eta} \\ \kappa_\xi \\ \kappa_\eta \\ \kappa_{\xi\eta} \end{array}\right\}_k = \left[\begin{array}{cccccc} \alpha_{11} & \alpha_{12} & 0 & \beta_{11} & \beta_{12} & 0 \\ \alpha_{12} & \alpha_{22} & 0 & \beta_{21} & \beta_{22} & 0 \\ 0 & 0 & \alpha_{66} & 0 & 0 & \beta_{66} \\ \beta_{11} & \beta_{21} & 0 & \delta_{11} & \delta_{12} & 0 \\ \beta_{12} & \beta_{22} & 0 & \delta_{12} & \delta_{22} & 0 \\ 0 & 0 & \beta_{66} & 0 & 0 & \delta_{66} \end{array}\right]_k \left\{\begin{array}{c} N_\xi \\ N_\eta \\ N_{\xi\eta} \\ M_\xi \\ M_\eta \\ M_{\xi\eta} \end{array}\right\}_k \tag{5.19}$$

where the calculation of the elements of the compliance matrix (α_{ij},β_{ij}, δ_{ij}) are given by [9], ϵ^o_ξ, ϵ^o_η, $\gamma^0_{\xi\eta}$ are the strains of the reference surface of the wall, κ_ξ, κ_η, $\kappa_{\xi\eta}$ are the curvatures of the

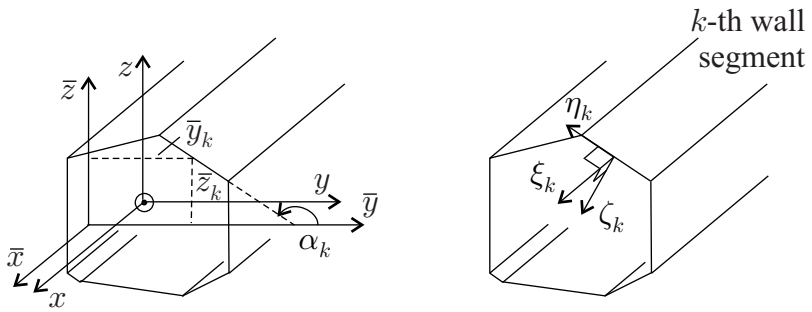

Figure 23: Coordinate systems employed in the analysis of thin-walled beams with arbitrary layup

wall, N_ξ, N_η, $N_{\xi\eta}$ are the in plane forces (per unit length) and M_ξ, M_η, $M_{\xi\eta}$ are the moments (per unit length) as illustrated in Figure 25.

The first and third rows of Equation (5.19) are

$$\epsilon^o_{\xi k} = (\alpha_{11})_k N_{\xi k} + (\alpha_{12})_k N_{\eta k} + (\beta_{11})_k M_{\xi k} + (\beta_{12})_k M_{\eta k} \tag{5.20}$$

$$\gamma^0_{\xi\eta k} = (\alpha_{66})_k N_{\xi\eta k} + (\beta_{66})_k M_{\xi\eta k} \tag{5.21}$$

By definition $N_{\xi\eta k}$ is the shear flow, and we write

$$N_{\xi\eta k} = q \tag{5.22}$$

$N_{\eta k}$ and $M_{\eta k}$ are small and can be neglected (see Assumption 3)

$$N_{\eta k} \cong 0 \qquad M_{\eta k} \cong 0 \tag{5.23}$$

From Equations (5.20) and (5.21) we obtain

$$\epsilon^o_{\xi k} = (\alpha_{11})_k N_{\xi k} + (\beta_{11})_k M_{\xi k} \tag{5.24}$$

$$\gamma^0_{\xi\eta k} = (\alpha_{66})_k q + (\beta_{66})_k M_{\xi\eta k} \tag{5.25}$$

When the wall is symmetrical $\left(\beta_{ij}\right)_k = 0$, and consequently Equations (5.24) and (5.25) become

$$N_{\xi k} = \frac{1}{(\alpha_{11})_k} \epsilon^o_{\xi k} \tag{5.26}$$

$$\gamma^0_{\xi\eta k} = (\alpha_{66})_k q \tag{5.27}$$

(Note however, that these relationships can be applied for unsymmetrical layups, provided that $(\alpha_{11})_k$ is evaluated at the "tension neutral" and $(\alpha_{66})_k$ at the "torque neutral" surface (see Appendix D).)

By substituting Equations (5.18) and (5.27) (together with $\epsilon^o_{\xi k} = \partial u/\partial x$) into Equation (5.26) we have

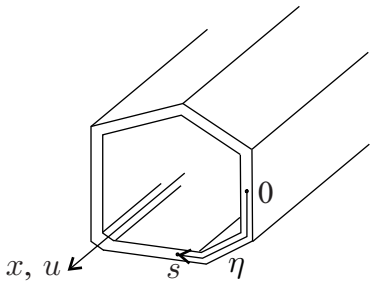

Figure 24: Definition of u, s, η

$$N_{\xi k}(s) = \frac{1}{(\alpha_{11})_k} \frac{d}{dx} \left(- \int_0^s r d\eta \vartheta + \int_0^s \alpha_{66} q d\eta \right) \tag{5.28}$$

The equilibrium equation in the axial direction (see Figure 26) results in

$$\frac{\partial N_{\xi k}}{\partial x} + \frac{\partial q_k}{\partial \eta} = 0 \tag{5.29}$$

We substitute Equation (5.28) into Equation (5.29), and write

$$\frac{1}{(\alpha_{11})_k} \frac{\partial^2}{\partial x^2} \left(- \int_0^s r d\eta \vartheta + \int_0^s \alpha_{66} q d\eta \right) + \frac{\partial q_k}{\partial \eta} = 0 \tag{5.30}$$

By differentiating with respect to η, after algebraic manipulation, we obtain

$$-r_k \frac{\partial^2 \vartheta}{\partial x^2} + (\alpha_{66})_k \frac{\partial^2 q_k}{\partial x^2} + (\alpha_{11})_k \frac{\partial^2 q_k}{\partial \eta^2} = 0 \tag{5.31}$$

This second order differential equation is valid for every wall segment ($k = 1, \ldots, K$). The following continuity conditions must be satisfied.

The shear flow must be continuous, hence, we have:

$$q_k \mid_{\frac{b_k}{2}} = q_{k+1} \mid_{-\frac{b_{k+1}}{2}} \qquad k = 1, \ldots, K \tag{5.32}$$

The axial displacements (u) of the adjacent walls must be identical. A necessary condition is that the derivative of the axial strains are identical. Consequently, we write

$$(\alpha_{11})_k \frac{\partial q_k}{\partial \eta} \mid_{\frac{b_k}{2}} = (\alpha_{11})_{k+1} \frac{\partial q_{k+1}}{\partial \eta} \mid_{-\frac{b_{k+1}}{2}} \qquad k = 1, \ldots, K \tag{5.33}$$

(Note that in the above equations $K + 1$ must be replaced by 1, see Figure 22.)

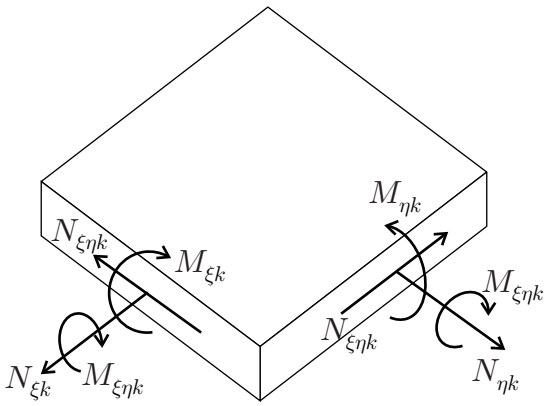

Figure 25: In plane forces and moments of a plate element

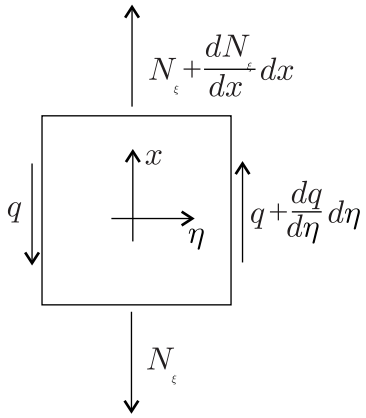

Figure 26: Forces on an element of the wall

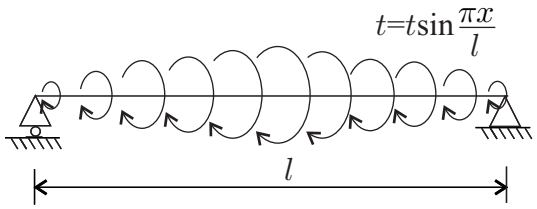

Figure 27: Simply supported beam subjected to a sinusoidal torque

5.5 "Exact" solution for sinusoidal loads

We consider a simply supported beam (Figure 27) subjected to a sinusoidal torque $t = \widetilde{t} \sin \pi x/l$, we assume that the beam undergoes pure torsion. (At a simple support $\psi = 0$, $\psi'' = 0$.) The solution of this problem is assumed to be in the form of the following functions

$$\vartheta = \widetilde{\vartheta} \cos \frac{\pi x}{l} \qquad q_k = \widetilde{q}_k (\eta) \cos \frac{\pi x}{l} \tag{5.34}$$

where $\widetilde{q}_k$ is a function of η only.

Note that these functions satisfy the boundary conditions at $x = 0$ and $x = l$. By substituting Equation (5.34) into Equation (5.31) we obtain

$$\left(r_k \frac{\pi^2}{l^2} \widetilde{\vartheta} - (\alpha_{66})_k \frac{\pi^2}{l^2} \widetilde{q}_k + (\alpha_{11})_k \frac{\partial \widetilde{q}_k}{\partial \eta^2} \right) \cos \frac{\pi x}{l} = 0 \tag{5.35}$$

which results in the following second order, ordinary, inhomogeneous differential equation:

$$(\alpha_{66})_k \frac{\pi^2}{l^2} \widetilde{q}_k - (\alpha_{11})_k \frac{\partial \widetilde{q}_k}{\partial \eta^2} = r_k \frac{\pi^2}{l^2} \widetilde{\vartheta} \tag{5.36}$$

The general solution is [14]

$$\frac{\widetilde{q}_k}{\vartheta_{\widetilde{\vartheta}0}} = \frac{r_k}{(\alpha_{66})_k} + C_{1,k} e^{-\lambda_k \left(\frac{b_k}{2} + \eta \right)} + C_{2,k} e^{-\lambda_k \left(\frac{b_k}{2} - \eta \right)} \tag{5.37}$$

where

$$\lambda_k = \frac{\pi}{l}\sqrt{\frac{(\alpha_{66})_k}{(\alpha_{11})_k}} \tag{5.38}$$

By substituting Equation (5.37) into Equations (5.32) and (5.33) we have

$$C_{1,k}e^{-\lambda_k b_k} + C_{2,k} - C_{1,k+1} - C_{2,k+1}e^{-b_{k+1}\lambda_{k+1}} = \frac{r_k}{(\alpha_{66})_k} - \frac{r_k}{(\alpha_{66})_k} \tag{5.39}$$

$$\begin{aligned} -(\alpha_{11})_k \lambda_k e^{-\lambda_k b_k} C_{1,k} + (\alpha_{11})_k \lambda_k C_{2,k} \quad &= \quad -(\alpha_{11})_{k+1} \lambda_{k+1} C_{1,k+1} + \\ &\quad + (\alpha_{11})_{k+1} \lambda_{k+1} e^{-b_{k+1}\lambda_{k+1}} C_{2,k+1} \end{aligned} \tag{5.40}$$

where $k = 1, \ldots, K$.

There are $2\times K$ equations from which the $2\times K$ unknowns ($C_{1,k}$, $C_{2,k}$ $\quad k = 1, \ldots, K$) can be calculated for a given $\widetilde{\vartheta}$. From the shear flow the torque and the load can be calculated (for a given $\widetilde{\vartheta}$) as

$$\widehat{T} = \oint q r d\eta \tag{5.41}$$

$$t = \int_0^l \widehat{T} dx = \int_0^l \oint q r d\eta dx \tag{5.42}$$

We emphasize that the shear flow (Equation 5.37) is the exact solution of the differential equation system, and hence, they can be used even in the case when the stiffnesses of the walls differ significantly.

5.6 Solution by the Ritz method

In the following we derive an approximate solution of the above differential equations by the Ritz method. The potential energy of the beam is

$$\Pi = \frac{1}{2}\int\int \left(N_\xi \epsilon_\xi^o + q\gamma_{\xi\eta}^0\right) d\eta dx - \int \vartheta t dx \tag{5.43}$$

where the first term is the strain energy and the second is the work done by the external load.

The axial force per unit length is (Equation 5.29):

$$N_\xi = -\int \frac{\partial q}{\partial \eta} dx \tag{5.44}$$

Equations (5.26), (5.27), (5.34), (5.44) and (5.43) result in

$$\Pi = \frac{1}{2}\int\int \left(\alpha_{11}\frac{l^2}{\pi^2}\left(\frac{\partial^2 q}{\partial \eta^2}\right)^2 + \alpha_{66} q^2\right) d\eta dx - \int \vartheta t dx \tag{5.45}$$

The shear flow is assumed to be in the form of

$$q \quad = \quad \widetilde{q}(\eta) \sin\frac{\pi x}{l} \tag{5.46}$$

$$\widetilde{q}(\eta) \quad = \quad \sum_{k=1}^{2K} C_k \phi_k(\eta) \tag{5.47}$$

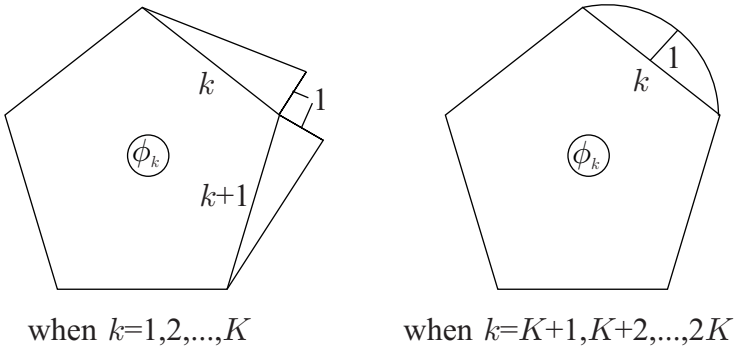

Figure 28: Functions ϕ_k

where C_k are yet unknown constants and the functions ϕ_k are illustrated in Figure 28 and are given below

$$\phi_k = \left\{ \begin{array}{lll} \frac{\eta}{b_k} + \frac{1}{2} & \text{when} & i = k \\ -\frac{\eta}{b_{k+1}} + \frac{1}{2} & \text{when} & i = k+1 \\ 0 & \text{else} & \end{array} \right\} \text{ when } k \leq K \tag{5.48}$$

$$\phi_k = \left\{ \begin{array}{lll} -\frac{4\eta^2}{b_k^2} + 1 & \text{when} & i = k \\ 0 & \text{else} & \end{array} \right\} \text{ when } k > K$$

The shear flow on the k-th wall consists of three parts

$$\widetilde{q}_k = C_{k-1}\phi_{k-1} + C_k\phi_k + C_{K+k}\phi_{K+k} \tag{5.49}$$

By substituting Equation (5.46) into Equation (5.45) we obtain

$$\Pi = \frac{1}{2}\mathbf{c}^T [F]\, \mathbf{c} - \mathbf{c}^T \mathbf{f} \tag{5.50}$$

where the kth element of the $\mathbf{c}$ and $\mathbf{f}$ vectors are

$$\mathbf{c}_k = C_k \qquad \mathbf{f}_k = \int \vartheta \phi_k r_k d\eta \qquad k = 1, \ldots, K \tag{5.51}$$

and the ik element of matrix $[F]$ is

$$F_{ik} = \int_{-b_k/2}^{b_k/2} \left((\alpha_{11})_k \frac{l^2}{\pi^2} \frac{\partial \phi_k}{\partial \eta} \frac{\partial \phi_i}{\partial \eta} + (\alpha_{66})_k \phi_k \phi_i \right) d\eta \tag{5.52}$$

According to the principle of stationary potential energy, we have

$$\Pi = \frac{1}{2}\mathbf{c}^T [F]\, \mathbf{c} - \mathbf{c}^T \mathbf{f} = \text{stacionary!} \tag{5.53}$$

The necessary condition for Equation (5.53) is $\partial\pi/\partial C_k = 0$, which result in the following equation:

$$[F]\,\mathbf{c} - \mathbf{f} = 0 \tag{5.54}$$

The unknown constants can be calculated as

$$\mathbf{c} = [F]^{-1}\,\mathbf{f} \tag{5.55}$$

When the constants are known, q can be calculated by Equation (5.46). From q the torque load can be calculated by Equation (5.42).

5.7 Beam theory

5.7.1 Assumptions

The first three assumptions in Section 5.3 are valid. In addition, the present beam theory uses the assumption in Section 2.6.1, which is reiterated here:

The axial strain is (Equation 2.22):

$$\epsilon_x^o = \frac{du}{dx} - y\frac{d\chi_y}{dx} - z\frac{d\chi_z}{dx} - \omega\frac{d\vartheta_B}{dx} \tag{5.56}$$

where

$$\begin{aligned} \chi_y &= \frac{dv}{dx} - \gamma_y \\ \chi_z &= \frac{dw}{dx} - \gamma_z \\ \vartheta_B &= \frac{d\psi}{dx} - \vartheta_S \end{aligned} \tag{5.57}$$

Couplings between normal and shearing effects are neglected.

5.7.2 Pure torsion - Governing equations

For convenience we separate the shear flow q as

$$q = q_0 + q_\omega \tag{5.58}$$

where q_0 is uniform around the circumference (Figure 29). These shear flows result in the following torques

$$\widehat{T}_{sv} = \oint q_0 r d\eta \qquad \widehat{T}_\omega = \oint q_\omega r d\eta \tag{5.59}$$

and the total torque is

$$\widehat{T} = \widehat{T}_{sv} + \widehat{T}_\omega \tag{5.60}$$

The shear flow results in a rate of twist

$$\vartheta = \frac{\oint q\alpha_{66} d\eta}{2A} \tag{5.61}$$

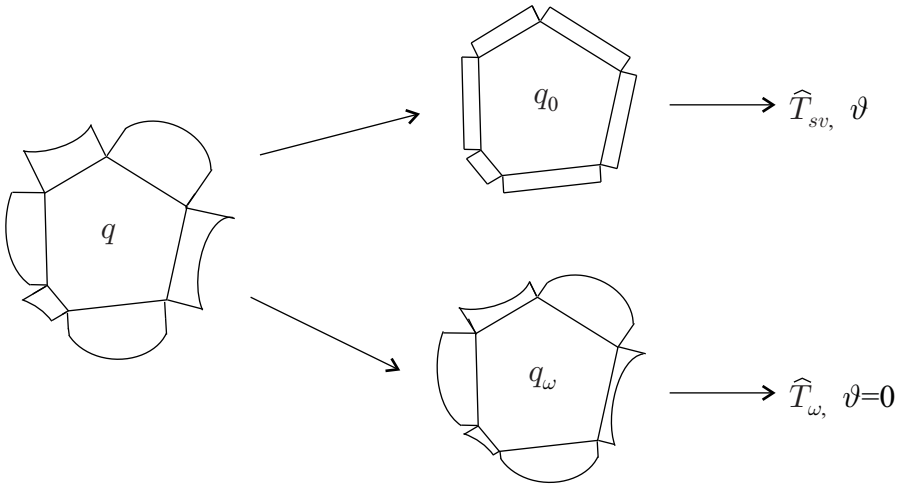

Figure 29: Shear flow $q = q_0 + q_\omega$

where A is the enclosed area.

We separate q (Equation 5.58) such that q_ω does not cause a twist. Hence we have

$$\frac{\oint q_\omega \alpha_{66} d\eta}{2A} = 0 \tag{5.62}$$

and

$$\vartheta = \frac{\oint q_0 \alpha_{66} d\eta}{2A} = q_0 \frac{\oint \alpha_{66} d\eta}{2A} \tag{5.63}$$

We define the bimoment $\widehat{M}^*_{\overline{\omega}}$ such that the first derivative of $\widehat{M}^*_{\overline{\omega}}$ is equal to $\widehat{T}_{\overline{\omega}}$. (See Equation 4.1 for open section beams.)

$$\widehat{T}_{\overline{\omega}} = \frac{d\widehat{M}^*_{\overline{\omega}}}{dx} \tag{5.64}$$

Note, however, that Vlasov's definition for the bimoment, $\widehat{M}_{\overline{\omega}} = \oint N_\xi r d\eta$, is different, Equations (5.44), (5.64) and (5.59) give

$$\widehat{M}^*_{\overline{\omega}} = \frac{\int \oint q_\omega r d\eta dx}{-\oint \int \frac{dq}{d\eta} dx r d\eta} \widehat{M}_{\overline{\omega}} \tag{5.65}$$

With Equation (5.64) we obtain the same equilibrium equations as for open section beams.

$$\begin{bmatrix} -\frac{d}{dx} & -\frac{d}{dx} & \\ & -1 & \frac{d}{dx} \end{bmatrix} \begin{Bmatrix} \widehat{T}_{\overline{sv}} \\ \widehat{T}_{\overline{\omega}} \\ \widehat{M}^*_{\overline{\omega}} \end{Bmatrix} = \begin{Bmatrix} t \\ 0 \end{Bmatrix} \tag{5.66}$$

Similarly, as for open section beams, we assume that the rate of twist consists of two terms, $\overline{\vartheta} = \overline{\vartheta}_S + \overline{\vartheta}_B$ (Equation 2.25) and write the strain-displacement relationship as (Equation 4.3)

$$\begin{Bmatrix} \overline{\vartheta} \\ \overline{\vartheta}_S \\ \overline{\Gamma} \end{Bmatrix} = \begin{bmatrix} \frac{d}{dx} & \\ \frac{d}{dx} & -1 \\ & -\frac{d}{dx} \end{bmatrix} \begin{Bmatrix} \overline{\psi} \\ \overline{\vartheta}_B \end{Bmatrix} \tag{5.67}$$

and assume that these generalized strains are related to the internal forces by

$$\begin{Bmatrix} \widehat{T}_{\overline{sv}} \\ \widehat{T}_{\overline{\omega}} \\ \widehat{M}^*_{\overline{\omega}} \end{Bmatrix} = \begin{bmatrix} \overline{GI}_t & & \\ & \overline{S}_{\omega\omega} & \\ & & \overline{EI}_\omega \end{bmatrix} \begin{Bmatrix} \overline{\vartheta} \\ \overline{\vartheta}_S \\ \overline{\Gamma} \end{Bmatrix} \tag{5.68}$$

where $\overline{GI}_t$, $\overline{S}_{\omega\omega}$ and $\overline{EI}_\omega$ are yet unknown stiffnesses. In the following section we will determine expressions for the stiffnesses to obtain an acceptable description for the beam with the above governing equations.

5.7.3 Replacement stiffnesses

To determine the stiffnesses $\overline{GI}_t$, $\overline{S}_{\omega\omega}$ and $\overline{EI}_\omega$ of the beam, we will make use of the derived solution for the case of beams subjected to a *sinusoidal load* (Sections 5.5, 5.6, Figure 27).

The strain energy of the beam is

$$U = \frac{1}{2}\left(\int_0^l \oint \left(\underbrace{\alpha_{11} N_\xi}_{\epsilon^o_\xi} N_\xi + \underbrace{\alpha_{66} q}_{\gamma^0_{\xi\eta}} q \right) d\eta \right) dx \tag{5.69}$$

We introduced the internal forces, generalized strains and the stiffnesses of the beam in the previous section. By using these definitions the strain energy can be written as

$$U = \frac{1}{2}\int_0^l \left(\widehat{T}_{\overline{sv}}\vartheta + \widehat{T}_{\overline{\omega}}\vartheta_s + \widehat{M}^*_{\overline{\omega}}\Gamma \right) dx = \frac{1}{2}\int_0^l \left(\frac{\widehat{T}^2_{\overline{sv}}}{\overline{GI}_t} + \frac{\widehat{T}^2_{\overline{\omega}}}{\overline{S}_{\omega\omega}} + \frac{\widehat{M}^{*2}_{\overline{\omega}}}{\overline{EI}_\omega} \right) dx \tag{5.70}$$

We recall (Equation 5.34) that for a sinusoidal load q and ϑ are trigonometrical functions, and hence, $\widehat{T}_{\overline{sv}}$, $\widehat{T}_{\overline{\omega}}$ and $\widehat{M}^*_{\overline{\omega}}$ are also trigonometrical functions and the integration with respect to x can be performed. From Equations (5.69) and (5.70), together with Equation (5.44) we obtain

$$U = \frac{1}{2}\frac{l}{\pi}\oint \alpha_{11}\frac{l^2}{\pi^2}\left(\frac{\partial^2 q}{\partial \eta^2}\right)^2 + \alpha_{66} q^2 d\eta \tag{5.71}$$

and

$$U = \frac{1}{2}\frac{l}{\pi}\left(\frac{\widehat{T}^2_{\overline{sv}}}{\overline{GI}_t} + \frac{\widehat{T}^2_{\overline{\omega}}}{\overline{S}_{\omega\omega}} + \frac{\widehat{M}^{*2}_{\overline{\omega}}}{\overline{EI}_\omega} \right) \tag{5.72}$$

We introduce $q = q_0 + q_\omega$ (Equation 5.58) into Equation (5.71) and obtain

$$U = \frac{1}{2}\frac{l}{\pi}\left(\int \alpha_{66} q_0^2 d\eta + \int \alpha_{66} q_\omega^2 d\eta + \frac{l^2}{\pi^2}\int \alpha_{11}\left(\frac{\partial^2 q}{\partial \eta^2}\right)^2 d\eta + 2q_0 \underbrace{\int q_\omega \alpha_{66} d\eta}_{0} \right) \tag{5.73}$$

As a consequence of Equation (5.62) the last term in Equation (5.73) is zero.

Introducing Equations (5.59) and (5.64) into Equation (5.72) we obtain

$$U = \frac{1}{2}\frac{l}{\pi}\left(\frac{\left(\oint q_0 r ds\right)^2}{\overline{GI}_t} + \frac{\left(\oint q_\omega r ds\right)^2}{\overline{S}_{\omega\omega}} + \frac{\left(\frac{l}{\pi}\oint q_\omega r ds\right)^2}{\overline{EI}_\omega}\right) \tag{5.74}$$

By comparing Equations (5.73) and (5.74) we have

$$\overline{GI}_t = \frac{\left(\oint q_0 r ds\right)^2}{\int \alpha_{66} q_0^2 d\eta} \tag{5.75}$$

$$\overline{S}_{\omega\omega} = \frac{\left(\oint q_\omega r ds\right)^2}{\int \alpha_{66} q_\omega^2 d\eta} \tag{5.76}$$

$$\overline{EI}_\omega = \frac{\left(\oint q_\omega r ds\right)^2}{\int \alpha_{11}\left(\frac{\partial^2 q}{\partial \eta^2}\right)^2 d\eta} \tag{5.77}$$

q_0 is uniform around the circumference, hence Equation (5.75) becomes

$$\overline{GI}_t = \frac{\left(\oint r ds\right)^2}{\int \alpha_{66} d\eta} = \frac{4A^2}{\int \alpha_{66} d\eta} \tag{5.78}$$

To determine $\overline{S}_{\omega\omega}$ and $\overline{EI}_\omega$ the distribution of q_ω must be known. In Sections 5.5 and 5.6 we determined q_ω, and obtained that q_ω depends on the length l, and as a consequence, $\overline{S}_{\omega\omega}$ and $\overline{EI}_\omega$ also depend on l. To derive stiffnesses which are independent of the length l we will assume that $l/b_k \gg 1$, where b_k is the widths of the kth wall segment.

To calculate the stiffnesses we may either use the "exact" solution (see Equation 5.37) or the approximate solution obtained via the Ritz method (see Equation 5.46). To obtain simpler results the approximate solution will be used. First the expressions for a doubly symmetrical box beam is derived then a general cross section undergoing pure torsion will be considered.

Doubly symmetrical, box section beams We consider a simply supported, doubly symmetrical box beam seen in Figure 27 and 30. $\overline{GI}_t$ is given by Equation (5.78), which results in

$$\overline{GI}_t = \frac{2b_1^2 b_2^2}{(\alpha_{66})_1 b_1 + (\alpha_{66})_2 b_2} \tag{5.79}$$

The beam is subjected to a torque load $t = \widetilde{t}\sin \pi x/l$. Under the applied load the beam undergoes a rate of twist $\vartheta = \widetilde{\vartheta}\sin \pi x/l$.

The box beam has four wall segments, hence the number of functions in the Ritz method is $2K = 2 \times 4 = 8$, and $\widetilde{q}$ is

$$\widetilde{q} = \sum_{k=1}^{8} C_k \phi_k \tag{5.80}$$

Because of symmetry (see Figure 31)

$$C_1 = C_2 = C_3 = C_4 \qquad C_5 = C_7 \qquad C_6 = C_8 \tag{5.81}$$

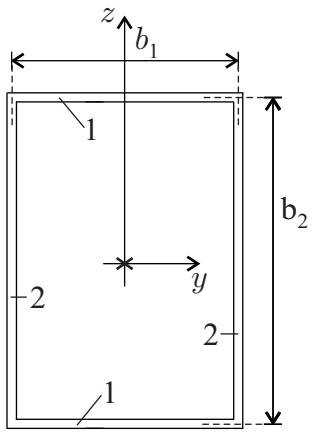

Figure 30: Box-section beam

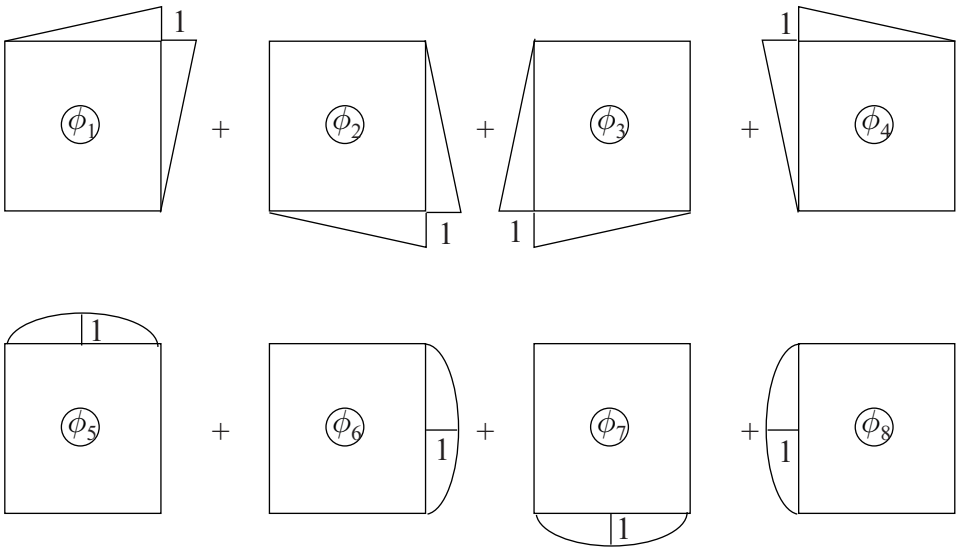

Figure 31: Functions ϕ_k for a box beam

Hence we use the basic functions given in Figure 32.

With these simplifications Equation (5.55) becomes

$$\mathbf{c} = [F]^{-1}\,\mathbf{f} \tag{5.82}$$

where

$$\mathbf{c} = \begin{Bmatrix} C_1 \\ C_2 \\ C_2 \end{Bmatrix} \qquad \mathbf{f} = \begin{Bmatrix} \frac{A}{2} \\ \frac{A}{3} \\ \frac{A}{3} \end{Bmatrix} \tag{5.83}$$

$$[F] = \frac{l^2}{\pi^2}\begin{bmatrix} \frac{\pi^2}{l^2}\frac{(\alpha_{66})_1 b_1}{2} + \frac{\pi^2}{l^2}\frac{(\alpha_{66})_2 b_2}{2} & \frac{\pi^2}{l^2}\frac{(\alpha_{66})_1 b_1}{3} & \frac{\pi^2}{l^2}\frac{(\alpha_{66})_2 b_2}{3} \\ \frac{\pi^2}{l^2}\frac{(\alpha_{66})_1 b_1}{3} & \frac{16(\alpha_{11})_1}{3b_1} + \frac{\pi^2}{l^2}\frac{8(\alpha_{66})_1 b_1}{15} & \\ \frac{\pi^2}{l^2}\frac{(\alpha_{66})_2 b_2}{3} & & \frac{16(\alpha_{11})_2}{3b_2} + \frac{\pi^2}{l^2}\frac{8(\alpha_{66})_2 b_2}{15} \end{bmatrix} \tag{5.84}$$

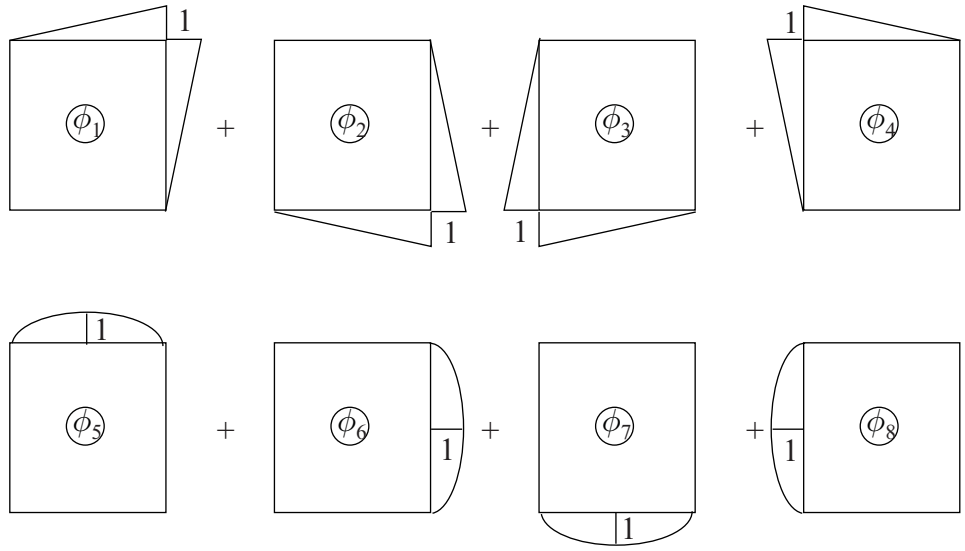

Figure 32: Functions ϕ_k for a doubly symmetrical box beam

Solution of Equation (5.82) results in

$$
\begin{aligned}
C_1 &= \widetilde{\vartheta}\frac{\pi^2}{l^2}A^2\frac{\frac{1}{2}-\frac{\frac{1}{3}\frac{(\alpha_{66})_1 b_1}{3}A\frac{\pi^2}{l^2}}{A\frac{16(\alpha_{11})_1}{3b_1}+A\frac{\pi^2}{l^2}\frac{8(\alpha_{66})_1 b_1}{15}}-\frac{\frac{1}{3}\frac{(\alpha_{66})_2 b_2}{3}A\frac{\pi^2}{l^2}}{A\frac{16(\alpha_{11})_2}{3b_2}+A\frac{\pi^2}{l^2}\frac{8(\alpha_{66})_2 b_2}{15}}}{\frac{(\alpha_{66})_1 b_1}{2}A\frac{\pi^2}{l^2}+\frac{(\alpha_{66})_2 b_2}{2}A\frac{\pi^2}{l^2}-2\frac{\left(\frac{(\alpha_{66})_1 b_1}{3}A\frac{\pi^2}{l^2}\right)^2}{A\frac{16(\alpha_{11})_1}{3b_2}+A\frac{\pi^2}{l^2}\frac{8(\alpha_{66})_1 b_1}{15}}-2\frac{\left(\frac{(\alpha_{66})_2 b_2}{3}A\frac{\pi^2}{l^2}\right)^2}{A\frac{16(\alpha_{11})_2}{3b_2}+A\frac{\pi^2}{l^2}\frac{8(\alpha_{66})_2 b_2}{15}}} \\
C_2 &= \widetilde{\vartheta}\frac{\frac{\pi^2}{l^2}\frac{A^2}{3}-2\frac{(\alpha_{66})_1 b_1}{3}A\frac{\pi^2}{l^2}C_1}{A\frac{16(\alpha_{11})_1}{3b_1}+A\frac{\pi^2}{l^2}\frac{8(\alpha_{66})_1 b_1}{15}} \\
C_3 &= \widetilde{\vartheta}\frac{\frac{\pi^2}{l^2}\frac{A^2}{3}-2\frac{(\alpha_{66})_2 b_2}{3}A\frac{\pi^2}{l^2}C_1}{A\frac{16(\alpha_{11})_2}{3b_2}+A\frac{\pi^2}{l^2}\frac{8(\alpha_{66})_2 b_2}{15}}
\end{aligned}
\tag{5.85}
$$

The Taylor series expression of these expressions with respect to $\sqrt{A}\pi/l$ are as follows

$$
\begin{aligned}
C_1 &= \widetilde{\vartheta}\left\{\frac{A}{X}+\frac{\pi^2}{l^2}\frac{2AY}{3X^2}\left(-\frac{(\alpha_{66})_1 b_1}{\frac{16(\alpha_{11})_1}{b_1}}+\frac{(\alpha_{66})_2 b_2}{\frac{16(\alpha_{11})_2}{b_2}}\right)\underbrace{+\frac{\pi^4}{l^4}\cdots}_{\text{neglected}}\right\} \\
C_2 &= \widetilde{\vartheta}\left\{\frac{\pi^2}{l^2}\frac{AY}{\frac{16(\alpha_{11})_1}{b_1}X}\underbrace{+\frac{\pi^4}{l^4}\cdots}_{\text{neglected}}\right\} \\
C_3 &= \widetilde{\vartheta}\left\{-\frac{\pi^2}{l^2}\frac{AY}{\frac{16(\alpha_{11})_2}{b_2}X}\underbrace{+\frac{\pi^4}{l^4}\cdots}_{\text{neglected}}\right\}
\end{aligned}
\tag{5.86}
$$

where

$$X = (\alpha_{66})_1 b_1 + (\alpha_{66})_2 b_2 \tag{5.87}$$

$$Y = (\alpha_{66})_2 b_2 - (\alpha_{66})_1 b_1 \tag{5.88}$$

In these expressions we neglect the terms containing $\left(\sqrt{A}\pi/l\right)^i$ when $i \geq 4$.

The uniform shear flow q_0 can be calculated by Equation (5.63), which is

$$\widetilde{\vartheta} \sin\frac{\pi x}{l} = \widetilde{q}_0 \sin\frac{\pi x}{l} \frac{\oint \alpha_{66} d\eta}{2A} \tag{5.89}$$

Equation (5.89) gives

$$\widetilde{q}_0 = \widetilde{\vartheta} \frac{2A}{\oint \alpha_{66} d\eta} \tag{5.90}$$

For the box beam $\oint \alpha_{66} d\eta = 2\,(\alpha_{66})_1 b_1 + 2\,(\alpha_{66})_2 b_2 = 2X$ and hence

$$\widetilde{q}_0 = \widetilde{\vartheta} \frac{A}{X} \tag{5.91}$$

The shear flow q_ω is calculated as

$$q_\omega = q - q_0 \tag{5.92}$$

Equations (5.80) and (5.92) give

$$\widetilde{q}\omega = (C_1 - \widetilde{q}_0)\,\phi_1 + C_2\phi_2 + C_3\phi_3 \tag{5.93}$$

By introducing Equation (5.93) into (5.76) and (5.77) we obtain

$$\overline{S}_{\omega\omega} = \frac{A^2 Y^2}{2X^2} \times \tag{5.94}$$

$$\times \frac{\left(\frac{b_1}{(\alpha_{11})_1} + \frac{b_2}{(\alpha_{11})_2}\right)^2}{\frac{(\alpha_{66})_1 b_1}{5}\left(\frac{b_1}{(\alpha_{11})_1}\right)^2 + \frac{(\alpha_{66})_2 b_2}{5}\left(\frac{b_2}{(\alpha_{11})_2}\right)^2 + \frac{(\alpha_{66})_1 b_1 (\alpha_{66})_2 b_2}{X}\left(\frac{b_1}{(\alpha_{11})_1} + \frac{b_2}{(\alpha_{11})_2}\right)^2}$$

$$\overline{EI}_\omega = \frac{A^2 Y^2}{24X^2}\left(\frac{b_1}{(\alpha_{11})_1} + \frac{b_2}{(\alpha_{11})_2}\right) \tag{5.95}$$

(A, X, Y are given by Equations **??**, 5.87, 5.88.)

General cross-section beams We consider a thin walled closed section beam consisting of K plane wall segments (Figure 22). The torsional stiffness $\overline{GI}_t$ is given by Equation (5.78) which results in

$$\overline{GI}_t = \frac{4A^2}{\sum_{k=1}^{K} (\alpha_{66})_k\, b_k} \tag{5.96}$$

where b_k and $(\alpha_{66})_k$ are the width and the shear compliance of the k-th wall segment, and A is the enclosed area.

$[A_1]$	$\begin{cases} \frac{(\alpha_{11})_j}{b_j} + \frac{(\alpha_{11})_i}{b_i} & i = j \\ -\frac{(\alpha_{11})_i}{b_i} & \text{when } i = j+1 \\ -\frac{(\alpha_{11})_j}{b_j} & i = j-1 \\ 0 & \text{else} \end{cases}$	$[B_1]$	$\begin{cases} \frac{(\alpha_{66})_i b_i}{3} + \frac{(\alpha_{66})_j b_j}{3} & i = j \\ \frac{(\alpha_{66})_i b_i}{6} & \text{when } i = j+1 \\ \frac{(\alpha_{66})_j b_j}{6} & i = j-1 \\ 0 & \text{else} \end{cases}$
$[A_2]$	$\begin{cases} \frac{16(\alpha_{11})_i}{3b_i} & \text{when } i = j \\ 0 & \text{else} \end{cases}$	$[B_2]$	$\begin{cases} \frac{(\alpha_{66})_i b_i}{3} & i = j \\ \frac{(\alpha_{66})_j b_j}{3} & \text{when } i = j-1 \\ 0 & \text{else} \end{cases}$
$\mathbf{f}$	$\begin{cases} \frac{b_k r_k}{2} & \text{when } k \le K \\ \frac{2b_k r_k}{3} & k > K \end{cases}$	$[B_3]$	$\begin{cases} \frac{8(\alpha_{66})_i b_i}{15} & \text{when } i = j \\ 0 & \text{else} \end{cases}$

Table 10: Elements of matrices $[A_1]$, $[A_2]$, $[B_1]$, $[B_2]$ and $[B_3]$ and vector $\mathbf{f}$

The beam is subjected to a torque load $t = \widetilde{t} \sin \pi x/l$ and the beam undergoes a rate of twist $\vartheta = \widetilde{\vartheta} \sin \pi x/l$. The shear flow of the beam is approximated by (see Equation 5.46)

$$\widetilde{q} = \sum_{k=1}^{2K} C_k \phi_k \tag{5.97}$$

where ϕ_k is illustrated in Figure 28, and C_k are yet unknown constants. The equation to determine these constants were derived in Section 5.46, and is reiterated below

$$[F]\,\mathbf{c} = \mathbf{f} \tag{5.98}$$

where

$$\mathbf{c} = \begin{Bmatrix} C_1 \\ C_2 \\ \vdots \\ C_{2K} \end{Bmatrix} \qquad \mathbf{f} = \begin{Bmatrix} f_1 \\ f_2 \\ \vdots \\ f_{2K} \end{Bmatrix} \tag{5.99}$$

and $[F]$ is

$$[F] = \frac{l^2}{\pi^2} \underbrace{\begin{bmatrix} [A_1] & \\ & [A_2] \end{bmatrix}}_{[A]} + \underbrace{\begin{bmatrix} [B_1] & [B_2] \\ [B_2]^T & [B_3] \end{bmatrix}}_{[B]} \tag{5.100}$$

where the elements of vector $\mathbf{f}$ and matrices $[A_1]$, $[A_2]$, $[B_1]$, $[B_2]$ and $[B_3]$ are given in Table .

Solution of Equation (5.98) is assumed to be in the form of

$$\mathbf{c} = \widetilde{\mathbf{c}} + \frac{\pi^2}{l^2}\widetilde{\widetilde{\mathbf{c}}} + \frac{\pi^4}{l^4}\widetilde{\widetilde{\widetilde{\mathbf{c}}}} + \ldots \tag{5.101}$$

By introducing Equations (5.100) and (5.101) into Equation (5.98) we obtain

$$\left(\frac{l^2}{\pi^2}[A] + [B]\right)\left(\widetilde{\mathbf{c}} + \frac{\pi^2}{l^2}\widetilde{\widetilde{\mathbf{c}}} + \frac{\pi^4}{l^4}\widetilde{\widetilde{\widetilde{\mathbf{c}}}} + \ldots\right) = \mathbf{f} \tag{5.102}$$

which gives

$$[A]\,\widetilde{\mathbf{c}} + \frac{\pi^2}{l^2}\left([B]\,\widetilde{\mathbf{c}} + [A]\,\widetilde{\widetilde{\mathbf{c}}}\right) \underbrace{+\frac{\pi^4}{l^4}\ldots}_{\text{neglected}} = \frac{\pi^2}{l^2}\mathbf{f} \tag{5.103}$$

In this equation we neglect the terms π^i/l^i when $i \geq 4$. In order to obtain the "best" solution we make equal the multipliers of π^i/l^i in the two sides of Equation (5.103), and write

$$[A]\,\widetilde{\mathbf{c}} = 0 \tag{5.104}$$

$$[B]\,\widetilde{\mathbf{c}} + [A]\,\widetilde{\widetilde{\mathbf{c}}} = \mathbf{f} \tag{5.105}$$

Matrix $[A]$ is singular. The non trivial solution of (Equation 5.104) is

$$\widetilde{\mathbf{c}}_1 = \widetilde{\mathbf{c}}_2 = \ldots = \widetilde{\mathbf{c}}_K = \text{const} \qquad \widetilde{\mathbf{c}}_{K+1} = \widetilde{\mathbf{c}}_{K+2} = \ldots = \widetilde{\mathbf{c}}_{2K} = 0 \tag{5.106}$$

The choice of the constant is not unambiguous. Here we propose the constant value to be equal to the shear flow resulting in an infinitely long beam. Hence we write (Equation 5.90):

$$\widetilde{\mathbf{c}}_1 = \widetilde{\mathbf{c}}_2 = \ldots = \widetilde{\mathbf{c}}_K = \widetilde{\underline{q}}_0 = \widetilde{\vartheta}\frac{2A}{\sum_{k=1}^{K}(\alpha_{66})_k\, b_k} \tag{5.107}$$

Equation (5.105) gives $2K$ equations to determine $\widetilde{\widetilde{\mathbf{c}}}$.

$$[A]\,\widetilde{\widetilde{\mathbf{c}}} = \mathbf{f} - [B]\,\widetilde{\mathbf{c}} \tag{5.108}$$

$[A]$ is singular and, consequently, the elements of $\widetilde{\widetilde{\mathbf{c}}}$ can not be determined unambiguously from Equation (5.108) only. However we have an additional condition which is discussed below.

We may observe (see Equation 5.106 and 5.91)

$$\widetilde{q}_0 = \sum_{k=1}^{2K}\widetilde{C}_k\phi_k = \sum_{k=1}^{K}\widetilde{C}_k\phi_k \tag{5.109}$$

and, consequently

$$\widetilde{q}_\omega = \sum_{k=1}^{2K}\widetilde{\widetilde{C}}_k\phi_k \tag{5.110}$$

We now make use of Equation (5.62), which can be given in the following form

$$\sum_{k=1}^{K}\widetilde{\widetilde{C}}_k\left(\frac{(\alpha_{66})_k\, b_k}{2} + \frac{(\alpha_{66})_{k+1}\, b_{k+1}}{2}\right) + \sum_{k=K}^{k+K}\widetilde{\widetilde{C}}_k\frac{2\,(\alpha_{66})_k\, b_k}{3} = 0 \tag{5.111}$$

The elements of $\widetilde{\widetilde{C}}_k$ are determined from the following $2K$ equations: The 2nd through $2K$th equations of Equation (5.108)

$$\sum_{j=1}^{2K}A_{jk}\widetilde{\widetilde{C}}_k = \mathbf{f}_k - \sum_{j=1}^{2K}B_{jk}\widetilde{C}_k \qquad k = 2,3,\ldots,2K \tag{5.112}$$

and from Equation (5.111). We introduce then $\widetilde{C}_k$ into Equations (5.76) and (5.77) which results in

$$\overline{S}_{\omega\omega} = \frac{\left(\sum_{k=1}^{K} r_k b_k\left(\frac{\underline{c}_{1k-1}+\underline{c}_{1k}}{2} + \frac{2}{3}\underline{c}_{1K+k}\right)\right)^2}{\sum_{k=1}^{K}(\alpha_{66})_k\, b_k\left(\frac{\underline{c}_{1k-1}^2+\underline{c}_{1k}^2+\underline{c}_{1k-1}\underline{c}_{1k}}{3} + \frac{8}{15}\underline{c}_{1K+k}^2 + \frac{2}{3}\underline{c}_{1K+k}\left(\underline{c}_{1k-1}+\underline{c}_{1k}\right)\right)} \tag{5.113}$$

$$\overline{EI}_\omega = \frac{\left(\sum_{k=1}^{K} r_k b_k\left(\frac{\underline{c}_{1k-1}+\underline{c}_{1k}}{2} + \frac{2}{3}\underline{c}_{1K+k}\right)\right)^2}{\sum_{k=1}^{K}\frac{(\alpha_{11})_k}{b_k}\left(\left(-\underline{c}_{1k-1}+\underline{c}_{1k}\right)^2 + \frac{16}{3}\underline{c}_{1K+k}^2\right)} \tag{5.114}$$

Note that we derived explicit expressions for $\overline{GI}$, $\overline{S}_{\omega\omega}$ and $\overline{EI}_{\omega}$ which are independent of the beam's length.

5.7.4 Unsymmetrical beams

In the previous section we considered beams undergoing pure torsion.

As a rule beams undergo lateral and torsional deformations simultaneously. By combining Equation (4.2) and Equation (5.68) we write

$$\begin{Bmatrix} \gamma_{\overline{y}} \\ \gamma_{\overline{z}} \\ \overline{\vartheta} \\ \overline{\vartheta}_s \end{Bmatrix} = \begin{bmatrix} \overline{s}_{yy} & \overline{s}_{yz} & \overline{s}_{y0} & \overline{s}_{y\omega} \\ \overline{s}_{yz} & \overline{s}_{zz} & \overline{s}_{z0} & \overline{s}_{z\omega} \\ \overline{s}_{y0} & \overline{s}_{z0} & \overline{s}_{00} & \overline{s}_{0\omega} \\ \overline{s}_{y\omega} & \overline{s}_{z\omega} & \overline{s}_{\omega 0} & \overline{s}_{\omega\omega} \end{bmatrix} \begin{Bmatrix} \widehat{V}_{\overline{y}} \\ \widehat{V}_{\overline{z}} \\ \widehat{T}_{\overline{sv}} \\ \widehat{T}_{\overline{\omega}} \end{Bmatrix} \tag{5.115}$$

where $\overline{s}_{ij}$ are the shear compliances. To determine the shear compliances we write the shear flow as

$$q = q_y + q_z + q_T \tag{5.116}$$

where q_y, q_z, q_T are the shear flows from the shear forces $\widehat{V}_{\overline{y}}$ and $\widehat{V}_{\overline{z}}$ and from the torque $\widehat{T}$, respectively. The shear flow from the torque is separated as Equation (5.58):

$$q_T = q_0 + q_\omega \tag{5.117}$$

Hence we have

$$\begin{aligned} \widehat{V}_{\overline{y}} &= \int q_y d\eta \\ \widehat{V}_{\overline{z}} &= \int q_z d\eta \\ \widehat{T}_{\overline{sv}} &= \int r q_0 d\eta \\ \widehat{T}_{\overline{\omega}} &= \int r q_\omega d\eta \end{aligned} \tag{5.118}$$

The compliances are determined similarly as for pure torsion. The strain energy of the beam is

$$U = U_N + U_q = \frac{1}{2}\int \alpha_{11}\frac{l^2}{\pi^2}\left(\frac{\partial^2 q}{\partial \eta^2}\right)^2 d\eta + \frac{1}{2}\int \alpha_{66} q^2 d\eta \tag{5.119}$$

With the internal forces in Equation (5.115) we write

$$\begin{aligned} U_q = {} & \frac{1}{2}\widehat{V}_{\overline{y}}^2\overline{s}_{yy} + \frac{1}{2}\widehat{V}_{\overline{z}}^2\overline{s}_{zz} + \frac{1}{2}\widehat{T}_{\overline{sv}}^2\overline{s}_{00} + \frac{1}{2}\widehat{T}_{\overline{\omega}}^2\overline{s}_{\omega\omega} + \widehat{V}_{\overline{y}}\widehat{V}_{\overline{z}}\overline{s}_{yz} + \widehat{V}_{\overline{y}}\widehat{T}_{\overline{sv}}\overline{s}_{y0} + \widehat{V}_{\overline{z}}\widehat{T}_{\overline{sv}}\overline{s}_{z0} \\ & + \widehat{V}_{\overline{y}}\widehat{T}_{\overline{\omega}}\overline{s}_{y\omega} + \widehat{V}_{\overline{z}}\widehat{T}_{\overline{\omega}}\overline{s}_{z\omega} + \widehat{T}_{\overline{sv}}\widehat{T}_{\overline{\omega}}\overline{s}_{\omega 0} \end{aligned} \tag{5.120}$$

By introducing Equations (5.116 and 5.117) into the second part of Equation (5.119) we have

$$U_q = \frac{1}{2}\int \alpha_{66}\left(q_y^2 + q_z^2 + q_0^2 + q_\omega^2 + 2q_y q_z + 2q_y q_0 + 2q_y q_\omega + 2q_z q_0 + 2q_z q_\omega + 2q_0 q_\omega\right) d\eta \tag{5.121}$$

By comparing Equation (5.120) and Equation (5.121) we obtain

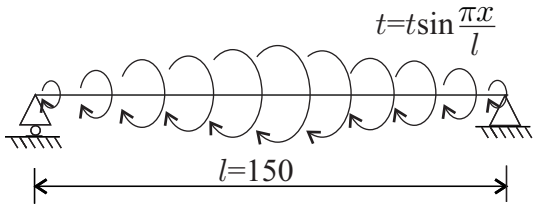

Figure 33: Beam in the numerical example

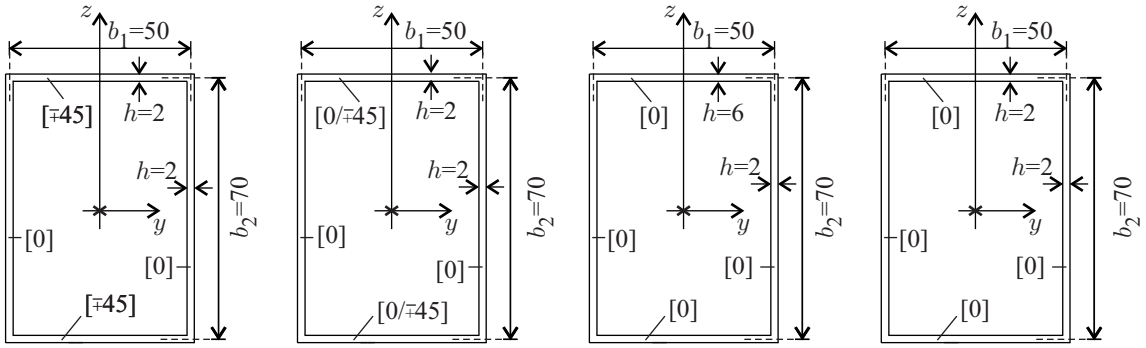

Figure 34: The cross sections in the numerical examples

$$\overline{s}_{ij} = \frac{\int \alpha_{66} q_i q_j d\eta}{\int q_i(r) d\eta \int q_j(r) d\eta} \tag{5.122}$$

The shear flows q_0 and q_ω can be calculated according to the previous section, while q_y and q_z according to classical textbooks.

Equation (5.62) results in

$$\overline{s}_{\omega 0} = 0 \tag{5.123}$$

5.7.5 Verification

In this section we demonstrate the utility of the presented theory through numerical examples.

First we consider a simply supported beam subjected to a sinusoidal load (Figure 33).

The cross section of the beam is shown in Figure 34a. The cross-sections in the numerical examples The material properties are given in Table 12. The thickness of the wall is 2 mm. For simplicity the dimensions are omitted below (the forces are given in N and the distances in mm). With these properties the value of α_{11} and α_{66} for the flanges and for the webs are

$$\begin{aligned} \alpha^1_{11} &= 3.0799 \times 10^{-5} \qquad \alpha^2_{66} = 1.432 \times 10^{-5} \\ \alpha^2_{11} &= 3.3784 \times 10^{-6} \qquad \alpha^2_{66} = 1.0989 \times 10^{-4} \end{aligned} \tag{5.124}$$

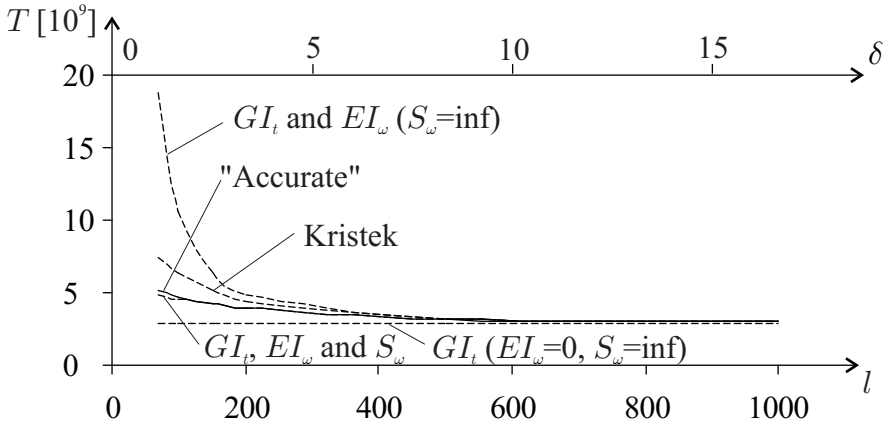

Figure 35: Comparision of the "accurate" solution with the results of the different theories (The cross section is given in Figure 34a)

The stiffnesses of the beam are calculated by Equations (5.79), (5.94), (5.95), (??), (5.87) and (5.88). With $b_1 = 50$ mm and $b_2 = 70$ mm we obtain

$$A = 3500 \qquad X = 0.0084083 \qquad Y = -0.0069763 \tag{5.125}$$

$$\overline{GI}_t = 2.9138 \times 10^9 \qquad \overline{S}_{\omega\omega} = 2.1308 \times 10^9 \qquad \overline{EI}_\omega = 7.8507 \times 10^{12} \tag{5.126}$$

The twist is given in Appendix B (Equation 2.11).

$$\overline{\psi} = \sum \widetilde{\psi}_k \sin \frac{\pi k x}{l} \tag{5.127}$$

$$\widetilde{\psi}_k = \frac{l^2}{\pi^2 k^2 \left(\overline{GI}_t + \overline{S}_{\omega\omega} \left(1 - \frac{\overline{S}_{\omega\omega}}{\overline{S}_{\omega\omega} + \overline{EI}_\omega \frac{\pi^2 k^2}{l^2}} \right) \right)} \widetilde{t}_k$$

For $l = 150$ mm and $t = \widetilde{t}_k \sin \pi x/l$, at the midspan, we have

$$\widetilde{\psi}_k = 5.3893 \times 10^{-7} \widetilde{t}_k \tag{5.128}$$

We calculated the twist of the middle section also by solving the differential equation system of the walls (page 63, "accurate solution"), and we obtained

$$\widetilde{\psi}_k = 5.3352 \times 10^{-7} \widetilde{t}_k \tag{5.129}$$

The difference is only -1.01%. Note that by neglecting $\overline{S}_{\omega\omega}$ we obtain $\widetilde{\psi}_k = 3.5870 \times 10^{-7} \widetilde{t}_k$ and by using Kristek's theory [7] $\widetilde{\psi}_k = 4.4204 \times 10^{-7} \widetilde{t}_k$. The inaccuracy of these values are 32.77% and 17.15%, respectively, which are not acceptable.

In Figure 35 we show the results for the same beam as a function of the beam length. We assumed that the maximum rate of twist on the beam is unity ($\overline{\vartheta} = \cos \pi x/l$) and we calculated

the torque ($\widehat{T} = \widetilde{T}\cos \pi x/l$) which results in $\overline{\vartheta}$. In this figure we included the results for the case when only $\overline{GI}_t$ is considered and when only $\overline{GI}_t$ and $\overline{EI}_\omega$ are taken into account, however $\overline{S}_{\omega\omega}$ is assumed to be infinity. The results of Kristek's theory is also presented. The shorter the beam the more important the effect of $\overline{S}_{\omega\omega}$.

For very short beams even the presented method becomes inaccurate. (The reason is that the function of q differs very much from a second order parabola (see Equation 5.80) for very short beams. This is the also the reason, why Vlasov's theory is inaccurate for short beams.) In these cases we should model the beam as a shell structure. The question arises at which beam length may the above theory be used? By coinciding Equation (5.86) we can see that the term $\frac{\pi^2}{l^2}\frac{8\alpha^k_{66}b_k}{15}$ was neglected with respect to $\frac{16\alpha^k_{11}}{3b_k}$ for each wall segment. Hence we write

$$\frac{16\alpha^k_{11}}{3b_k} \gg \frac{\pi^2}{l^2}\frac{8\alpha^k_{66}b_k}{15} \tag{5.130}$$

which yields

$$\frac{l^2}{b_k^2}\frac{\alpha^k_{11}}{\alpha^k_{66}} \gg 1 \tag{5.131}$$

We made several numerical comparisons; on the basis of these we suggest that our beam theory can be used when

$$\delta = \frac{l}{K}\sum_{k=1}^{K}\frac{1}{b_k}\sqrt{\frac{\alpha^k_{11}}{\alpha^k_{66}}} \geq 1 \div 3 \tag{5.132}$$

where K is the number of the wall segments.

(Note that for isotropic beams the above condition gives $l/K\sum_{k=1}^{K} b_k > 2 \div 5$)

For the beam shown in Figures 34a and 33 $\delta = 2.3877$. In Figure 35 the results, as a function of δ, are also presented (see top axis).

We also considered the cross-sections shown in Figure 34b and c. The compliances of the walls for the beam in Figure 34b are

$$\alpha^1_{11} = 0.6100 \times 10^{-5} \qquad \alpha^1_{66} = 2.3498 \times 10^{-5} \tag{5.133}$$

$$\alpha^2_{11} = 3.3784 \times 10^{-6} \qquad \alpha^2_{66} = 1.0989 \times 10^{-4} \tag{5.134}$$

for the section given in Figure 34c are

$$\alpha^1_{11} = \times 10^{-5} \qquad \alpha^1_{66} = \times 10^{-5} \tag{5.135}$$

$$\alpha^2_{11} = 3.3784 \times 10^{-6} \qquad \alpha^2_{66} = 1.0989 \times 10^{-4} \tag{5.136}$$

while for the section given in Figure 34d are

$$\alpha^1_{11} = \alpha^2_{11} = 3.3784 \times 10^{-6} \qquad \alpha^1_{66} = \alpha^2_{66} = 1.0989 \times 10^{-4} \tag{5.137}$$

The results are shown in Figure 36 and Figure 37. In these figures we included our beam solution, the "accurate" solution, and Kristek's solution. It is seen that for beams, when $\delta \geq 1$, the presented beam model is acceptable.

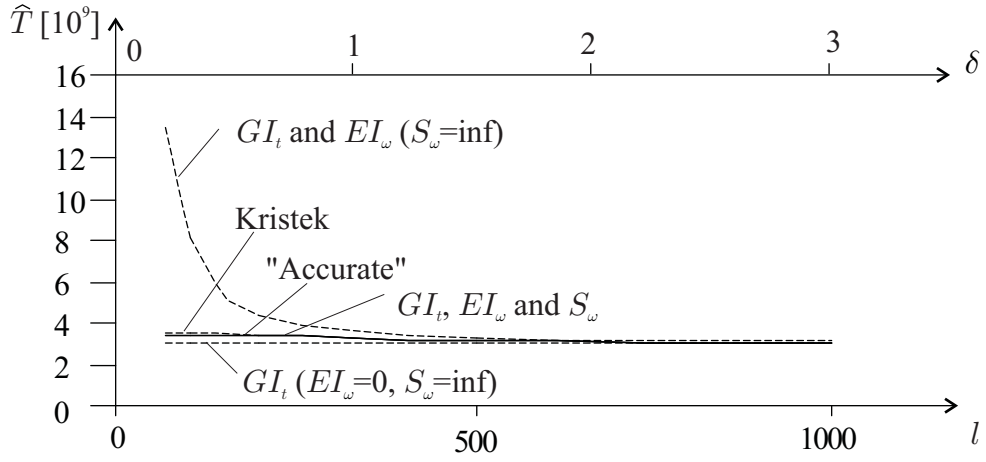

Figure 36: Comparision of the "accurate" solution with the results of the different theories (The cross section is given in Figure 34b)

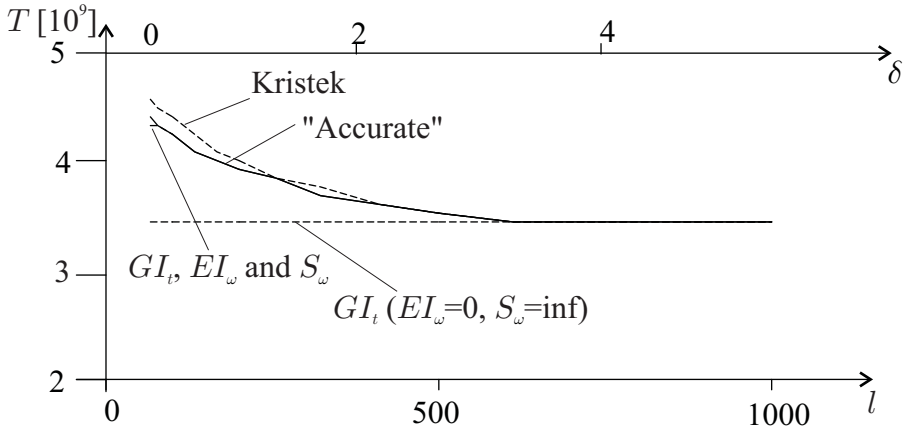

Figure 37: Comparision of the "accurate" solution with the results of the different theories (The cross section is given in Figure 34c)

Note that the for the case when the layup and the thickness of the wall segments are identical (Figure 34d) the simple theory, considering $\overline{GI}_t$ only, is applicable.

For further verification we considered beams with artificial materials, where the compliances are significantly differ from each other. The values of α_{11} and α_{66} are shown in Figure 38. The results of our calculations are shown in Figures 39 and 40.

We consider a cantilever beam subjected to a concentrated torque at the end (Figure 41).The cross-section is shown in Figure 34a.

The stiffnesses of the beam $\overline{GI}_t$, $\overline{S}_{\omega\omega}$ and $\overline{EI}_\omega$ are given by Equation (**??**). The function of the twist is given by Equation (2.23).

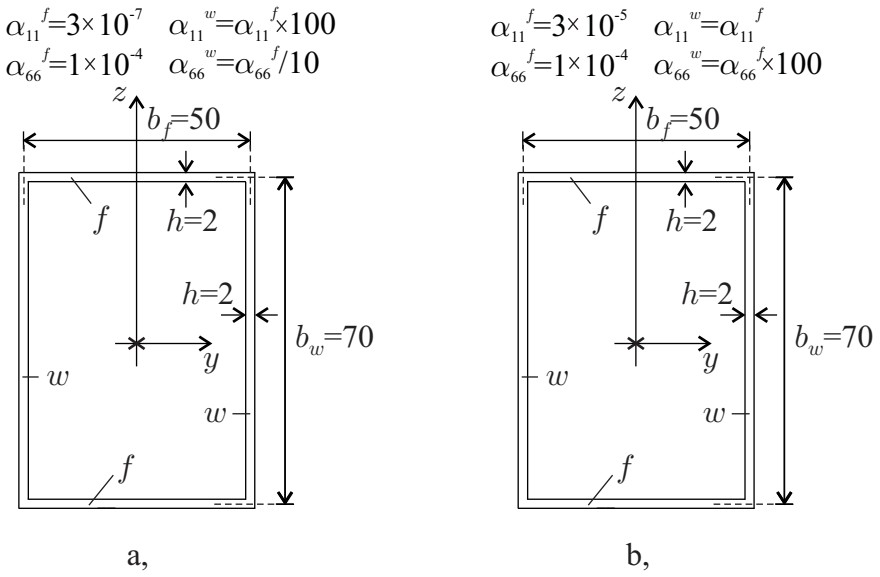

Figure 38: Cross-sections with artifitial materials

With $l = 150$ mm Equation (2.23) in Appendix B yields

$$\begin{aligned}\{\overline{\psi}_0\} = 0.1448\times10^{-4}e^{0.0125x} \quad & -245.18i\times e^{8.9582\times10^{-10}ix}\{-1.0000+0.3647\times10^{-7}i\}+\\ & +245.18i\times e^{-8.9582\times10^{-10}ix}\{-1.0000-0.3647\times10^{-7}i\}+\\ & -0.3384\times10^{-6}e^{-0.0125x}\end{aligned} \tag{5.138}$$

The maximum twist at $x = l$ is

$$\overline{\psi} = 5.1751\times10^{-5} \tag{5.139}$$

When only $\overline{GI}_t$ is considered we obtain

$$\overline{\psi} = \frac{\widehat{T}}{\overline{GI}_t}l = 6.5893\times10^{-5} \tag{5.140}$$

which overestimates $\overline{\psi}$ by 27.32%.

When $\overline{GI}_t$ and $\overline{EI}_\omega$ are considered ($\overline{S}_{\omega\omega} = \infty$) the maximum twist is

$$\overline{\psi} = \frac{\widehat{T}}{\widehat{GI}_t}\left(\frac{sh\,(\nu l)}{\nu ch(\nu l)}\,(ch(\nu x)-1)+x-\frac{sh(\nu x)}{\nu}\right) = 4.3232\times10^{-5} \tag{5.141}$$

$$\nu = \sqrt{\frac{\widehat{GI}_t}{\widehat{EI}_\omega}} \tag{5.142}$$

We observe that this value underestimates $\overline{\psi}$ (Equation 5.138) by 16.46%.

6 Effect of shear deformation and restrained warping

Different beam theories often neglect the effects of shear deformation and restrained warping (or both) (see Section 1). The designer would be well served with simple rules which enable him to decide whether these effects are negligible or not [25].

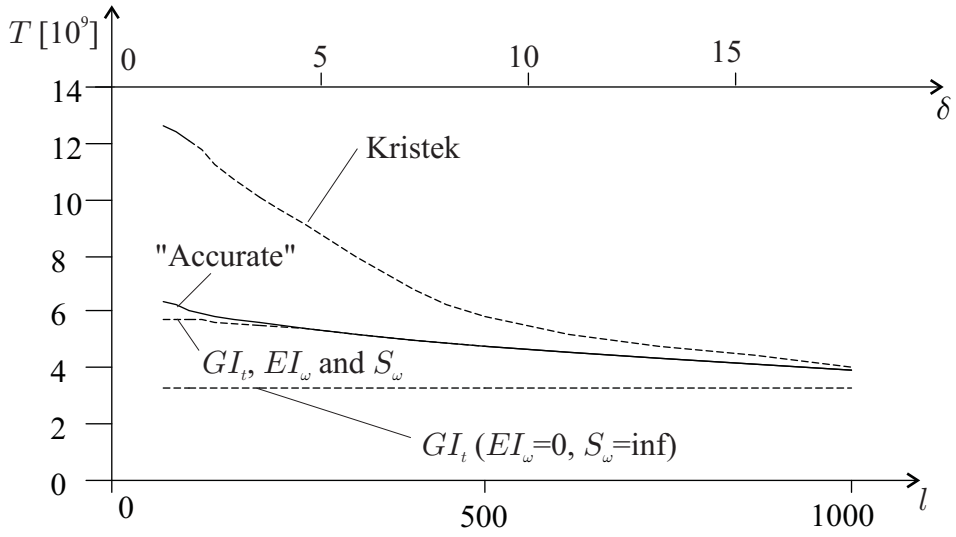

Figure 39: Comparision of the "accurate" solution with the results of the different theories (The cross section is given in Figure 38a)

6.1 Problem statement

We consider thin walled composite beams subjected to end loads or distributed loads as illustrated in Figure 42. The beam has either an open cross-section or a single cell closed cross-section (examples are shown in Figure 43).

The layups of the walls can be orthotropic or anisotropic, balanced or unbalanced. When every wall is orthotropic the beam is called "orthotropic" otherwise it is called "generally anisotropic". When every wall is balanced, the beam is called "balanced". For an orthotropic laminate the 1,6 and 2,6 elements of the stiffness matrices are zero: $A_{16} = A_{26} = B_{16} = B_{26} = D_{16} = D_{26} = 0$. For a balanced laminate the 1,6 and 2,6 elements of the $[A]$ matrix are zero: $A_{16} = A_{26} = 0$.

The different beam theories apply different approximations, and there are circumstances when the simplified theories yield inaccurate results.

In this section we have two tasks: First we will investigate the effect of shear deformation and the effect of restrained warping and we wish to give "rules" when these effects must be taken into account and when they can be neglected. Second, we will demonstrate that for *balanced*, anisotropic open section beams the effect of restrained warping can be taken into account by using the warping stiffness derived for orthotropic beams.

6.2 Effect of shear deformation

The effect of shear deformation is dependent upon three factors: the length to height ratio, the material properties, and the shape of the beam cross-section. The maximum deflection w of a beam with shear deformation is calculated by

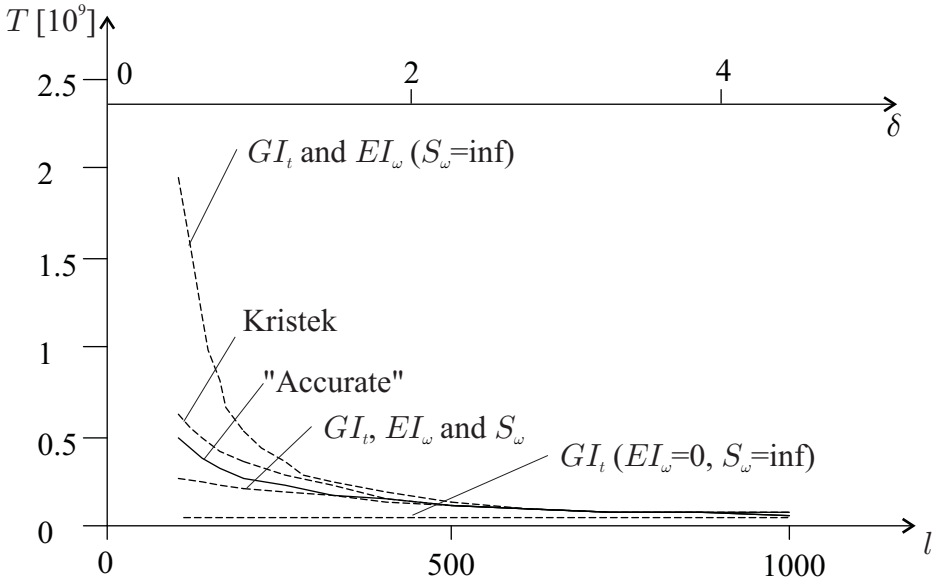

Figure 40: Comparision of the "accurate" solution with the results of the different theories (The cross section is given in Figure 38b)

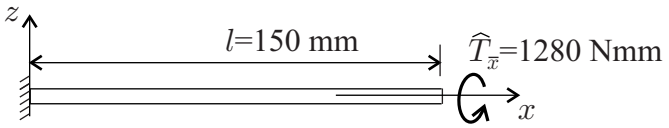

Figure 41: Cantilever beam subjected to a torque at the end

$$w = w_B + w_S \tag{6.1}$$

where w_B and w_S are the deflections due to bending and shear deformation, respectively, as shown in Table 11 for different loading conditions.

For assessing the effect of shear deformation we define a parameter α as follows

$$\alpha = \frac{w_S}{w} \tag{6.2}$$

The α values are given in Table 11. When the beam is not simply supported it is necessary to introduce an "effective length" which is defined for different end conditions, in the second column of Table 11.

The constant in the expression varies between 9.6 and 12, we take as an approximation π^2 into account. With this value α becomes

$$\alpha = \frac{1}{1 + \frac{l^2 \widehat{S}}{\pi^2 \widehat{EI}}} \tag{6.3}$$

Next, we estimate α for thin-walled beams. First we develop an expression for a doubly symmetrical, orthotropic I-beam. Then, we apply these results to anisotropic C, Z and box-section

	loads	l	w_B	w_S	α
1	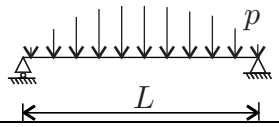	L	$\frac{qL^4}{\pi^4 \widehat{EI}}$	$\frac{qL^2}{\pi^2 \widehat{S}}$	$\frac{1}{1+\frac{l^2 \widehat{S}}{\pi^2 \widehat{EI}}}$
2	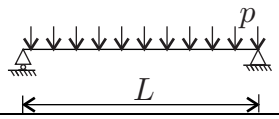	L	$\frac{5qL^4}{384\widehat{EI}}$	$\frac{qL^2}{8\widehat{S}}$	$\frac{1}{1+\frac{l^2 \widehat{S}}{9.6\widehat{EI}}}$
3	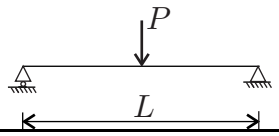	L	$\frac{PL^3}{48\widehat{EI}}$	$\frac{PL}{4\widehat{S}}$	$\frac{1}{1+\frac{l^2 \widehat{S}}{12\widehat{EI}}}$
4	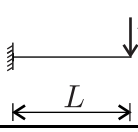	$2L$	$\frac{PL^3}{3\widehat{EI}}$	$\frac{PL}{\widehat{S}}$	$\frac{1}{1+\frac{l^2 \widehat{S}}{12\widehat{EI}}}$
5	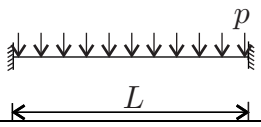	$L/2$	$\frac{qL^4}{384\widehat{EI}}$	$\frac{qL^2}{8\widehat{S}}$	$\frac{1}{1+\frac{l^2 \widehat{S}}{12\widehat{EI}}}$

Table 11: The bending (w_B) and shear (w_S) deflections of beams with different loading conditions. l is the effective length

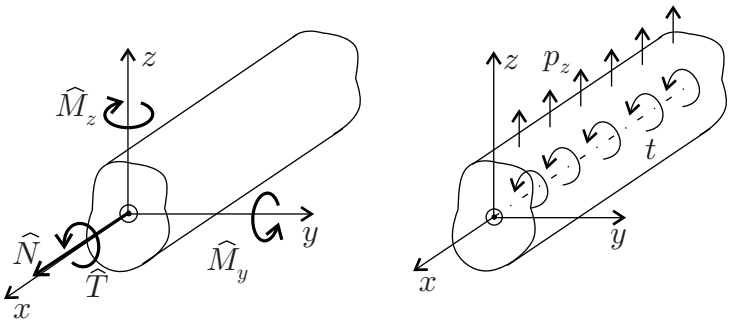

Figure 42: thin walled composite beams subjected to end loads and distributed loads

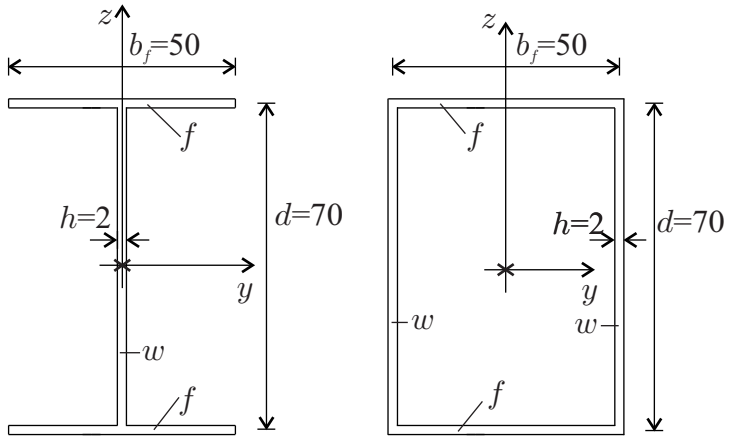

Figure 43: Cross-sections in the numerical calculations

beams.

The bending stiffnesses of an I-beam (Figure 44) are [5]:

$$\widehat{EI}_{yy} = \frac{b_1}{(\alpha^{\rho}_{11})_1}\frac{d^2}{2} + \frac{2b_1}{(\delta^{\rho}_{11})_1} + \frac{b_2^3}{12\,(\alpha^{\rho}_{11})_2} \tag{6.4}$$

$$\widehat{EI}_{zz} = \frac{b_2}{(\delta^{\rho}_{11})_2} + \frac{b_1^3}{6\,(\alpha^{\rho}_{11})_1} \tag{6.5}$$

where α^{ρ}_{11} and δ^{ρ}_{11} are the elements of the compliance matrices ($[\alpha]$ and $[\delta]$), which are evaluated at the "tension neutral" surface (Equation 4.1 in Appendix D), and is given by Equation (4.3) in Appendix D. Subscripts 1 and 2 refer to the flange and web, respectively.

The shear stiffnesses are [5]

$$\widehat{S}_{zz} = \frac{1}{\frac{(\alpha^{\nu}_{66})_2}{d} + \frac{1}{6}\frac{(\alpha^{\nu}_{66})_1 b_1}{d^2}} \tag{6.6}$$

$$\widehat{S}_{yy} = \frac{2b_1}{1.2\,(\alpha^{\nu}_{66})_1} \tag{6.7}$$

where α^{μ}_{66} is evaluated at the "torque neutral" surface (Equation 4.4 in Appendix D), and are given by Equation (4.5) in Appendix D. When the walls are thin we may approximate the bending

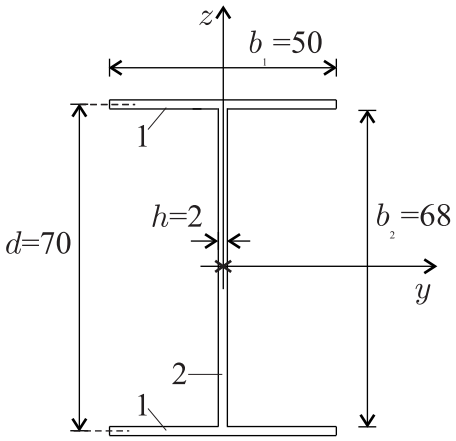

Figure 44: Cross section of an I-beam

stiffnesses by

$$\widehat{EI}_{yy} = \frac{b_1}{(\alpha^{\rho}_{11})_1}\frac{d^2}{2} \qquad \widehat{EI}_{zz} = \frac{b_1^3}{6\,(\alpha^{\rho}_{11})_1} \tag{6.8}$$

while $\widehat{S}_{zz}$ and $\widehat{S}_{yy}$ are approximated by

$$\widehat{S}_{zz} = \frac{d}{(\alpha^{\nu}_{66})_2} \qquad \widehat{S}_{yy} = \frac{2b_1}{1.2\,(\alpha^{\nu}_{66})_1} \tag{6.9}$$

Using Equation (6.3) into account, we obtain expression for an I-beam loaded in the $x-z$ plane

$$\alpha = \frac{1}{1+\frac{l^2\widehat{S}_{zz}}{\pi^2\widehat{EI}_{yy}}} = \frac{1}{1+\frac{2l^2\left(\alpha^{\rho}_{11}\right)_1}{\pi^2 b_f d\left(\alpha^{\nu}_{66}\right)_2}} \qquad \text{in the } x-z \text{ plane,} \tag{6.10}$$

while for an I-beam loaded in the $x-y$ plane

$$\alpha = \frac{1}{1+\frac{l^2\widehat{S}_{yy}}{\pi^2\widehat{EI}_{zz}}} = \frac{1}{1+\frac{10l^2\left(\alpha^{\rho}_{11}\right)_1}{\pi^2 b_f^2\left(\alpha^{\nu}_{66}\right)_2}} \qquad \text{in the } x-y \text{ plane.} \tag{6.11}$$

The above expressions of α, developed for doubly symmetrical, orthotropic, I-beams, also prove reasonable estimates for thin-walled anisotropic C, I and box-section beams. To verify this statement we made comparisons with FE calculations for the loading case illustrated in the third row of Table 11.

In Figure 45 and 46 the results for orthotropic I-beams with different symmetrical and unsymmetrical layups are presented. The cross-section is shown in Figure 44, the material properties of unidirectional ply are given in Table 12.

It can be seen that the finite element calculations are in a close agreement with the α value given by Equations (6.10) and (6.11).

Equation (6.10) can be used as an approximation for the cross-sections shown in Figure 47.

Comparisons with the FE calculations are shown in Figure 48. (For box beams $(\alpha^{\nu}_{66})_2$ is taken to be the sum of α^{ν}_{66} of the two walls $(\alpha^{\nu}_{66})_2 = (\alpha^{\nu}_{66})_2 + (\alpha^{\nu}_{66})_4$.) It can be seen that Equation (6.10) is a reasonable estimate for α. We also made comparisons for anisotropic I-beams. The

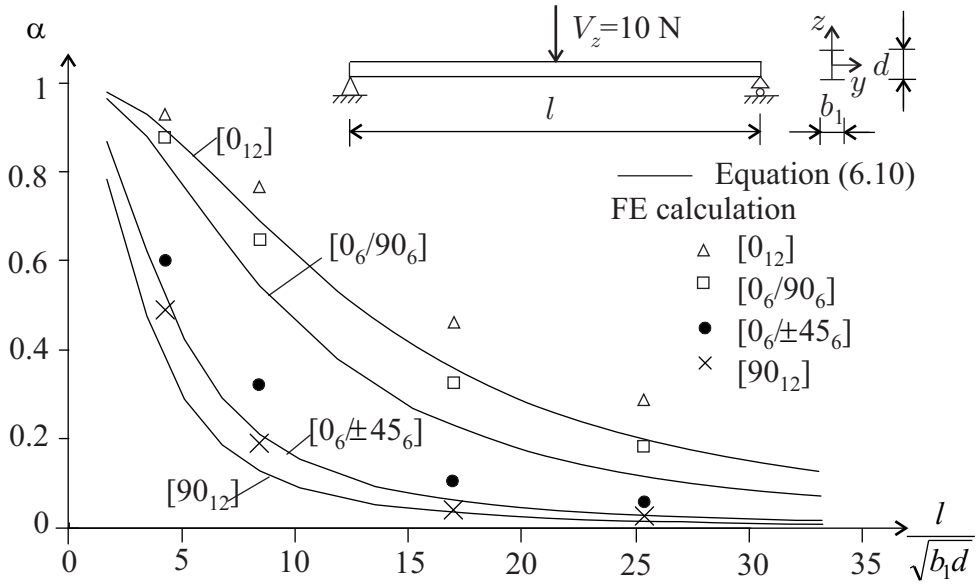

Figure 45: Effect of shear deformation $\left(\alpha = \frac{w_S}{w}\right)$ on simply supported I-beams with orthotropic layup loaded in the $x - z$ plane

results, for five different layups are shown in Figure 49. In all five layups $(\alpha^{\nu}_{66})_2 \,/\, (\alpha^{\rho}_{11})_1 \approx 6.6$ and consequently, Equation (6.10) gives a single curve. We observe that Equation (6.10) is a reasonable estimate also for beams with anisotropic layups.

The correction factor α (Equations 6.10 and 6.11) is plotted in Figures 50 and 51.

6.3 Effect of restrained warping

We investigate the two cross-sections shown in Figure 43, with five different layups as given in Table 13, each made of graphite epoxy plies. The material properties are given in Table 12 and the ply thickness is 1/6=0.166 mm.

The stiffness matrices of these layups are given in Section 3. We also included the case of an *isotropic beam* (last row in Table 13) where infinite number of randomly oriented plies are considered. For this case the Young modulus, is equal to $E = 54168$ N/mm^2, while the Poisson ratio, is equal to $\nu = 0.33$.

6.3.1 Open section beams

A cantilever beam (Figure 52) with open cross-section (Figure 43a) is subjected to a torque at the end of the cantilever. The rotation of the cross-section $\overline{\psi}$ and the rate of twist ($\overline{\vartheta} = d\overline{\psi}/dx$) were calculated by the ANSYS FE program. The results, for $\widehat{T}_{\overline{x}} = 630$ Nmm, are shown in Figure 53.

We also calculated the rate of twist by the theory presented in Section 3, where the restrained

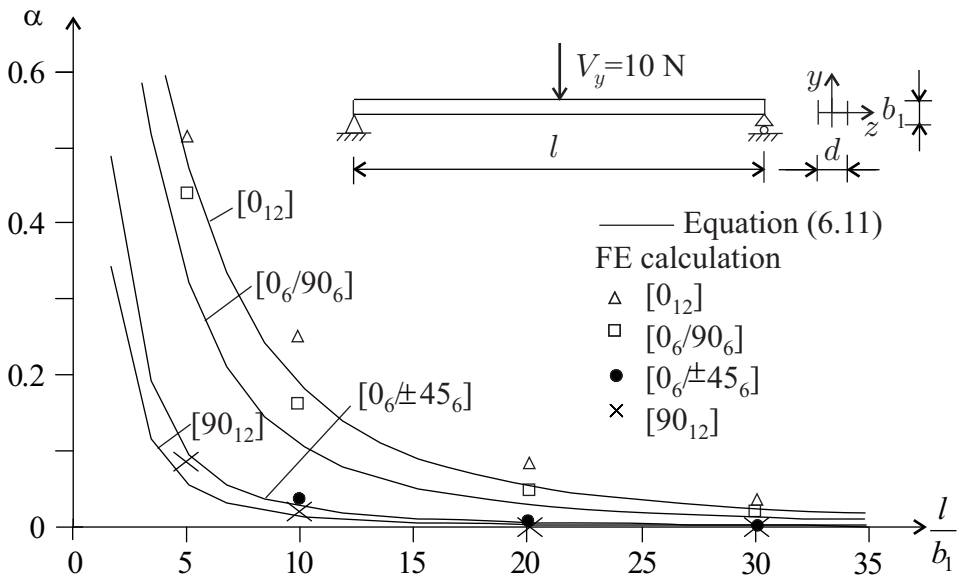

Figure 46: Effect of shear deformation $\left(\alpha = \frac{w_S}{w}\right)$ on simply supported I-beams with orthotropic layup loaded in the $x - y$ plane

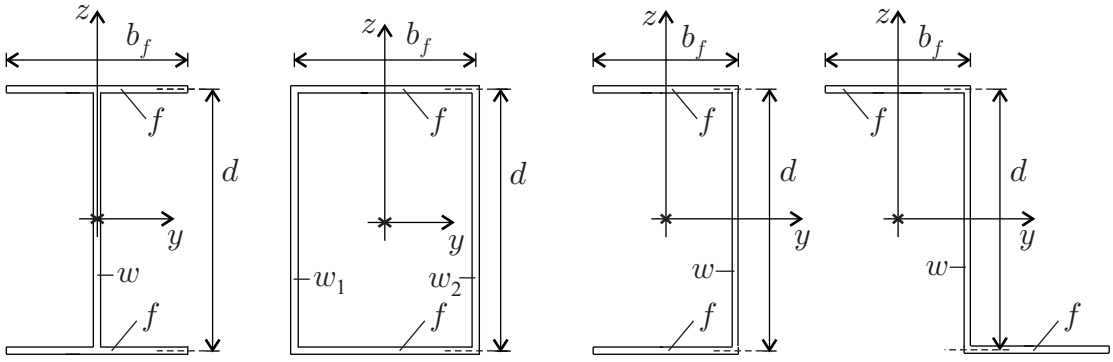

Figure 47: Cross sections of I, box, C, and Z beams

warping induced stresses were neglected and ϑ is calculated by

$$\overline{\vartheta} = \overline{W}_{44} \times \widehat{T}_{\overline{x}} \tag{6.12}$$

where $\overline{W}_{44}$ is the 4,4 element of matrix $\left[\overline{W}\right] = \left[\overline{P}\right]^{-1}$, where $\left[\overline{P}\right]$ is given in Section 3. The values of $\overline{W}_{44}$ are given in Table 13. The results are compared to the rate of twist calculated for $x/d = 10$ by the ANSYS program (see Table 14).

It can be seen that the effect of restrained warping cannot be neglected even in the case of relatively slender beams. In Table 14 we also included the ratio $\delta_{66}/\alpha^{\rho}_{11}$ where α^{ρ}_{11} is evaluated at the "tensile neutral" surface (see Equations 4.1 and 4.3). It can be seen that the effect of restrained warping is highest for the unidirectional beam, where the value of $\delta_{66}/\alpha^{\rho}_{11}$ is the highest.

Approximate calculations

	E_1 [MPa]	E_2 [MPa]	G_{12} [MPa]	ν_{12}
T300/934	148000	9650	4550	0.3

Table 12: Material properties of a graphite epoxy ply

layup		I-beam	Closed section beam
		$\frac{1}{\overline{W}_{44}}$ $[10^6\text{Nm}]$	$\frac{1}{\overline{W}_{44}}$ $[10^6\text{Nm}]$
$[0_{12}]$	orthotropic and balanced	2.0627	1.8579
$[45_{12}]$	anisotropic and balanced	5.2915	3.5926
$[45_6/-45_6]$	anisotropic and unbalanced	7.2991	15.6056
$[0_6/45_6]$	anisotropic and unbalanced	3.7059	3.9910
$[10_4/20_4/30_4]$	anisotropic and unbalanced	5.3432	2.9790
isotropic		9.2625	8.3434

Table 13: The layups used in the numerical comparisions, and the torsional stifffnesses (by $1/\overline{W}_{44}$) for I and box section beams shown in Figure 43

layup	$[0_{12}]$	$[45_{12}]$	$[0_6/45_6]$	$[45_6$/-$45_6]$	$[10_4/20_4/30_4]$	isotropic
$\overline{\boldsymbol{\vartheta}}_N$ $\left[10^{-5}\right]$(ANSYS)	6.9814	10.6396	8.4554	7.5576	7.6782	5.0116
$\overline{\vartheta}$ $\left[10^{-5}\right]$(Equation 6.12)	30.542	11.9070	16.9997	8.6311	11.7908	6.8016
$\frac{\overline{\boldsymbol{\vartheta}}_N-\overline{\vartheta}}{\overline{\boldsymbol{\vartheta}}_N}\times 100$ [%]	-337.47	-11.90	-101.05	-14.20	-53.56	-35.72
$\delta_{66}/\alpha_{11}^{\rho}$	32.5275	1.4037	9.9738	0.8953	7.0116	7.9535

Table 14: Rate of twist ($\overline{\vartheta}$) of a cantilever I-beam at a distance x=700 mm for different layups

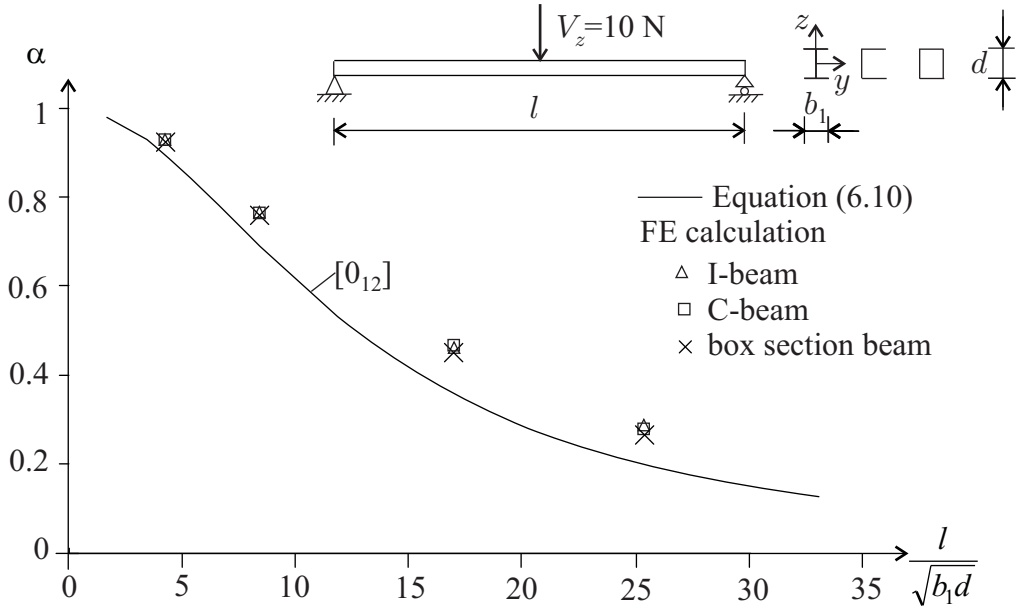

Figure 48: Effect of shear deformation ($\alpha = \frac{w_S}{w}$) on simply supported beams with different cross-sections. The layup is $[0_{12}]$

In Section 3 we derived the stiffness matrix of open section anisotropic beams by neglecting the effect of restrained warping, however we showed above numerically that for open section beams this approximation is not acceptable. When the beam is *balanced*, i.e. each layup is balanced, we approximate the displacements of the beam by combining the stiffnesses derived for a generally anisotropic beam and the warping stiffness derived for an orthotropic beam. Consequently, the material law is given below as:

$$\begin{Bmatrix} \epsilon^o_{\overline{x}} \\ \frac{1}{\rho_{\overline{y}}} \\ \frac{1}{\rho_{\overline{z}}} \\ \overline{\vartheta} \\ \overline{\Gamma} \end{Bmatrix} = \begin{bmatrix} \overline{W}_{11} & \overline{W}_{12} & \overline{W}_{13} & \overline{W}_{14} & \\ \overline{W}_{12} & \overline{W}_{22} & \overline{W}_{23} & \overline{W}_{24} & \\ \overline{W}_{13} & \overline{W}_{23} & \overline{W}_{33} & \overline{W}_{34} & \\ \overline{W}_{14} & \overline{W}_{24} & \overline{W}_{34} & \overline{W}_{44} & \\ & & & & 1/\widehat{EI}_\omega \end{bmatrix} \begin{Bmatrix} \widehat{N}_{\overline{x}} \\ \widehat{M}_{\overline{y}} \\ \widehat{M}_{\overline{z}} \\ \widehat{T}_{sv} \\ \widehat{M}_\omega \end{Bmatrix} \tag{6.13}$$

where $\epsilon^o_{\overline{x}}$ is the axial strain of the $\overline{x}$ axis, $\frac{1}{\rho_{\overline{y}}}$ and $\frac{1}{\rho_{\overline{z}}}$ are the curvatures of the $\overline{x}$ axis about the $\overline{y}$ and $\overline{z}$ axes, $\overline{\Gamma}$ is the second derivative of the twist, $\overline{\vartheta}$ is the rate of the twist, $\widehat{N}_{\overline{x}}$ is the normal force, $\widehat{M}_{\overline{y}}$ and $\widehat{M}_{\overline{z}}$ are the bending moments about the $\overline{y}$ and $\overline{z}$ axes, $\widehat{T}_{sv}$ is the Saint Venant torque, $\widehat{M}_\omega$ is the bimoment. The total torque is defined as:

$$\widehat{T} = \widehat{T}_{sv} + \widehat{T}_\omega \tag{6.14}$$

where $\widehat{T}_\omega$ is the restrained warping induced torque, and calculated by [17]

$$\widehat{T}_\omega = \frac{d\widehat{M}_\omega}{dx} \tag{6.15}$$

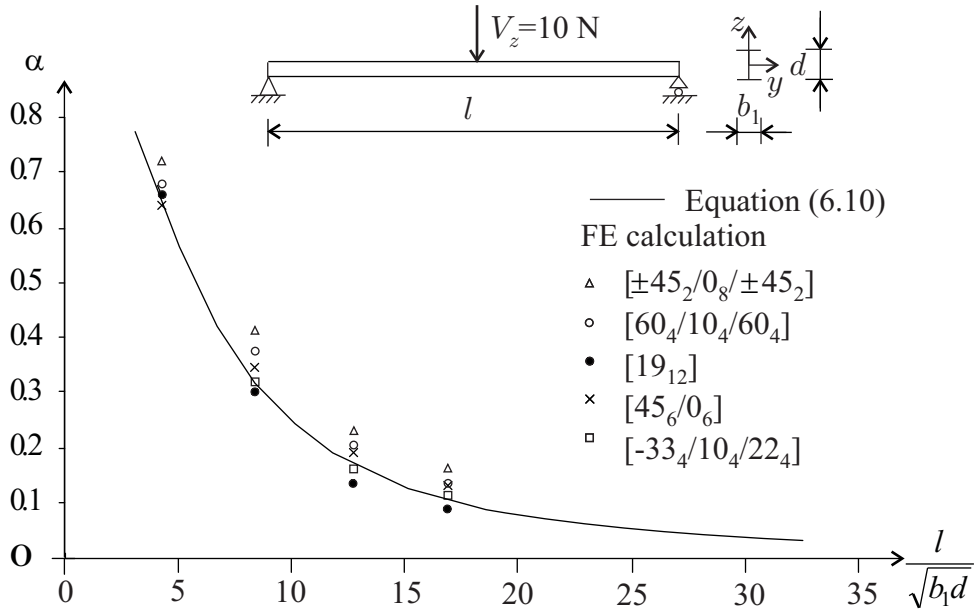

Figure 49: Effect of shear deformation ($\alpha = \frac{w_S}{w}$) on simply supported I-beams with anisotropic layups

For pure torque Equation (6.13) yields

$$\widehat{T}_{sv} = \frac{1}{\overline{\overline{W}}_{44}}\overline{\vartheta} \tag{6.16}$$

$$\widehat{T}_{\omega} = \widehat{EI}_{\omega}\overline{\Gamma} \tag{6.17}$$

And for cantilever beam we have [17]

$$\overline{\psi} = \frac{\widehat{T}}{\widehat{GI}_t}\left(\frac{sh\,(\nu l)}{\nu ch(\nu l)}\,(ch(\nu x)-1)+x-\frac{sh(\nu x)}{\nu}\right) \tag{6.18}$$

$$\overline{\vartheta} = \frac{d\overline{\psi}}{dx} = \frac{\widehat{T}}{\widehat{GI}_t}\left(1-\frac{ch(\nu(l-x))}{ch(\nu l)}\right) \tag{6.19}$$

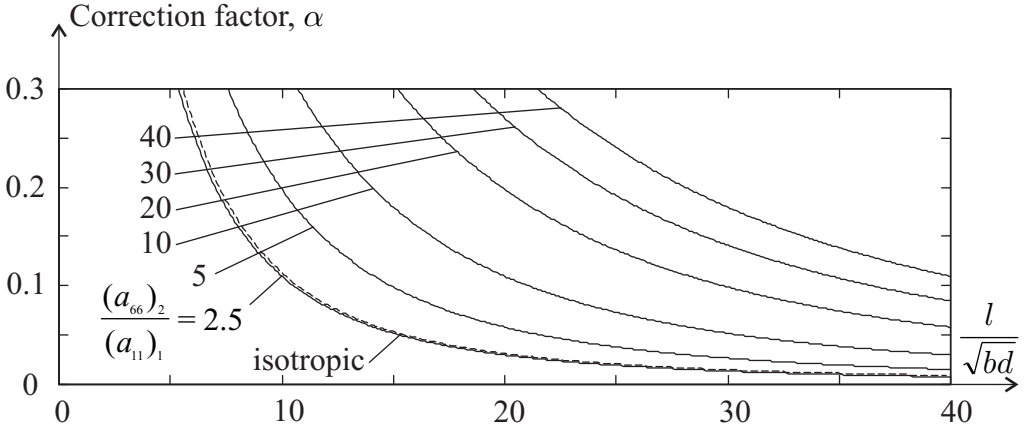

Figure 50: The correction factor α Equation (6.10)

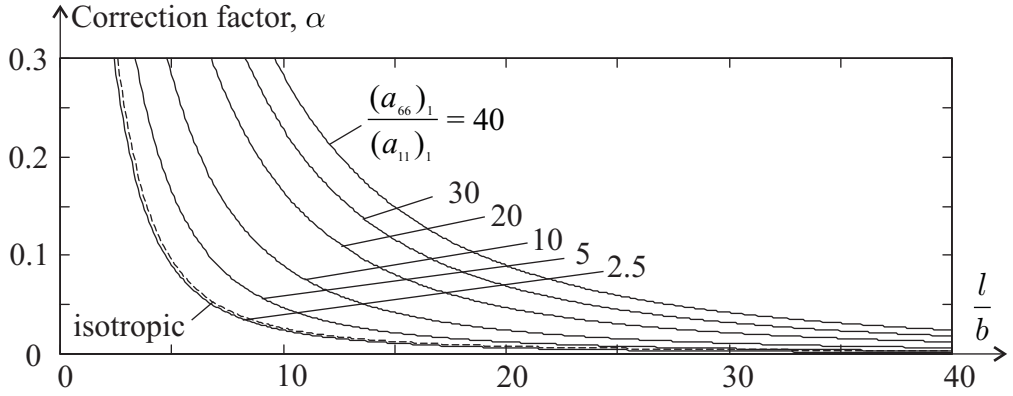

Figure 51: The correction factor α Equation (6.11)

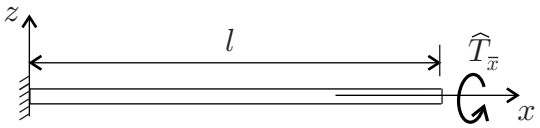

Figure 52: Cantilever beam subjected to a torque at the end

where

$$\nu = \sqrt{\frac{\widehat{GI}_t}{\widehat{EI}_\omega}} \tag{6.20}$$

$\widehat{EI}_\omega$ and $\widehat{GI}_t$ are the warping and torsional stiffnesses. For an orthotropic beam the warping stiffness is calculated by the expression given for an isotropic beam by replacing Eh by $1/\alpha^\rho_{11}$ [5], where the superscript ρ indicates that α^ρ_{11} is evaluated at the flange's "tension neutral" surface. Hence, for an I-beam we have

$$\widehat{EI}_\omega = \frac{\frac{1}{\alpha^\rho_{11}} b_f^3}{24} d^2 \tag{6.21}$$

$\widehat{GI}_t$ is replaced by the inverse of $\overline{W}_{44}$ (see Equation 6.16). With these stiffnesses and with Equation (6.18) we calculated $\overline{\vartheta}$ which is compared to the FE calculation in Figure 54 for the cantilever I-beam investigated in the previous section.

The warping and torsional stiffnesses for the examined balanced layups are given in Table 15.

6.3.2 Closed section beam

A cantilever beam with the cross-section given in Figure 43b, is subjected to an applied torque at the end of the cantilever (Figure 52). We calculated the rate of twist with the ANSYS FE program. The results, for $\widehat{T}_{\bar{x}} = 1280$ Nmm, are shown in Figure 55.

The rate of twist was also calculated by the theory given in Section 3, where the restrained warping induced stresses were neglected, which results in a uniform rate of twist along the beam. Accordingly, the rate of twist is calculated by Equation (6.12). The values of $\overline{W}_{44}$ are given in Table **??**.

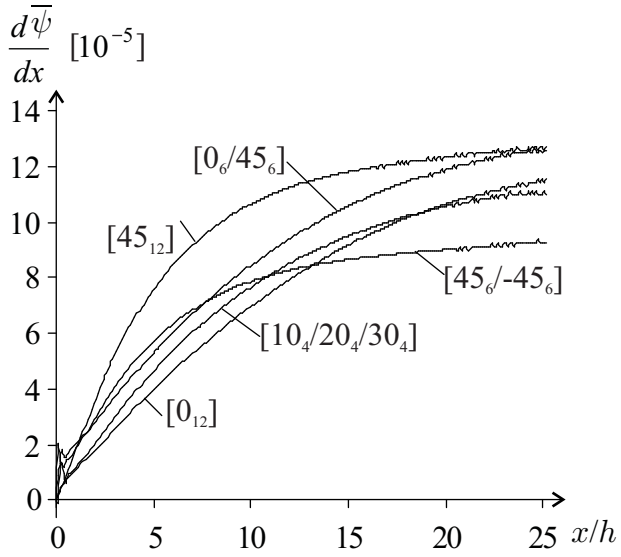

Figure 53: Rate of twist of a cantilever I-beam subjected to an end torque (see Figures 43 and 52) (FE solution)

These results are compared to the FE calculations in which $x/h = 10$ in Table 16.

It can be seen that the rate of twist is predicted reasonably well even close to the built-in end (see Figure 55) where the effect of restrained warping is the most dominant.

We note however that in all the numerical calculations the wall segments of the beam were identical. We have shown in Section **??** that for beams with different wall segments the restrained warping may play an important role.

6.4 Numerical example

An $L = 2000$ mm long C-beam, with the cross-section shown in Figure 56, is made of T300/934 graphite epoxy. The layup is $[45_4/0_4/-45_4]$. The beam is simply supported and is subjected to a uniformly distributed load ($p_z = 0.1345$) acting at point A (see Figure 56). We calculate the deformations at the midspan of the beam at point A.

First we will determine the effect of shear deformations. For the above layup both the "tensile neutral" and the "torque neutral" surfaces coincide with the midplane ($\rho = \nu = 0$). The elements of the compliance matrices are

$$(\alpha_{11}^{\rho})_f = 8.5937 \times 10^{-6} \text{ mm/N} \qquad (\alpha_{66}^{\nu})_w = 5.3184 \times 10^{-5} \text{ mm/N} \tag{6.22}$$

Here and below the forces are given in N and the distances in mm. For simplicity the dimensions are omitted below.

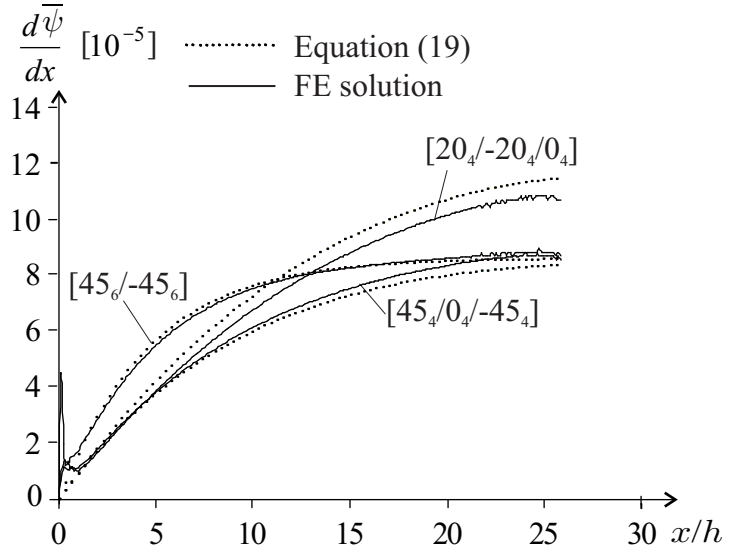

Figure 54: Rate of twist of a cantilever I-beam with balanced layups subjected to an end torque (see Figures 43 and 52) (FE solution)

By taking these values and assuming $L = l = 2000$, $b_f = 50$, $d = 70$, Equation (6.10) yields

$$\alpha = \frac{1}{1 + \frac{2l^2\left(\alpha^{\rho}_{11}\right)_f}{\pi^2 b_f d\left(\alpha^{\mu}_{66}\right)_w}} = \frac{1}{1 + \frac{2\times 2000^2}{\pi^2\times 50\times 70} \times \frac{8.5937\times 10^{-6}}{5.3184\times 10^{-5}}} = 0.0007 \tag{6.23}$$

Consequently, the effect of shear deformation is small and it is not taken into account.

The displacements can be calculated by solving the equilibrium equations, the stress-strain relationships, the strain-displacement relationships together with the imposed boundary conditions.

The stress-strain relationships in matrix form are (the inverse of Equation 6.13)

$$\left\{\begin{array}{c} \widehat{N}_{\overline{x}} \\ \widehat{M}_{\overline{y}} \\ \widehat{M}_{\overline{z}} \\ \widehat{T}_{sv} \\ \widehat{M}_{\omega} \end{array}\right\} = \left[\begin{array}{ccccc} \overline{P}_{11} & \overline{P}_{12} & \overline{P}_{13} & \overline{P}_{14} & \\ \overline{P}_{12} & \overline{P}_{22} & \overline{P}_{23} & \overline{P}_{24} & \\ \overline{P}_{13} & \overline{P}_{23} & \overline{P}_{33} & \overline{P}_{34} & \\ \overline{P}_{14} & \overline{P}_{24} & \overline{P}_{34} & \overline{P}_{44} & \\ & & & & \widehat{EI}_{\omega} \end{array}\right] \left\{\begin{array}{c} \epsilon^{o}_{\overline{x}} \\ \frac{1}{\rho_{\overline{y}}} \\ \frac{1}{\rho_{\overline{z}}} \\ \overline{\vartheta} \\ \overline{\Gamma} \end{array}\right\} \tag{6.24}$$

where the $\overline{P}_{ij}$ $(i, j = 1, 2, 3, 4)$ elements were calculated according to Table 1, and are

$$\left[\begin{array}{cccc} \overline{P}_{11} & \overline{P}_{12} & \overline{P}_{13} & \overline{P}_{14} \\ \overline{P}_{12} & \overline{P}_{22} & \overline{P}_{23} & \overline{P}_{24} \\ \overline{P}_{13} & \overline{P}_{23} & \overline{P}_{33} & \overline{P}_{34} \\ \overline{P}_{14} & \overline{P}_{24} & \overline{P}_{34} & \overline{P}_{44} \end{array}\right] = \left[\begin{array}{cccc} 0.0020 & 0 & 0.0207 & 0.0003 \\ 0 & 1.8431 & 0 & 0 \\ 0.0207 & 0 & 0.7726 & 0.0026 \\ 0.0003 & 0 & 0.0026 & 0.0007 \end{array}\right] \times 10^{10} \tag{6.25}$$

and the torsional stiffness is calculated using the expression derived for isotropic C-beams [19] by

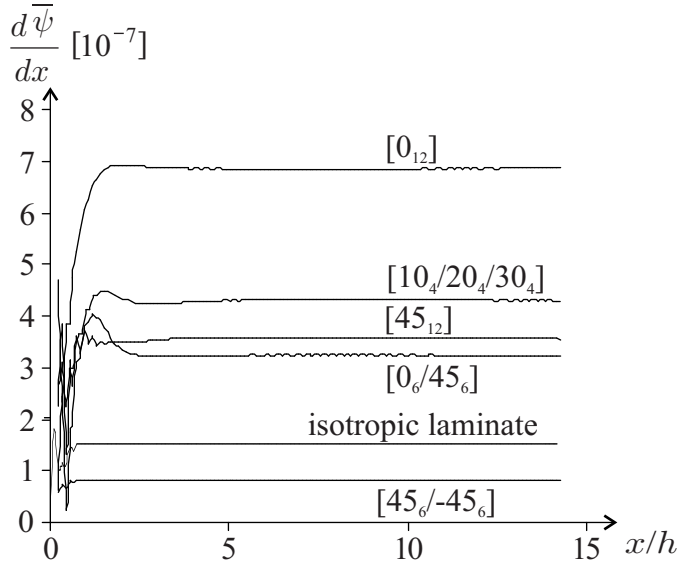

Figure 55: Rate of twist of a cantilever box-beam subjected to an end torque (see Figures 43 and 52)

replacing Eh by $1/\alpha_{11}^{\rho}$ [4]. It yields

$$\widehat{EI}_{\omega} = \frac{\frac{1}{\alpha_{11}^{\rho}} b_f^3}{12} d^2 \frac{\frac{3b_f}{\left(\alpha_{11}^{\rho}\right)_f} + \frac{2d}{\left(\alpha_{11}^{\rho}\right)_w}}{\frac{6b_f}{\left(\alpha_{11}^{\rho}\right)_f} + \frac{d}{\left(\alpha_{11}^{\rho}\right)_w}} = 4.6552 \times 10^{12} \tag{6.26}$$

The strain-displacement relationships (Equation 3.2) in matrix form are

$$\begin{Bmatrix} \epsilon_{\overline{x}}^{o} \\ \frac{1}{\rho_{\overline{y}}} \\ \frac{1}{\rho_{\overline{z}}} \\ \overline{\vartheta} \\ \overline{\Gamma} \end{Bmatrix} = \begin{bmatrix} \frac{d}{dx} & & & \\ & -\frac{d^2}{dx^2} & & \\ & & -\frac{d^2}{dx^2} & \\ & & & \frac{d}{dx} \\ & & & -\frac{d^2}{dx^2} \end{bmatrix} \begin{Bmatrix} \overline{u} \\ \overline{w} \\ \overline{v} \\ \overline{\psi} \end{Bmatrix} \tag{6.27}$$

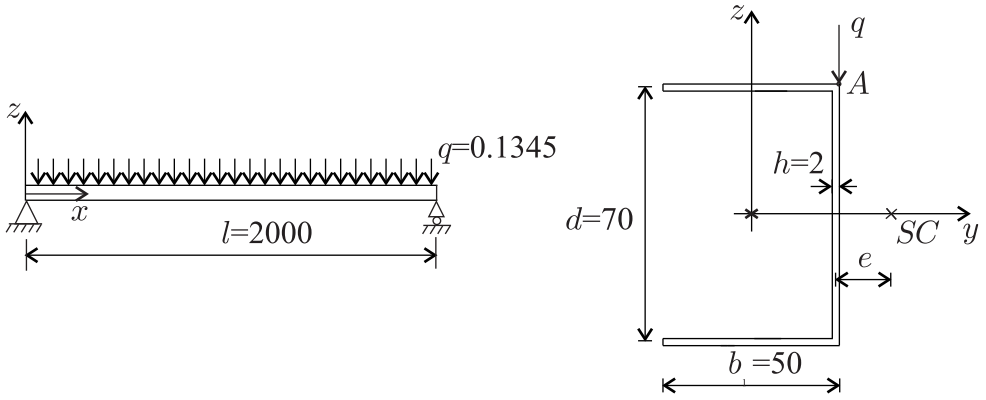

Figure 56: Beam in the numerical example

while *the equilibrium equations* are [6]

$$\begin{bmatrix} -\frac{d}{dx} & & & & \\ & -\frac{d^2}{dx^2} & & & \\ & & -\frac{d^2}{dx^2} & & \\ & & & -\frac{d}{dx} & -\frac{d^2}{dx^2} \end{bmatrix} \begin{Bmatrix} \widehat{N}_{\overline{x}} \\ \widehat{M}_{\overline{y}} \\ \widehat{M}_{\overline{z}} \\ \widehat{T}_{sv} \\ \widehat{M}_{\omega} \end{Bmatrix} = \begin{Bmatrix} p_{\overline{x}} \\ p_{\overline{y}} \\ p_{\overline{z}} \\ t \end{Bmatrix} \tag{6.28}$$

The loads $p_{\overline{z}}$ and t must be calculated with respect to the shear center. The location of the shear center is calculated from the expression given for isotropic beams [19], by replacing Eh by $1/\alpha_{11}^{\rho}$. It yields (Figure 56)

$$e = \frac{\frac{3b_f^2}{\left(\alpha_{11}^{\rho}\right)_f}}{\frac{6b_f}{\left(\alpha_{11}^{\rho}\right)_f} + \frac{d}{\left(\alpha_{11}^{\rho}\right)_w}} = \frac{3 \cdot 50^2}{6 \cdot 50 + 70} = 20.2702 \tag{6.29}$$

Hence the loads are

$$p_{\overline{z}} = 0.1345 \tag{6.30}$$

$$t = p_{\overline{z}} \cdot e = 2.7263 \tag{6.31}$$

We have 14 equations (Equation 6.28, Equation 6.27, Equation 6.24) to determine 14 unknown parameters including: $\widehat{N}_{\overline{x}}$, $\widehat{M}_{\overline{y}}$, $\widehat{M}_{\overline{z}}$, $\widehat{T}_{sv}$, $\widehat{M}_{\omega}$, $\epsilon_{\overline{x}}^{o}$, $\frac{1}{\rho_{\overline{y}}}$, $\frac{1}{\rho_{\overline{z}}}$, $\overline{\vartheta}$, $\overline{\Gamma}$, $\overline{u}$, $\overline{w}$, $\overline{v}$, $\overline{\psi}$.

The boundary conditions at $x = 0$ are

$$\widehat{M}_{\overline{y}} = \widehat{M}_{\overline{z}} = \widehat{M}_{\omega} = \overline{u} = \overline{v} = \overline{w} = \overline{\psi} = 0 \tag{6.32}$$

while at $x = L$ are

$$\widehat{N}_{\overline{x}} = \widehat{M}_{\overline{y}} = \widehat{M}_{\overline{z}} = \widehat{M}_{\omega} = \overline{v} = \overline{w} = \overline{\psi} = 0 \tag{6.33}$$

Solution of the above system of equations prescribed with the boundary conditions are given in Appendix E.

The derived displacement functions are (see Equation 5.15)

$$\begin{Bmatrix} \overline{u} \\ \overline{w} \\ \overline{v} \\ \overline{\psi} \end{Bmatrix} = \begin{Bmatrix} -0.0519 \\ 0 \\ 0.1777 \\ 0.2768 \end{Bmatrix} + \begin{Bmatrix} 0.6633 \times 10^{-4} \\ 0.0025 \\ -0.3757 \times 10^{-3} \\ -0.4162 \times 10^{-3} \end{Bmatrix} x + e^{-0.0012x} \begin{Bmatrix} 0.0406 \\ 0 \\ \text{-0.1944} \\ \text{-0.2549} \end{Bmatrix} + e^{0.0012x} \begin{Bmatrix} 0.0034 \\ 0 \\ 0.0167 \\ \text{-0.0219} \end{Bmatrix} + x^3 \begin{Bmatrix} 0 \\ -0.1236 \times 10^{-8} \\ 0 \\ 0 \end{Bmatrix} + x^2 \begin{Bmatrix} 0 \\ 0 \\ 0.1926 \times 10^{-6} \\ 0 \end{Bmatrix} + x^3 \begin{Bmatrix} 0 \\ 0 \\ -0.4682 \times 10^{-10} \\ 0 \end{Bmatrix} + 10^{-9} \times \begin{Bmatrix} -31.2172x^2 \\ -0.00031x^2 \\ 0 \\ 208.1145x^2 \end{Bmatrix} \tag{6.34}$$

The displacements of the origin of the coordinate system at the midspan ($x = 1000$) are obtained from Equation (6.34)

$$\left\{ \begin{array}{c} \overline{u} \\ \overline{w} \\ \overline{v} \\ \overline{\psi} \end{array} \right\} = \left\{ \begin{array}{c} 0.0070 \\ 1.5447 \\ -0.0522 \\ -0.0808 \end{array} \right\} \tag{6.35}$$

The displacements of the point A are

$$\left\{ \begin{array}{c} \overline{u}^A \\ \overline{w}^A \\ \overline{v}^A \\ \overline{\psi}^A \end{array} \right\} = \left\{ \begin{array}{c} \overline{u} \\ \overline{w} \\ \overline{v} \\ \overline{\psi} \end{array} \right\} + \left\{ \begin{array}{c} 0 \\ \overline{\psi} \times e \\ \overline{\psi} \times d/2 \\ 0 \end{array} \right\} = \left\{ \begin{array}{c} 0.0070 \\ -3.1838 \\ 2.7779 \\ -0.0808 \end{array} \right\} \tag{6.36}$$

(Note that $\overline{\vartheta}$ is zero at the midspan and hence the warping is also zero.)

These displacements were also calculated by the ANSYS finite element program and we obtained

$$\left\{ \begin{array}{c} \overline{u}_N^A \\ \overline{w}_N^A \\ \overline{v}_N^A \\ \overline{\psi}_N^A \end{array} \right\} = \left\{ \begin{array}{c} 0.0079 \\ -3.0797 \\ 2.6211 \\ -0.0746 \end{array} \right\} \tag{6.37}$$

The analytical and numerical calculations agree reasonably well.

7 Conclusions

In Section 3 we presented a beam theory for thin-walled open and closed section composite beams with arbitrary layups which neglects the effect of restrained warping and transverse shear deformation, and developed expressions for the stiffness matrix.

For anisotropic beams, by neglecting the tension-twist or bending-twist coupling result in unaccaptable errors.

Through numerical examples we demonstrated that the local bending stiffnesses of the walls may be neglected only if the layup is either symmetrical or orthotropic. For symmetrical layup the compliances α_{11}, α_{22}, α_{12} and α_{66} must be evaluated at the midsurface, while a "tension neutral" surface, defined by Equation (3.100), must be defined for orthotropic and unsymmetrical laminates and α_{66} must be replaced by the expression given by Equation (3.102).

In Section 5 we gave the basic differential equation system of thin-walled, closed section, orthotropic beams subjected to a torque load. We have solved the problem for sinusoidal load. Solution only for isotropic case can be found in the literature[21], which gives inaccurate results when the stiffnesses of the wall segments differ from each other significantly.

We presented in Section 5 a beam theory for thin-walled, closed section, orthotropic beams taking the restrained warping and the shear deformation into account. We gave numerical examples to demonstrate the accuracy our beam model.

The results of the beam models available in the literature compared to our results are given in Table 17.

By making numerical comparisons in Section 6 we may arrive at the following conclusions:

The restrained warping induced stresses may be neglected for closed section beams, while must be taken into account for open section beams. In the latter case, when the layup of the beam is balanced, the restrained warping induced torque may be calculated with the warping stiffness derived for orthotropic beams.

The effect of shear deformation can be estimated by Equations (6.10) and (6.11). Accordingly, the effect of shear deformation is less then 5 percent for box beams I, C, and Z beams loaded in the vertical plane (Figure 47) when

$$\frac{l}{\sqrt{bd}}\sqrt{\frac{(\alpha_{11}^{\rho})_f}{(\alpha_{66}^{\mu})_w}} < 10 \tag{7.1}$$

and for box beams I, C, and Z beams loaded in the horizontal plane, when

$$\frac{l}{b}\sqrt{\frac{(\alpha_{11}^{\rho})_f}{(\alpha_{66}^{\mu})_w}} < 4.4 \tag{7.2}$$

For beams made of a single layer of orthotropic material $\alpha_{66}^{\mu} = 1/G_{12}h$ and $\alpha_{11}^{\rho} = 1/E_1 h$ where E_1 is the longitudinal Young modulus, G_{12} is the shear modulus and h is the thickness. Consequently, Equation (7.1) and (7.2) becomes

$$\frac{l}{\sqrt{bd}}\sqrt{\frac{Eh_w}{Gh_f}} < 10 \qquad \begin{array}{l}\text{I, C, Z, and box-beams}\\ \text{in the } x-z \text{ plane}\end{array} \tag{7.3}$$

$$\frac{l}{b}\sqrt{\frac{Eh_w}{Gh_f}} < 5 \qquad \begin{array}{l}\text{I-beams}\\ \text{in the } x-y \text{ plane}\end{array} \tag{7.4}$$

8 References

References

[1] O. A. Bachau, A Beam Theory for Anisotropic Materials. Journal of Applied Mechanics. Vol. 52. 416-422. (1985)

[2] L. C. Bank, Modifications to Beam Theory for Bending and Twisting of Open-Section Composite Beams. Composite Structures. Vol. 15. 93-114. (1990)

[3] L. C. Bank, Shear Coefficients for Thin-Walled Composite Beams. Composite Structures. Vol. 8. 47-61. (1987)

layup	$\widehat{GI}_t$ $[10^6\mathrm{Nm}]$	$\widehat{EI}_\omega$ $[10^{12}\mathrm{Nm}^4]$
$[45_6/\text{-}45_6]$	7.2991	0.7358
$[45_4/0_4/\text{-}45_4]$	6.7632	2.9697
$[20_4/\text{-}20_4/0_4]$	3.5212	4.8721

Table 15: The torsional and warping stiffnesses of an I-beam (Figure 43) with different layups

layup	$[0_{12}]$	$[45_{12}]$	$[0_6/45_6]$	$[45_6/\text{-}45_6]$	$[10_4/20_4/30_4]$	isotropic
$\overline{\vartheta}_N$ $[10^{-7}]$(ANSYS)	6.8474	3.5644	3.2294	0.8214	4.3282	1.5410
$\overline{\vartheta}$ $[10^{-7}]$(Equation 6.12)	6.8790	3.5629	3.2072	0.8203	4.2968	1.5341
$\frac{\overline{\vartheta}_N-\overline{\vartheta}}{\overline{\vartheta}_N}\times 100$ [%]	-0.46	0.04	0.69	0.14	0.72	0.44

Table 16: Rate of twist ($\overline{\vartheta}$) of a cantilever, closed section beam at a distance x=700 mm for different layups

cross-section	layup	beam theories	
		classical	with restrained warping
open	isotropic	several authors	Vlasov [21]
	ortotropic		Barbero [5]
	symmetrical	*Mansfield and Sobey [16]**	Bauld and Tzeng [6]
	generally anisotropic	Kollár and Pluzsik [24]	
closed	isotropic ortotropic	several authors	
	symmetrical	Mansfield and Sobey [16]	
	generally anisotropic	Kollár and Pluzsik [24]	
cross-section	layup	beam theories	
		with shear deformations	with restrained warping and shear deformations
open	isotropic	Timoshenko [19]	-
	ortotropic	Barbero [5]	Kollár [12]*Barbero [5]**
	symmetrical	*Bank [3]**	Kobelev and Larichev [11]
	generally anisotropic		*Wu and Sun [23]**
closed	isotropic	Timoshenko [19]	*Urban [20]*, Vlasov [21]**
	ortotropic	Barbero [5]	Pluzsik and Kollár [Section 5]
	symmetrical		
	generally anisotropic		*Wu and Sun [23]**

Table 17: The beam theories with different assumptions. The beam models denoted by * are either inaccurate, or not applicable for all practical cases, or do not give the whole stiffness matrix

[4] E. J. Barbero, R. Lopez-Anido, and J.F. Davalos, On the Mechanics of Thin-Walled Laminated Composite Beams. J. of Composite Materials. Vol. 27. 806-829. (1993)

[5] J. C. Massa and E. J. Barbero, A Strength of Materials Formulation for Thin Walled Composite Beams with Torsion. J. of Composite Materials. Vol. 32. 1560-1594. (1998)

[6] N. R. Bauld and L.S. Tzeng, A Vlasov Theory of Fiber Reinforced Beams with Thin-walled open cross-sections. International Journal of Solids and Structures. Vol. 20. 277-297. (1984)

[7] V. Kristek, Theory of Box Girders. John Wiley & Sons, New York. (1979)

[8] D. H. Hodges, Review of Composite Rotor Blade Modeling. AIAA Journal, Vol. 28. 561-565. (1990)

[9] R. M. Jones, Mechanics of Composite Materials. Scripta Book Company,Washington. (1975)

[10] M. Z. Kabir and A. N. Sherbourne, Shear Strain Effects on Flexure and Torsion of Thin-walled Pultruded Composite Beams. Can. J. Civ. Eng. Vol. 26. 852-868. (1999)

[11] V. V. Kobelev and A. D. Larichev, Model of Thin-Walled Anisotropic Rods. Mechanika Kompozinykh Materialov, Vol. 24. 102-109. (1988)

[12] L. P. Kollár, Flexural-torsional buckling of open section composite coloumns with shear deformation. International Journal of Solids and Structures, 38. 7525-7541. (2001)

[13] L.P. Kollar and G.S. Springer, Mechanics of Composite Structures. Cambridge University Press. (2003)

[14] E. Kreyszig, Advanced Engineering Mathematics. John Wiley and Sons, INC., New York (1993)

[15] S. G. Lekhnitskii, Theory of Elasticity of an Anisotropic Body. Mir Publishers, Moscow. (1981)

[16] E. H. Mansfield and A. J. Sobey, The Fiber Composite Helicopter Blade-Part 1: Stiffness Properties- Part 2: Prospectors for Aeroelastic Tailoring. Aeronautical Quarterly, Vol. 30. 413-449. (1979)

[17] T. H. G. Megson, Aircraft Structures for Engineering Students. 2nd Edition. Halsted Press, John Wiley & Sons, New York. (1990)

[18] T. M. Roberts and H. Al-Ubaidi, Influence of Shear Deformation on Restrained Torsional Warping of Pultruded FRP Bars of Open Cross-Section. Thin-Walled Structures. Vol. 39. 395-414. (2001)

[19] S. P. Timoshenko and J.M. Gere, Theory of Elastic Stability. 2nd Edition. McGraw-Hill, New York (1961)

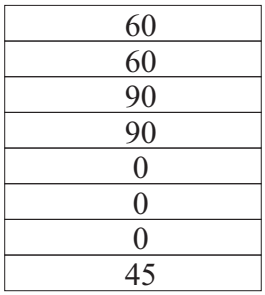

Figure 57: Example of laminated plate

[20] I. V. Urban, Teoria Rascota Sterznevih Tonkostennih Konstrukcij. Gosudarstvennoe Transportnoe Zeleznodoroznoe Izdatelstvo, Moscow. (1955)

[21] V. Z. Vlasov, Thin-walled elastic beams. Office of Technical Services. U.S. Department of Commerce, Wasington 25, DC, TT-61-11400 (1961)

[22] Wilkinson, The algebraic eigenvalue problem. Clarendon Press, Oxford. (1996)

[23] X. Wu and C. T. Sun, Simplified Theory for Composite Thin-Walled Beams. AIAA Journal, Vol. 30. 2945-2951. (1992)

[24] L. P. Kollár and A. Pluzsik, Analysis of Thin-Walled Composite Beams with Arbitrary Layup. Journal of Reinforced Plastics & Composites, Vol.21. 1423-1465 (2002)

[25] A. Pluzsik and L. P. Kollár, Effects of the different engineering approximations in the analysis of composite beams. Journal of Reinforced Plastics & Composites, Vol.21. (2002)

A Stiffness matrix of a laminated composite plate

Here we summarise the stiffness matrix of a laminated composite on the basis of [9]. A composite plate may consist of several plies. In a ply the orientation of the fibers are the same, the angle of the fibers with respect to the x axis is denoted by Θ. The laminate code gives the values of Θ for each ply from the bottom to the top. For example the laminate code of the layup shown in Figure 57 is $[45/0_3/90_2/60_2]$.

The stress-strain relationship for a ply (for plane-stress conditions) is:

$$\left\{ \begin{array}{c} \sigma_\xi \\ \sigma_\eta \\ \tau_{\xi\eta} \end{array} \right\}_k = \left[\begin{array}{ccc} Q_{11} & Q_{12} & Q_{16} \\ Q_{12} & Q_{22} & Q_{26} \\ Q_{16} & Q_{26} & Q_{66} \end{array} \right]_k \left\{ \begin{array}{c} \epsilon_\xi \\ \epsilon_\eta \\ \gamma_{\xi\eta} \end{array} \right\}_k \tag{1.1}$$

For a thin plate element the plate theory defines the following internal forces and moments (see

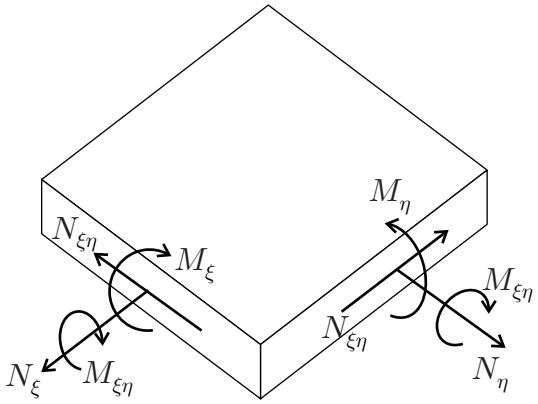

Figure 58: Internal forces and moments defined on a thin plate element

Figure 58):

$$N_\xi = \int_h \sigma_\xi dz \qquad N_\eta = \int_h \sigma_\eta dz \qquad N_{\xi\eta} = \int_h \tau_{\xi\eta} dz \tag{1.2}$$

$$M_\xi = \int_h z\sigma_\xi dz \qquad M_\eta = \int_h z\sigma_\eta dz \qquad M_{\xi\eta} = \int_h z\tau_{\xi\eta} dz \tag{1.3}$$

The strains in the reference surface can be calculated from the displacements of the reference plane:

$$\epsilon^o_\xi = \frac{\partial u^0}{\partial x} \qquad \epsilon^o_\eta = \frac{\partial v^0}{\partial y} \qquad \gamma^0_{\xi\eta} = \frac{\partial u^0}{\partial y} + \frac{\partial v^0}{\partial x} \tag{1.4}$$

$$\kappa_\xi = \frac{\partial^2 w^0}{\partial x^2} \qquad \kappa_\eta = \frac{\partial^2 w^0}{\partial y^2} \qquad \kappa_{\xi\eta} = -\frac{2\partial^2 w^0}{\partial x \partial y} \tag{1.5}$$

where u^0, v^0 and w^0 are the ξ, η, and ζ components of the displacement of the reference plane, respectively. The stiffness matrix of the plate gives the relationship between these internal forces and strains:

$$\begin{Bmatrix} N_\xi \\ N_\eta \\ N_{\xi\eta} \\ M_\xi \\ M_\eta \\ M_{\xi\eta} \end{Bmatrix} = \begin{bmatrix} A_{11} & A_{12} & A_{16} & B_{11} & B_{12} & B_{16} \\ A_{12} & A_{22} & A_{26} & B_{21} & B_{22} & B_{26} \\ A_{16} & A_{26} & A_{66} & B_{61} & B_{62} & B_{66} \\ B_{11} & B_{21} & B_{61} & D_{11} & D_{12} & D_{16} \\ B_{12} & B_{22} & B_{62} & D_{12} & D_{22} & D_{26} \\ B_{16} & B_{26} & B_{66} & D_{16} & D_{26} & D_{66} \end{bmatrix} \begin{Bmatrix} \epsilon^o_\xi \\ \epsilon^o_\eta \\ \gamma^0_{\xi\eta} \\ \kappa_\xi \\ \kappa_\eta \\ \kappa_{\xi\eta} \end{Bmatrix} \tag{1.6}$$

The compliance matrix of the plate is the inverse of the stiffness matrix:

$$\begin{bmatrix} \alpha_{11} & \alpha_{12} & \alpha_{16} & \beta_{11} & \beta_{12} & \beta_{16} \\ \alpha_{12} & \alpha_{22} & \alpha_{26} & \beta_{21} & \beta_{22} & \beta_{26} \\ \alpha_{16} & \alpha_{26} & \alpha_{66} & \beta_{11} & \beta_{61} & \beta_{66} \\ \beta_{11} & \beta_{21} & \beta_{61} & \delta_{11} & \delta_{12} & \delta_{16} \\ \beta_{12} & \beta_{22} & \beta_{62} & \delta_{12} & \delta_{22} & \delta_{26} \\ \beta_{16} & \beta_{26} & \beta_{66} & \delta_{16} & \delta_{26} & \delta_{66} \end{bmatrix} = \begin{bmatrix} A_{11} & A_{12} & A_{16} & B_{11} & B_{12} & B_{16} \\ A_{12} & A_{22} & A_{26} & B_{21} & B_{22} & B_{26} \\ A_{16} & A_{26} & A_{66} & B_{61} & B_{62} & B_{66} \\ B_{11} & B_{21} & B_{61} & D_{11} & D_{12} & D_{16} \\ B_{12} & B_{22} & B_{62} & D_{12} & D_{22} & D_{26} \\ B_{16} & B_{26} & B_{66} & D_{16} & D_{26} & D_{66} \end{bmatrix}^{-1} \tag{1.7}$$

.

From the stiffness matrices $[\overline{Q}]_k$ of the plies (Equation 1.1) we can obtain the elements of the stiffness matrix of the plate as follows:

$$A_{ij} = \int_h \overline{Q}_{ij} dz \tag{1.8}$$

$$B_{ij} = \int_h z\overline{Q}_{ij} dz \qquad i,j = 1,2,6 \tag{1.9}$$

$$D_{ij} = \int_h z^2\overline{Q}_{ij} dz \tag{1.10}$$

B Solution of the differential equation of beams in torsion

B.1 Simply supported beam

We consider a simply supported beam with the length l subjected to a torque with arbitrary distribution. The torque load is represented by its Fourier series expansion:

$$t = \sum \widetilde{t}_k \sin\frac{\pi k x}{l} \tag{2.1}$$

In the following we determine the rate of twist for the kth element of the load: $\widetilde{t}_k \sin \pi k x/l$.

The governing equations are given by Equations (5.66), (5.67) and (5.68) which - for pure torsion - are reiterated below

$$\begin{Bmatrix} \overline{\vartheta} \\ \overline{\vartheta}_S \\ \overline{\Gamma} \end{Bmatrix} = \begin{bmatrix} \frac{d}{dx} & \\ \frac{d}{dx} & -1 \\ & -\frac{d}{dx} \end{bmatrix} \begin{Bmatrix} \overline{\psi} \\ \overline{\vartheta}_B \end{Bmatrix} \tag{2.2}$$

$$\begin{Bmatrix} \widehat{T}_{\overline{sv}} \\ \widehat{T}_{\overline{\omega}} \\ \widehat{M}^*_{\overline{\omega}} \end{Bmatrix} = \begin{bmatrix} \overline{GI}_t & & \\ & \overline{S}_{\omega\omega} & \\ & & \overline{EI}_\omega \end{bmatrix} \begin{Bmatrix} \overline{\vartheta} \\ \overline{\vartheta}_S \\ \overline{\Gamma} \end{Bmatrix} \tag{2.3}$$

$$\begin{bmatrix} -\frac{d}{dx} & -\frac{d}{dx} & \\ & -1 & \frac{d}{dx} \end{bmatrix} \begin{Bmatrix} \widehat{T}_{\overline{sv}} \\ \widehat{T}_{\overline{\omega}} \\ \widehat{M}^*_{\overline{\omega}} \end{Bmatrix} = \begin{Bmatrix} \widetilde{t}_k \sin\frac{\pi k x}{l} \\ 0 \end{Bmatrix} \tag{2.4}$$

The boundary conditions are

$$\begin{aligned} \overline{\psi}(0) &= 0 \qquad & \frac{d^2\overline{\psi}}{dx^2}(0) = 0 \\ \overline{\psi}(l) &= 0 \qquad & \frac{d^2\overline{\psi}}{dx^2}(l) = 0 \end{aligned} \tag{2.5}$$

The rate of twist ϑ and ϑ_S are assumed in the form

$$\overline{\psi}_k = \widetilde{\psi}_k \sin\frac{\pi k x}{l} \tag{2.6}$$

$$\overline{\vartheta}_{Bk} = \widetilde{\vartheta}_{Bk} \cos\frac{\pi k x}{l} \tag{2.7}$$

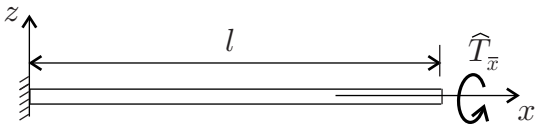

Figure 59: Cantilever beam subjected to a torque at the end

which satisfy the boundary conditions (Equation 2.5).

By introducing $\overline{\psi}_k$ and $\overline{\vartheta}_{Bk}$ into Equations (2.2), (2.3) and (2.4) we obtain

$$\left\{ \begin{array}{c} \overline{\vartheta} \\ \overline{\vartheta}_S \\ \overline{\Gamma} \end{array} \right\} = \left[\begin{array}{ccc} \frac{d}{dx} & & \\ \frac{d}{dx} & -1 & \\ & -\frac{d}{dx} & \end{array} \right] \left\{ \begin{array}{c} \widetilde{\psi}_k \sin\frac{\pi k x}{l} \\ \widetilde{\vartheta}_{Bk} \cos\frac{\pi k x}{l} \end{array} \right\} = \left\{ \begin{array}{c} \widetilde{\psi}_k \frac{\pi k}{l} \cos\frac{\pi k x}{l} \\ \left(\widetilde{\psi}_k \frac{\pi k}{l} - \widetilde{\vartheta}_{Bk}\right) \cos\frac{\pi k x}{l} \\ \widetilde{\vartheta}_{Bk} \frac{\pi k}{l} \sin\frac{\pi k x}{l} \end{array} \right\} \tag{2.8}$$

$$\left\{ \begin{array}{c} \widehat{T}_{\overline{sv}} \\ \widehat{T}_{\overline{\omega}} \\ \widehat{M}^*_{\overline{\omega}} \end{array} \right\} = \left[\begin{array}{ccc} \overline{GI}_t & & \\ & \overline{S}_{\omega\omega} & \\ & & \overline{EI}_\omega \end{array} \right] \left\{ \begin{array}{c} \overline{\vartheta} \\ \overline{\vartheta}_S \\ \overline{\Gamma} \end{array} \right\} = \left\{ \begin{array}{c} \overline{GI}_t \widetilde{\psi}_k \frac{\pi k}{l} \cos\frac{\pi k x}{l} \\ \overline{S}_{\omega\omega} \left(\widetilde{\psi}_k \frac{\pi k}{l} - \widetilde{\vartheta}_{Bk}\right) \cos\frac{\pi k x}{l} \\ \overline{EI}_\omega \widetilde{\vartheta}_{Bk} \frac{\pi k}{l} \sin\frac{\pi k x}{l} \end{array} \right\} \tag{2.9}$$

$$\begin{aligned} \left[\begin{array}{ccc} -\frac{d}{dx} & -\frac{d}{dx} & \\ & -1 & \frac{d}{dx} \end{array} \right] \left\{ \begin{array}{c} \widehat{T}_{\overline{sv}} \\ \widehat{T}_{\overline{\omega}} \\ \widehat{M}^*_{\overline{\omega}} \end{array} \right\} &= \left\{ \begin{array}{c} \overline{GI}_t \widetilde{\psi}_k \frac{\pi^2 k^2}{l^2} \sin\frac{\pi k x}{l} + \overline{S}_{\omega\omega} \left(\widetilde{\psi}_k \frac{\pi^2 k^2}{l^2} - \widetilde{\vartheta}_{Bk} \frac{\pi k}{l}\right) \sin\frac{\pi k x}{l} \\ -\overline{S}_{\omega\omega} \left(\widetilde{\psi}_k \frac{\pi k}{l} - \widetilde{\vartheta}_{Bk}\right) \cos\frac{\pi k x}{l} + \overline{EI}_\omega \widetilde{\vartheta}_{Bk} \frac{\pi^2 k^2}{l^2} \cos\frac{\pi k x}{l} \end{array} \right\} = \\ &= \left\{ \begin{array}{c} \widetilde{t}_k \sin\frac{\pi k x}{l} \\ 0 \end{array} \right\} \end{aligned} \tag{2.10}$$

From these equations, after algebraic manipulation, we obtain

$$\overline{\psi} = \sum \widetilde{\psi}_k \sin\frac{\pi k x}{l} \tag{2.11}$$

$$\widetilde{\psi}_k = \frac{l^2}{\pi^2 k^2 \left(\overline{GI}_t + \overline{S}_{\omega\omega} \left(1 - \frac{\overline{S}_{\omega\omega}}{\overline{S}_{\omega\omega} + \overline{EI}_\omega \frac{\pi^2 k^2}{l^2}}\right)\right)} \widetilde{t}_k \tag{2.12}$$

The rate of twist $\overline{\vartheta}$ is the derivative of $\overline{\psi}$, which is

$$\overline{\vartheta} = \sum \widetilde{\vartheta}_k \cos\frac{\pi k x}{l} \tag{2.13}$$

$$\widetilde{\vartheta}_k = \frac{l}{\pi k \left(\overline{GI}_t + \overline{S}_{\omega\omega} \left(1 - \frac{\overline{S}_{\omega\omega}}{\overline{S}_{\omega\omega} + \overline{EI}_\omega \frac{\pi^2 k^2}{l^2}}\right)\right)} \widetilde{t}_k \tag{2.14}$$

B.2 Cantilever beam subjected to a concentrated torque at the end

We consider a cantilever beam subjected to a torque $\widehat{T}$ at the end (Figure 59). The governing equations are given by Equations (2.2), (2.3) and (2.4), with $t = 0$.

Substituting Equation (2.2) into Equation (2.3) and then into Equation (2.4) we obtain

$$\left[\begin{array}{cc} \left(\overline{GI}_t + \overline{S}_{\omega\omega}\right) \frac{d^2}{dx^2} & -\overline{S}_{\omega\omega} \frac{d}{dx} \\ -\overline{S}_{\omega\omega} \frac{d}{dx} & \overline{S}_{\omega\omega} - \overline{EI}_\omega \frac{d^2}{dx^2} \end{array} \right] \left\{ \begin{array}{c} \overline{\psi} \\ \overline{\vartheta}_B \end{array} \right\} = \left\{ \begin{array}{c} 0 \\ 0 \end{array} \right\} \tag{2.15}$$

The boundary conditions are

$$\begin{aligned} \overline{\psi}(0) &= 0 \quad \overline{\vartheta}_B(0) = 0 \\ \widehat{M}^*_{\overline{\omega}}(l) &= 0 \quad \widehat{T}(l) = \widehat{T} \end{aligned} \tag{2.16}$$

Using Equations (2.2), (2.3) and (2.22) we get

$$\begin{aligned} \overline{\psi}(0) &= 0 \quad \overline{\vartheta}_B(0) = 0 \\ \frac{d\overline{\vartheta}_B}{dx}(l) &= 0 \quad \overline{GI}_t \frac{d\overline{\psi}}{dx}(l) + \overline{S}_{\omega\omega}\left(\frac{d\overline{\psi}}{dx}(l) - \overline{\vartheta}_B(l)\right) = \widehat{T} \end{aligned} \tag{2.17}$$

We assume the solution of Equation (2.15) as follows

$$\left\{ \begin{array}{c} \overline{\psi} \\ \overline{\vartheta}_B \end{array} \right\} = \left\{ \begin{array}{c} \overline{\psi}_0 \\ \overline{\vartheta}_{B0} \end{array} \right\} e^{\lambda x} = \left\{\overline{\psi}_0\right\} e^{\lambda x} \tag{2.18}$$

Substituting Equation (2.18) into Equation (2.15), and dividing by $e^{\lambda x}$, we obtain

$$\left[\begin{array}{cc} \left(\overline{GI}_t + \overline{S}_{\omega\omega}\right)\lambda^2 & -\overline{S}_{\omega\omega}\lambda \\ -\overline{S}_{\omega\omega}\lambda & \overline{S}_{\omega\omega} - \overline{EI}_\omega\lambda^2 \end{array} \right] \left\{ \begin{array}{c} \overline{\psi}_0 \\ \overline{\vartheta}_{B0} \end{array} \right\} = \left\{ \begin{array}{c} 0 \\ 0 \end{array} \right\} \tag{2.19}$$

which can be written as

$$\left(\lambda^2[K] + \lambda[L] + [M]\right)\left\{\overline{\psi}_0\right\} = \{0\} \tag{2.20}$$

where

$$[K] = \left[\begin{array}{cc} \overline{GI}_t + \overline{S}_{\omega\omega} & 0 \\ 0 & -\overline{EI}_\omega \end{array} \right] \quad [L] = \left[\begin{array}{cc} 0 & -\overline{S}_{\omega\omega} \\ v & 0 \end{array} \right] \quad [M] = \left[\begin{array}{cc} 0 & 0 \\ 0 & \overline{S}_{\omega\omega} \end{array} \right] \tag{2.21}$$

Equation (2.20) is an eigenvalue problem for λ. To obtain the values of λ and $\left\{\overline{\psi}_0\right\}$ we rearrange Equation (2.20) in the following form [22]

$$\lambda \left[\begin{array}{cc} K & L \\ 0 & E \end{array} \right] \left\{ \begin{array}{c} y \\ \overline{\psi}_0 \end{array} \right\} + \left[\begin{array}{cc} 0 & M \\ -E & 0 \end{array} \right] \left\{ \begin{array}{c} y \\ \overline{\psi}_0 \end{array} \right\} = \{0\} \tag{2.22}$$

where $\{y\} = \lambda\left\{\overline{\psi}_0\right\}$ and $[E]$ is a 2×2 unit matrix.

Equation (2.22) is an eigenvalue problem for λ, which results in 4 eigenvalue $\lambda_1, \ldots \lambda_4$ and four eigen vectors $y^1, \overline{\psi}_0^1, \ldots y^4, \overline{\psi}_0^4$.

With these results the solution of Equation (2.15) is

$$\left\{ \begin{array}{c} \overline{\psi}_0 \\ \overline{\vartheta}_{B0} \end{array} \right\} = C_1 e^{\lambda_1 x}\overline{\psi}_0^1 + C_2 e^{\lambda_2 x}\overline{\psi}_0^2 + C_3 e^{\lambda_3 x}\overline{\psi}_0^3 + C_4 e^{\lambda_4 x}\overline{\psi}_0^4 \tag{2.23}$$

Substituting these into the expressions of the boundary conditions (Equation 2.17) we obtain an algebraic equation system which yields the yet unknown constants C_i $(i = 1, 2, \ldots 4)$.

When $\overline{S}_{\omega\omega}$ is large $(\overline{S}_{\omega\omega} > 10l^2\overline{EI}_\omega)$ the results are very close to those given by the expression derived on the basis of $\overline{GI}_t$ and $\overline{EI}_\omega$ (while $\overline{S}_{\omega\omega} = \infty$) [17].

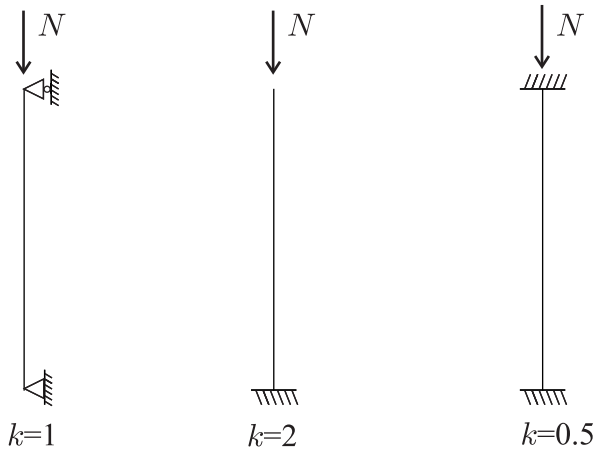

Figure 60: Coloumns with different end conditions subjected to a concentrated force at the end

C Buckling of composite columns subjected to concentrated loads

We consider a column which is subjected to a concentrated force at the end (Figure 60). The end conditions are shown in Figure 60.

We have shown in Section 5.7.2 that the governing equations of beams with open and closed cross-sections are identical, and hence, the results derived for open section beams can be directly applied for closed section beams. Consequently the critical loads are [12]

$$\begin{aligned} \frac{1}{\widehat{N}_{crz}} &= \frac{1}{\widehat{N}^B_{crz}} + \frac{1}{\overline{S}_{yy}} \qquad \frac{1}{\widehat{N}_{cry}} = \frac{1}{\widehat{N}^B_{cry}} + \frac{1}{\overline{S}_{zz}} \qquad \frac{1}{\widehat{N}_{cr\omega}} = \frac{1}{\widehat{N}^B_{cr\omega}} + \frac{1}{\frac{1}{i^2_\omega}\overline{S}_{\omega\omega}} \\ \widehat{N}^B_{crz} &= \frac{\pi^2 \overline{EI}_{zz}}{l^2} \qquad \widehat{N}^B_{cry} = \frac{\pi^2 \overline{EI}_{yy}}{l^2} \qquad \widehat{N}^B_{cr\omega} = \frac{1}{i^2_\omega}\frac{\pi^2 \overline{EI}_{\omega}}{l^2} \qquad i^2_\omega = \frac{\overline{EI}_{zz} + \overline{EI}_{yy}}{\overline{EA}} \end{aligned} \tag{3.1}$$

where k is given in Figure 60.

D The "neutral" surfaces of a laminate

In a laminated plate made of *isotropic plies* there is a neutral plane with the following features: (*i*) when forces (per unit length) N_x, N_y, and N_{xy} are applied at the neutral plane the plate remains plane, and (*ii*) when bending moments (per unit length) M_x, M_y, and M_{xy} are applied on the plate the strains in the neutral plane are zero.

In a laminated plate made of anisotropic plies no such a plane exists. However, we can define two surfaces with similar features as the above neutral plane.

"Tension neutral" surface. We can define a surface such that an axial force (per unit length) N_x applied at this surface does not cause a curvature in the $x-z$ plane ($\kappa_x = 0$, see Figure 61).

The location of this "tension neutral" surface is at a distance ρ from the reference surface which

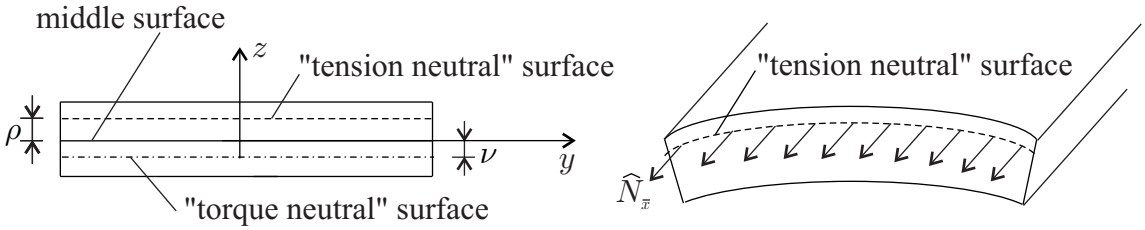

Figure 61: Tension and torque neutral surface (left) and the deformation of a plate element loaded in the "tension neutral surface" (right)

is calculated by

$$\rho = -\frac{\beta_{11}}{\alpha_{11}} \tag{4.1}$$

where α_{11} and β_{11} are the elements of the $[\alpha]$ and $[\beta]$ compliance matrices which are evaluated at the reference surface, and are defined as

$$\begin{bmatrix} \alpha & \beta \\ \beta^T & \delta \end{bmatrix} = \begin{bmatrix} A & B \\ B^T & D \end{bmatrix}^{-1} \tag{4.2}$$

where $[A]$, $[B]$, and $[D]$ are the stiffness matrices of a laminate. At the "tension neutral" surface the compliances α^{ρ}_{ij}, β^{ρ}_{ij}, and δ^{ρ}_{ij} are calculated by the parallel axis theorem, and are

$$\begin{aligned} \alpha^{\rho}_{ij} &= \alpha_{ij} + 2\rho\beta_{ij} + \rho^2\delta_{ij} \\ \beta^{\rho}_{ij} &= \beta_{ij} + \rho\delta_{ij} \\ \delta^{\rho}_{ij} &= \delta_{ij} \end{aligned} \tag{4.3}$$

"*Torque neutral" surface.* We can define a surface such that a shear flow N_{xy} applied at this surface does not cause the twist of the plate ($\kappa_{xy} = 0$). The location of this "torque neutral" surface is at a distance ν from the reference surface, which is

$$\nu = -\frac{\beta_{66}}{\alpha_{66}} \tag{4.4}$$

where α_{66} and β_{66} are evaluated at the reference surface. At the "torque neutral" surface the compliances are

$$\begin{aligned} \alpha^{\nu}_{ij} &= \alpha_{ij} + 2\nu\beta_{ij} + \nu^2\delta_{ij} \\ \beta^{\nu}_{ij} &= \beta_{ij} + \nu\delta_{ij} \\ \delta^{\nu}_{ij} &= \delta_{ij} \end{aligned} \tag{4.5}$$

We may observe that for an isotropic plate made of one layer the "tension neutral" and the "torque neutral" surfaces coincide with the neutral surface, which is at the midplane.

E Solution of a simply supported beam

First we substitute Equation (6.24) into Equation (4.1) and then Equation (6.27) into the resulting expression. We obtain

$$\begin{bmatrix} \overline{P}_{11}\frac{d^2}{dx^2} & 0 & -\overline{P}_{13}\frac{d^3}{dx^3} & \overline{P}_{14}\frac{d^2}{dx^2} \\ 0 & -\overline{P}_{22}\frac{d^4}{dx^4} & 0 & 0 \\ -\overline{P}_{31}\frac{d^3}{dx^3} & 0 & -\overline{P}_{33}\frac{d^4}{dx^4} & -\overline{P}_{34}\frac{d^3}{dx^3} \\ \overline{P}_{41}\frac{d^2}{dx^2} & 0 & -\overline{P}_{43}\frac{d^3}{dx^3} & \overline{P}_{44}\frac{d^2}{dx^2} - \widehat{EI}_{\omega}\frac{d^4}{dx^4} \end{bmatrix} \begin{Bmatrix} \overline{u} \\ \overline{w} \\ \overline{v} \\ \overline{\psi} \end{Bmatrix} = \begin{Bmatrix} 0 \\ p_{\overline{z}} \\ 0 \\ t \end{Bmatrix} \tag{5.1}$$

Homogeneous solution of the differential equation system (Equation 5.1): We assume the homogeneous solution of Equation (5.1) as follows

$$\begin{Bmatrix} \overline{u}_h \\ \overline{w}_h \\ \overline{v}_h \\ \overline{\psi}_h \end{Bmatrix} = \begin{Bmatrix} \overline{u}_0 \\ \overline{w}_0 \\ \overline{v}_0 \\ \overline{\psi}_0 \end{Bmatrix} e^{\lambda x} = \{\overline{u}_0\}\, e^{\lambda x} \tag{5.2}$$

Substituting Equation (5.2) into the homogeneous form of Equation (5.1), and dividing by $e^{\lambda x}$, we obtain

$$\begin{bmatrix} \overline{P}_{11}\lambda^2 & 0 & -\overline{P}_{13}\lambda^3 & \overline{P}_{14}\lambda^2 \\ 0 & -\overline{P}_{22}\lambda^4 & 0 & 0 \\ \overline{P}_{31}\lambda^3 & 0 & -\overline{P}_{33}\lambda^4 & \overline{P}_{34}\lambda^3 \\ \overline{P}_{41}\lambda^2 & 0 & -\overline{P}_{43}\lambda^3 & \overline{P}_{44}\lambda^2 - \widehat{EI}_{\omega}\lambda^4 \end{bmatrix} \begin{Bmatrix} \overline{u}_0 \\ \overline{w}_0 \\ \overline{v}_0 \\ \overline{\psi}_0 \end{Bmatrix} = \begin{Bmatrix} 0 \\ 0 \\ 0 \\ 0 \end{Bmatrix} \tag{5.3}$$

which can be written as

$$\lambda^2 \left(\lambda^2 [K] + \lambda [L] + [M]\right) \{u_0\} = \{0\} \tag{5.4}$$

where

$$[K] = \begin{bmatrix} 0 & 0 & 0 & 0 \\ 0 & -\overline{P}_{22} & 0 & 0 \\ 0 & 0 & -\overline{P}_{33} & 0 \\ 0 & 0 & 0 & -\widehat{EI}_{\omega} \end{bmatrix} \quad [L] = \begin{bmatrix} 0 & 0 & -\overline{P}_{13} & 0 \\ 0 & 0 & 0 & 0 \\ \overline{P}_{31} & 0 & 0 & \overline{P}_{34} \\ 0 & 0 & -\overline{P}_{43} & 0 \end{bmatrix}$$

$$[M] = \begin{bmatrix} \overline{P}_{11} & 0 & 0 & \overline{P}_{14} \\ 0 & 0 & 0 & 0 \\ 0 & 0 & 0 & 0 \\ \overline{P}_{41} & 0 & 0 & \overline{P}_{44} \end{bmatrix} \tag{5.5}$$

Equation (5.4) is an eigenvalue problem for λ. Two solutions are $\lambda_1 = \lambda_2 = 0$. To obtain the remaining values of λ and $\{u_0\}$ we rearrange Equation (5.4) in the following form [22]

$$\lambda \begin{bmatrix} K & L \\ 0 & E \end{bmatrix} \begin{Bmatrix} y \\ u_0 \end{Bmatrix} + \begin{bmatrix} 0 & M \\ -E & 0 \end{bmatrix} \begin{Bmatrix} y \\ u_0 \end{Bmatrix} = \{0\} \tag{5.6}$$

where $\{y\} = \lambda\{u_0\}$ and $[E]$ is a 4×4 unit matrix.

By solving Equation (5.6) we obtain the following values for λ and $[U_0] = \left[u_0^1, u_0^2, ..., u_0^6\right]$:

$$[\lambda] = \begin{bmatrix} \text{-0.0012} & 0.0012 & 0 & 0 & 0 & 0 \end{bmatrix} \tag{5.7}$$

$$[U_0] = \begin{bmatrix} 0.1257 & 0.1257 & 0 & 0 & 0 & 0 \\ 0 & 0 & 1 & \text{-1} & 0 & 0 \\ \text{-0.6017} & 0.6017 & 0 & 0 & 1 & \text{-1} \\ \text{-0.7888} & \text{-0.7888} & 0 & 0 & 0 & 0 \end{bmatrix} \tag{5.8}$$

Note that there are two additional eigenvalues ($\lambda_7 = \lambda_8 = -\infty$) which are not independent solutions of the original equation (Equation 5.1). With these results the homogeneous solution of Equation (5.1) is

$$\begin{Bmatrix} \overline{u}_h \\ \overline{w}_h \\ \overline{v}_h \\ \overline{\psi}_h \end{Bmatrix} = \begin{Bmatrix} C_1 \\ C_2 \\ C_3 \\ C_4 \end{Bmatrix} + \begin{Bmatrix} C_5 \\ C_6 \\ C_7 \\ C_8 \end{Bmatrix} x + C_9 e^{-0.0012x} \begin{Bmatrix} 0.1257 \\ 0 \\ \text{-0.6017} \\ \text{-0.7888} \end{Bmatrix} + C_{10} \times e^{0.0012x} \begin{Bmatrix} 0.1257 \\ 0 \\ 0.6017 \\ \text{-0.7888} \end{Bmatrix} + C_{11} x^2 \begin{Bmatrix} 0 \\ 1 \\ 0 \\ 0 \end{Bmatrix} + C_{12} x^3 \begin{Bmatrix} 0 \\ -1 \\ 0 \\ 0 \end{Bmatrix} + C_{13} x^2 \begin{Bmatrix} 0 \\ 0 \\ 1 \\ 0 \end{Bmatrix} + C_{14} x^3 \begin{Bmatrix} 0 \\ 0 \\ -1 \\ 0 \end{Bmatrix} \tag{5.9}$$

Inhomogeneous solution: We assume the inhomogeneous solution in the following form:

$$\begin{Bmatrix} \overline{u}_p \\ \overline{w}_p \\ \overline{v}_p \\ \overline{\psi}_p \end{Bmatrix} = \begin{Bmatrix} ax^2 \\ bx^4 \\ 0 \\ cx^2 \end{Bmatrix} \tag{5.10}$$

Substituting Equation (5.10) into the differential equation system (Equation 5.1) we obtain an algebraic equation which yields the yet unknown constants a, b, and c as:

$$\begin{Bmatrix} a \\ b \\ c \end{Bmatrix} = \begin{bmatrix} \overline{P}_{11} & 0 & \overline{P}_{14} \\ 0 & \text{-}24\overline{P}_{22} & 0 \\ \overline{P}_{41} & 0 & \overline{P}_{44} \end{bmatrix}^{-1} \begin{Bmatrix} 0 \\ -p_{\overline{z}} \\ t/2 \end{Bmatrix} = \begin{Bmatrix} -31.2172 \\ -0.00031 \\ 208.1145 \end{Bmatrix} \times 10^{-9} \tag{5.11}$$

Consequently, the inhomogeneous solution is (Equation 5.10 and 5.11)

$$\begin{Bmatrix} \overline{u}_p \\ \overline{w}_p \\ \overline{v}_p \\ \overline{\psi}_p \end{Bmatrix} = \begin{Bmatrix} -31.2172x^2 \\ -0.00031x^2 \\ 0 \\ 208.1145x^2 \end{Bmatrix} \times 10^{-9} \tag{5.12}$$

The solution of Equation (5.1) is the sum of the homogeneous solution (Equation 5.9) and the inhomogeneous solution (Equation 5.12).

$$\begin{aligned} \begin{Bmatrix} \overline{u} \\ \overline{w} \\ \overline{v} \\ \overline{\psi} \end{Bmatrix} = & \begin{Bmatrix} C_1 \\ C_2 \\ C_3 \\ C_4 \end{Bmatrix} + \begin{Bmatrix} C_5 \\ C_6 \\ C_7 \\ C_8 \end{Bmatrix} x + C_9 \times e^{-0.0012x} \begin{Bmatrix} 0.1257 \\ 0 \\ \text{-0.6017} \\ \text{-0.7888} \end{Bmatrix} + \\ & + C_{10} \times e^{0.0012x} \begin{Bmatrix} 0.1257 \\ 0 \\ 0.6017 \\ \text{-0.7888} \end{Bmatrix} + C_{11}x^2 \begin{Bmatrix} 0 \\ 1 \\ 0 \\ 0 \end{Bmatrix} + C_{12}x^3 \begin{Bmatrix} 0 \\ -1 \\ 0 \\ 0 \end{Bmatrix} + \\ & + C_{13}x^2 \begin{Bmatrix} 0 \\ 0 \\ 1 \\ 0 \end{Bmatrix} + C_{14}x^3 \begin{Bmatrix} 0 \\ 0 \\ -1 \\ 0 \end{Bmatrix} + 10^{-9} \times \begin{Bmatrix} -31.2172x^2 \\ -0.00031x^2 \\ 0 \\ 208.1145x^2 \end{Bmatrix} \end{aligned} \tag{5.13}$$

Substituting Equation (5.13) into Equation (6.27) and the resulting expression into Equation (6.24) we obtain the beam forces and the strains of the beam. Substituting these into the expressions of the boundary conditions (Equation 6.32 and 6.33) we obtain an algebraic equation system which

yields the yet unknown constants C_i $(i = 1, 2, ...14)$ as:

$$\left\{\begin{array}{c} C_1 \\ C_2 \\ C_3 \\ C_4 \\ C_5 \\ C_6 \\ C_7 \\ C_8 \\ C_9 \\ C_{10} \\ C_{11} \\ C_{12} \\ C_{13} \\ C_{14} \end{array}\right\} = \left\{\begin{array}{r} -0.0519 \\ 0 \\ 0.1777 \\ 0.2768 \\ 0.6633 \times 10^{-4} \\ 0.0025 \\ -0.3757 \times 10^{-3} \\ -0.4162 \times 10^{-3} \\ 0.3231 \\ 0.0278 \\ 0 \\ 0.1236 \times 10^{-8} \\ 0.1926 \times 10^{-6} \\ 0.4682 \times 10^{-10} \end{array}\right\} \tag{5.14}$$

With these values the solution of Equation (5.1) is

$$\left\{\begin{array}{c} \overline{u} \\ \overline{w} \\ \overline{v} \\ \overline{\psi} \end{array}\right\} = \left\{\begin{array}{c} -0.0519 \\ 0 \\ 0.1777 \\ 0.2768 \end{array}\right\} + \left\{\begin{array}{c} 0.6633 \times 10^{-4} \\ 0.0025 \\ -0.3757 \times 10^{-3} \\ -0.4162 \times 10^{-3} \end{array}\right\} x + e^{-0.0012x} \left\{\begin{array}{c} 0.0406 \\ 0 \\ \text{-0.1944} \\ \text{-0.2549} \end{array}\right\} + \tag{5.15}$$

$$e^{0.0012x} \left\{\begin{array}{c} 0.0034 \\ 0 \\ 0.0167 \\ \text{-0.0219} \end{array}\right\} + x^3 \left\{\begin{array}{c} 0 \\ -0.1236 \times 10^{-8} \\ 0 \\ 0 \end{array}\right\} + x^2 \left\{\begin{array}{c} 0 \\ 0 \\ 0.1926 \times 10^{-6} \\ 0 \end{array}\right\} +$$

$$x^3 \left\{\begin{array}{c} 0 \\ 0 \\ -0.4682 \times 10^{-10} \\ 0 \end{array}\right\} + 10^{-9} \times \left\{\begin{array}{c} -31.2172x^2 \\ -0.00031x^2 \\ 0 \\ 208.1145x^2 \end{array}\right\}$$